

SCALE-DOWN APPROACH: CHEMICAL PROCESS OPTIMISATION USING REACTION CALORIMETRY FOR THE EXPERIMENTAL SIMULATION OF INDUSTRIAL REACTORS DYNAMICS

THÈSE N° 3464 (2006)

PRÉSENTÉE LE 3 MARS 2006
À LA FACULTÉ SCIENCES DE BASE

Groupe de Sécurité des procédés chimiques
SÉCTION DE CHIMIE ET GÉNIE CHIMIQUE

ÉCOLE POLYTECHNIQUE FÉDÉRALE DE LAUSANNE

POUR L'OBTENTION DU GRADE DE DOCTEUR ÈS SCIENCES

PAR

Benoît ZUFFEREY

ingénieur chimiste diplômé EPF
de nationalité suisse et originaire de Staint-Luc (VS)

acceptée sur proposition du jury:

Prof. P. Vogel, président du jury
Prof. F. Stoessel, directeur de thèse
Prof. D. Bonvin, rapporteur
Prof. K. Hungerbühler, rapporteur
Prof. A. Renken, rapporteur
Dr C. Rivier, rapporteur



ÉCOLE POLYTECHNIQUE
FÉDÉRALE DE LAUSANNE

Lausanne, EPFL

2006

A mes parents
A Marie

Durch viele Zitate vermehrt man seinen Anspruch auf
Gelehrsamkeit, vermindert aber den auf Originalität,
und was ist Gelehrsamkeit ohne Originalität!
Man soll sie also nur gebrauchen, wo man
fremder Autorität wirklich bedarf.

Arthur Schopenhauer
(1788-1860)

ACKNOWLEDGEMENTS

I consider that I am not too close for a proper view when I affirm that this thesis was somehow unique. Having the opportunity to work in collaboration with so many industrial partners, so many competent and devoted people and in so many different environments and places is very uncommon. This may sound pretentious, but I hurry to say that I had nothing to do with it, or then just a little. All these people deserve to be named.

First of all, I would like to express my profound gratitude to Prof. Stoessel for having accepted me in his research group and for having trusted in me. I asked him for a thesis work because, in my opinion, his was a great professor. Now that I better know him, I can state positively that he is also a great scientist, researcher and man. He gave me the freedom to plan my work as I thought best, but was also always able to rapidly give me precious advice to keep me «on the right tracks». Moreover, I had with him very interesting discussions about themes of all kind.

I am also grateful to Prof. P. Vogel, Prof. D. Bonvin and Prof. A. Renken from the Swiss Federal Institute of Technology Lausanne, Prof. K. Hungerbühler from the Swiss Federal Institute of Technology Zurich and Dr. C. Rivier from Firmenich for having accepted to be part of my jury, taken the time to read my thesis and who gave me many hints.

I would like also to thank P. Favre and B. Umbricht, who contributed to improve this manuscript by their pertinent remarks and proofreading.

This research work was completely financed by industrial partners. I am infinitely grateful to the companies Ciba SC, Firmenich, Mettler-Toledo, Roche, the Swiss Institute for the Promotion of Safety & Security and Syngenta. However, behind this list that sounds a little bit cold, there are people who constantly helped me and improved the quality of my work. Among them, I would like to address my special thanks to Dr. A. Fiaux, Dr. H. Maire, Dr. P-A. Michaud, Dr. S. Raoul and Dr. P. Zaza from Ciba SC; Dr. C. Mahaim, Dr. P. Schneider and Dr. E. Walther from Firmenich; U. Groth, Dr. P. Meuer and Dr. O. Ubrich from Mettler-Toledo; Dr. C. Lautz, Dr. J. Schildknecht and Dr. R. Thieme from Roche; Dr. A. Sting and Dr. S. Wodiunig from Syngenta. To correctly

express my feelings, I should detail the passionate discussions (not only about science but life in general), the uninterrupted help and the close ties that unite us. This would undoubtedly need tens of pages, which would be quite boring for other readers (if there are...). However, I already had the opportunity to thank them all «viva voce» and I am confident that they know all the good I think about them.

I do really want to thank all the people whom I met at the EPFL and who helped me. I am grateful for the assistance of the secretariat and the technical support of both the electronics and mechanics staff. Special thanks to P. Lugon for his devotion and kindness. I had also the opportunity to know people from diverse horizons who latter became close friends, namely Dr. E. Baranova, Dr. I. Duo, Dr. J. Eaves, Dr. C. Horny, Dr. B. Marselli, P. Prechtel, M. Grasemann, K. Nikolajsen, Dr. G. Siné and many more besides. Thank you for all the good times we had (and will have) together. It goes without saying that I address my profound gratitude to: E. Joannet, F. Lavanchy, C. Mantelis, M. Molliet, P. Nising, P. Tribolet and B. Zen-Ruffinen for the summer 2004.

Thanks to Prof. Stoessel, I had the opportuneness to spend 1 ½ year at the Swiss Institute for the Promotion of Safety & Security in Basel. I was confronted there to the «real life», in other words to the industrial way of life (I did not say that the university was the «simple life»...). If my coffee consumption decreased due to fewer breaks, my efficiency and productivity consequently increased! I would like to thank Dr. M. Glor, Dr. H. Rüegg and Dr. G. Suter for having accepted me here in Basel. Special thanks to Dr. H. Fierz, who will always remain for me as the ideal balance between deep scientific and general knowledge, great shrewdness and sense of humour. Special appreciation to my two co-tenants H. Angly and M. Durrer for their welcome. I also owe thanks to the other «Mitarbeiter» for their kindness. Last but not least, I would like to express my profound acknowledgment to the «Young Connection»: Dr. P. «Schlagfertigkeit» Reuse, Valérie, Patrizia, Dr. Alexis «Peyvil», Marc, Philippe and Thuy Van. They helped me a lot when I was fed up during the inherent hard times of a thesis (like for example with a meal at the «Braunen Mutz»).

Finally, I wish to record my gratitude to my parents, who gave me the possibility to acquire such a strong scientific education but also an open-mindedness, thanks to which everyday things seem to me new and attractive. And of course a very special acknowledgment to Marie: my most sincere thanks for your fondness, patience, support and love.

ABSTRACT

This thesis deals with the combined utilisation of a reaction calorimeter, the RC1[®] commercialised by Mettler Toledo and equipped with a 2 L glass reactor, and the heat transfer dynamics modelling of industrial reactors. By doing so, the temperature evolution of the reaction medium of full scale equipment during a chemical process can be forecast already at laboratory scale. Thus, the selectivity, quality and safety issues arising during the transfer of a new process, respectively the optimisation of an existing one, from the laboratory to the production scale are earlier detected and more correctly apprehended. It follows that the proposed methodology is a process development tool aiming to accelerate the rate at which innovative processes can be introduced into the market, and for which the global safety can be guaranteed.

Chapter 3 of the thesis devotes to the heat transfer dynamics modelling of industrial reactors. To this intention, heating/cooling experiments have been performed at plant scale. First, it consisted in filling up the industrial reactor with a measured quantity of a solvent with known physical and chemical properties (typically water or toluene). Second, after a stabilisation phase at low temperature, the setpoint of the liquid was modified to a temperature about 20 °C below its boiling point, followed by a stabilisation phase at high temperature. Then, the setpoint was changed to a value about 20 °C higher than the fusion point, again followed by a stabilisation phase at low temperature. During the experiment, the solvent and jacket temperatures are measured and registered. The stirrer revolution speed or the liquid amount are changed, and the whole measurement cycle repeated. Not only the heat transfer between the utility fluid and the reaction medium was modelled, but also the thermal dynamics of the jacket itself. Nine industrial reactors have been characterised, their sizes ranging from 40 L to 25 m³.

Chapter 4 presents the developed methodology allowing to predict the thermal behaviour of full scale equipment during a chemical process. It is based on two on-line heat balances, namely one over the reaction calorimeter to determine the instantaneous heat release rate and the other over the industrial reactor dynamics to compute its hypothetical thermal evolution. The dynamic model of the industrial reactor is introduced in an Excel sheet. A Visual Basic window allows to establish the connection between the reaction calorimeter and the Excel sheet, meaning that the data from

the various sensors of the RC1[®] can be sent at regular intervals of 10 s to the Excel sheet. By controlling its jacket temperature, the calorimeter is then forced to track the predicted temperature of the industrial reactor. The advantage of the proposed methodology is that the kinetics modelling of the reaction, often a time-consuming and expensive step, is here not mandatory.

In chapter 5, the precision of the on-line heat balance over the RC1[®] was tested and validated with the help of an external voltage source controlling the power delivered by the calibration probe. In this way, the heat provided to the reaction medium was known with great accuracy. The error of the on-line heat balance on the heat release rate, q_{rx} , lies in the generally acceptable 5 % range for bench scale calorimeters. Afterwards, the chosen test reaction, the hydrolysis of acetic anhydride, has permitted, at laboratory scale using the RC1[®], to highlight that the thermal dynamics of industrial reactors has a great influence on the temperature evolution of the reaction medium and, hence, on process safety. Finally, the simulation of a polymerisation reaction with the help of a thickener permits to conclude that the «scale-down» methodology and the on-line heat balance over the reaction calorimeter are also applicable to reactions accompanied with large variations of the reaction medium viscosity.

Chapter 6 compares the temperature evolution of the reaction medium predicted in the calorimeter with that actually recorded at plant scale. Three reactions are presented: a neutralisation, a three steps reaction and an alkene oxidation by a peroxycarboxylic acid. For the neutralisation, the results precisely tallied with a mean temperature difference lesser than 0.5 °C. Due to technical difficulties, the results of the three steps reaction slightly differ. For the oxidation reaction, the temperature predicted in the reaction calorimeter corresponds to that of full scale equipment to the nearest 0.5 °C. Moreover, the final compositions of the reaction medium are from the gas chromatography analyses also comparable. Moreover, this reaction being thermosensitive, a final selectivity decrease of 13 % is obtained at laboratory scale if this reaction took place in the 25 m³ reactor. This effect is due to its slower dynamics, smaller cooling capacity and more unfavourable heat transfer area to volume ratio compared with smaller reactors. The effect being highlighted already at laboratory scale, the elaborated tool results in a shorter process development time, a safer process and, hence, a shorter time-to-market.

Finally, chapter 7 concludes with some outlooks concerning the continuation of the project. As this thesis did not deal with mixing issues, its logical continuation would be the scale-down of mixing effects. A few general guidelines are given for this field.

Keywords: Scale-up; Scale-down; Reaction calorimetry; Process development
Heat transfer; Safety

VERSION ABREGEE

Ce travail de thèse a pour objet l'utilisation combinée d'un calorimètre de réaction, le RC1[®] commercialisé par Mettler Toledo et équipé d'un réacteur en verre de deux litres, et de la modélisation de la dynamique du transfert de chaleur de réacteurs industriels. Ce faisant, l'évolution de la température du milieu réactionnel lors d'un procédé à grande échelle peut être prédite déjà au niveau du laboratoire. Ainsi, les problèmes de productivité, qualité et sécurité survenant lors du transfert d'un nouveau procédé, respectivement lors de l'optimisation d'un procédé existant, du laboratoire à sa taille de production peuvent être plus tôt et plus correctement appréhendés. Il s'en suit que la méthodologie établie peut servir d'outil de développement en accélérant la mise sur le marché de nouveaux procédés dont la sécurité peut, de plus, être garantie.

Le chapitre 3 de la présente thèse traite de la modélisation de la dynamique du transfert de chaleur de réacteurs industriels. Pour ce faire, des essais de chauffage/refroidissement ont été réalisés à grande échelle. Ces essais consistaient tout d'abord à remplir le réacteur d'une quantité mesurée d'un solvant dont les propriétés physico-chimiques sont connues (typiquement eau ou toluène). Après une phase de stabilisation à basse température, une phase de chauffage, suivie d'une phase de stabilisation à haute température puis d'une phase de refroidissement sont réalisées. Durant l'expérience, la température du solvant ainsi que celle de la jaquette sont mesurées et enregistrées. La vitesse d'agitation ou la quantité de solvant sont modifiées, puis un nouveau cycle de mesure répété. A partir de ces mesures et à l'aide d'équations de bilan de chaleur, un modèle dynamique de transfert de chaleur est identifié pour chaque réacteur industriel. Non seulement le transfert entre la jaquette et le milieu réactionnel a été modélisé, mais aussi la dynamique thermique de la jaquette elle-même. Neuf réacteurs industriels ont été modélisés, leur volume allant de 40 L jusqu'à 25 m³.

Le chapitre 4 présente la méthodologie développée pour permettre d'imposer au calorimètre RC1[®] le profil de température prédit du réacteur industriel lors d'une réaction chimique. Pour ce faire, deux bilans de chaleur en ligne sont réalisés: le premier sur le calorimètre lui-même pour déterminer la puissance de réaction instantanée, et le deuxième sur le réacteur industriel, dont la dynamique thermique a été identifiée, pour déterminer son profil de température hypothétique. Le modèle dynamique du réacteur est introduit dans une feuille Excel. Une fenêtre Visual Basic permet au

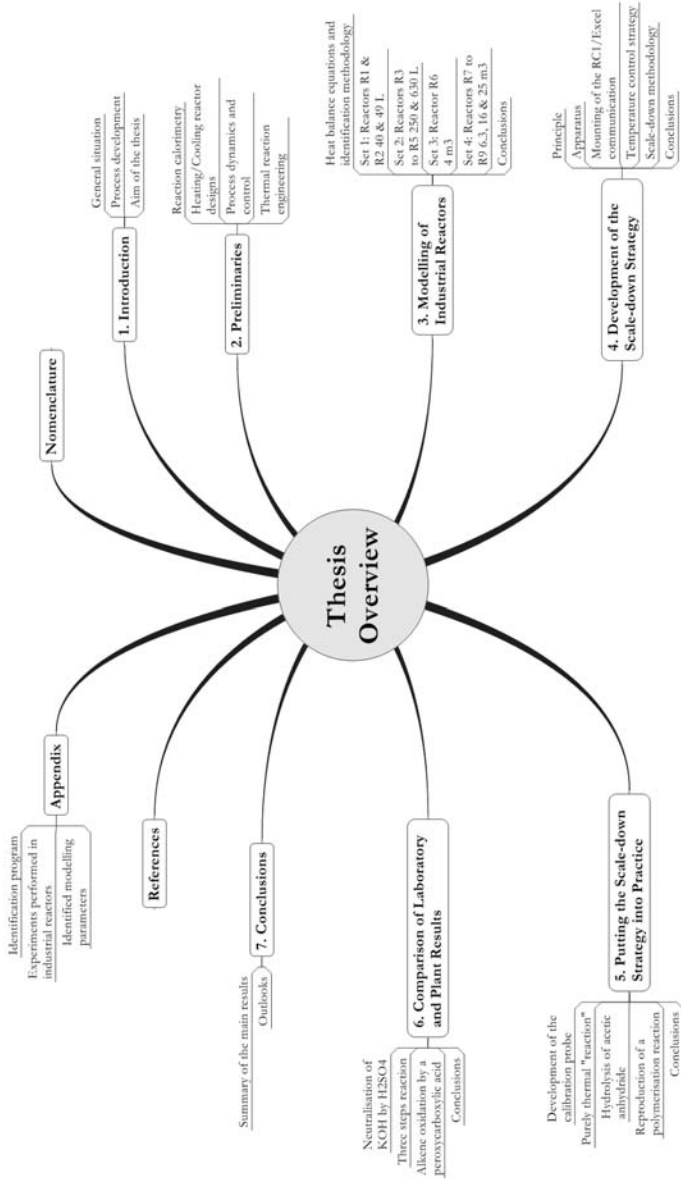
calorimètre RC1[®] et à la feuille Excel de communiquer, signifiant que des valeurs provenant des différents senseurs du calorimètre peuvent être envoyés, à intervalles réguliers de 10 s, vers la feuille Excel. La valeur de température du réacteur industriel prédite sert ensuite à contrôler la température de jaquette du RC1[®], forçant ce dernier à suivre les conditions thermales prédites pour le procédé à grande échelle. L'avantage de la méthode proposée est que la modélisation de la cinétique de la réaction, une étape souvent longue et coûteuse, n'est ici pas nécessaire.

Dans le chapitre 5, la précision du bilan de chaleur en ligne sur le calorimètre est testée et validée à l'aide d'une source de tension externe contrôlant la puissance dégagée par la sonde de calibration du RC1[®]. Ce faisant, la chaleur fournie au milieu réactionnel est connue avec une grande précision. L'erreur du bilan en ligne sur la puissance dégagée, q_{no} , se situe dans un domaine acceptable de 5 % pour des calorimètres de cette taille. Ensuite, une réaction test, l'hydrolyse de l'acide acétique, a permis de mettre en évidence l'effet de la dynamique thermique du réacteur industriel sur l'évolution de température globale de la masse réactionnelle, et donc sur la sécurité du procédé. Enfin, une simulation d'une réaction de polymérisation, impliquant un important changement de la viscosité, permet de conclure que la méthodologie développée et le bilan en ligne sur le calorimètre sont aussi valables dans des conditions réactionnelles plus drastiques.

Le chapitre 6 compare l'évolution de température du milieu réactionnel prédite à l'échelle du calorimètre avec celle effectivement mesurée lors de procédés à grande échelle. Trois réactions sont présentées: une neutralisation, une réaction en trois étapes et enfin une réaction d'oxydation d'un alcène par un acide peroxy-carboxylique. Pour la réaction de neutralisation, les résultats prédits sont proches de ceux obtenus dans les réacteurs industriels avec une différence de température moyenne inférieure à 0.5 °C. La réaction en trois étapes présente des difficultés techniques liées à son fonctionnement et de ce fait, les résultats diffèrent quelque peu. Pour la réaction d'oxydation, la température prédite dans le calorimètre de réaction correspond en moyenne à 0.5 °C près à celle obtenue à la production. La composition finale du milieu réactionnel est aussi comparable d'après les analyses chromatographiques réalisées. De plus, cette réaction étant thermosensible, une diminution de sélectivité de 13 % est prédite au laboratoire si cette réaction se déroulait dans le réacteur de 25 m³. Cet effet est dû à une plus lente dynamique, une capacité de refroidissement moindre et un rapport surface de transfert de chaleur sur volume plus défavorable pour ce réacteur comparés à des réacteurs de moindre taille. L'effet étant mis en évidence déjà à l'échelle du laboratoire, il en résulte un gain de temps appréciable du développement de procédé, et donc de la mise sur le marché de nouveaux produits, dont la sécurité de fabrication est assurée.

Finalement, le chapitre 7 conclue avec quelques perspectives pour la suite de cette thèse. Les problèmes de mélange résultant du passage d'un procédé du laboratoire à l'échelle de production, qui n'ont pas été pris en compte lors de ce travail, constituent une suite logique. Quelques directives et conseils généraux pour ce domaine sont présentés.

Mots-clefs: Scale-up; Scale-down; Calorimétrie de réaction; Développement de procédés
Transfert de chaleur; Sécurité



CONTENTS

NOMENCLATURE	xi
1 INTRODUCTION	1
1.1 General situation	1
1.2 Process development	3
1.2.1 Basic concepts	3
1.2.2 Computational tools	4
1.2.3 Safety aspects	4
1.3 Aim of the thesis	6
2 PRELIMINARIES	9
2.1 Reaction calorimetry	9
2.1.1 Introduction	9
2.1.2 Heat balance and principles of measurement	10
2.1.3 Short historical reminder of heat flow calorimetry	12
2.1.4 Safety aspects and reaction calorimetry	14
2.1.5 Process development and scale-up	18
2.1.6 On-line monitoring of chemical reactions	20
2.1.7 Scale-down	22
2.1.8 Current trend	23
2.2 Heating/Cooling reactor designs	24
2.2.1 Example A	24
2.2.2 Example B	26
2.2.3 Example C	27
2.3 Process dynamics and control	28
2.3.1 Historical background	28
2.3.2 Classification of control strategies	29
2.3.3 Parametric sensitivity	29
2.3.4 P, I, D control	30
2.3.5 Cascade control	32
2.3.6 Advanced control systems	33
2.4 Thermal reaction engineering	36
2.4.1 Isothermal control: $T_r = \text{const}(t)$	36

2.4.2 Isoperibolic control: $T_j = \text{const}(t)$	38
2.4.3 Adiabatic control: $q_{\text{ex}} = 0$	39
2.4.4 Programmed temperature control: $T_{\text{set}} = \text{Progr}(t)$	40
3 MODELLING OF INDUSTRIAL REACTORS DYNAMICS	43
3.1 Aims and strategy	43
3.2 Modelling - general equations	44
3.2.1 Mass balance	44
3.2.2 Heat balance - Reactor temperature	44
3.2.3 Heat balance - Jacket temperature	53
3.3 Experimental part	56
3.3.1 Standard experiments	56
3.3.2 Parameters identification of the dynamic model	57
3.4 First set of reactors - 40 & 49 L	57
3.4.1 Features and experiments	57
3.4.2 Experimental results	58
3.4.3 Modelling	59
3.4.4 Results	61
3.5 Second set of reactors - 250 to 630 L	63
3.5.1 Features and experiments	63
3.5.2 Modelling	64
3.6 Third set of reactor - 4 m ³	66
3.7 Fourth set of reactors - 6.3 to 25 m ³	69
3.7.1 Experiments and modelling	69
3.7.2 Results	71
3.8 Conclusions	74
4 DEVELOPMENT OF THE SCALE-DOWN METHODOLOGY	77
4.1 Principle	77
4.2 Apparatus	78
4.3 External data source communication	79
4.4 Temperature control strategy	81
4.4.1 Context	81
4.4.2 PI controller	82
4.5 Scale-down methodology	85
4.5.1 Initialisation phase	85
4.5.2 Data acquisition	87
4.5.3 Update	87

4.5.4 Heat balance over the RC1	89
4.5.5 Scale-up factor	90
4.5.6 Heat balance over the industrial reactor	90
4.5.7 Setpoint	91
4.5.8 Reiteration	91
4.5.9 Block diagram	91
4.6 Conclusions	94
5 PUTTING THE SCALE-DOWN STRATEGY INTO PRACTICE 95	
5.1 Introduction	95
5.2 Calibration probe controlled by an external voltage source	96
5.2.1 Principle	96
5.2.2 Development	96
5.2.3 Validation	97
5.3 Purely thermal reactions	98
5.3.1 Classical RC1	98
5.3.2 Modified RC1	100
5.4 Hydrolysis of acetic anhydride	106
5.4.1 Purpose	106
5.4.2 Experimental conditions	106
5.4.3 Classical RC1 results	107
5.4.4 Modified RC1 results	109
5.5 Reproduction of a polymerisation reaction	114
5.5.1 Purpose	114
5.5.2 Experimental conditions	116
5.5.3 Classical RC1 results	116
5.5.4 Modified RC1 results	118
5.6 Conclusions	120
6 COMPARISON OF LABORATORY AND PLANT RESULTS 121	
6.1 Introduction	121
6.2 Neutralisation of KOH by H_2SO_4	122
6.2.1 Introduction	122
6.2.2 Experimental part	122
6.2.3 Classical RC1 results	124
6.2.4 Modified RC1 results	124
6.3 Three steps reaction	128
6.3.1 Introduction	128
6.3.2 Experimental part	128

6.3.3 Classical RC1 results	129
6.3.4 Modified RC1 results	132
6.4 Alkene oxidation by a peroxycarboxylic acid.	137
6.4.1 Introduction.	137
6.4.2 Experimental part	137
6.4.3 Classical RC1 results	138
6.4.4 Modified RC1 results	140
6.5 Conclusions	144
7 CONCLUSIONS	147
7.1 Summary of the main results	147
7.2 Outlooks.	149
7.2.1 Mixing effects	149
7.2.2 Mixing issues	149
7.2.3 Continuation of the project - a few general guidelines	151
REFERENCES	155
APPENDIX	163
A.1 Identification program	163
A.2 Experiments performed in industrial reactors	165
A.2.1 First set of reactors.	165
A.2.2 Second set of reactors	166
A.2.3 Third set of reactors.	167
A.2.4 Fourth set of reactors.	168
A.3 Identified modelling parameters	169
INDEX	171

NOMENCLATURE

Symbols

A	Heat transfer area	$[\text{m}^2]$
C	Stirrer constant	$[-]$
C_1 to C_4	Parameters of the Uhl & Gray vortex equation	$[-]$, except m^2s^{-2} for C_1
C_p'	Specific heat capacity	$[\text{J}\cdot\text{kg}^{-1}\cdot\text{K}^{-1}]$
C_R	Reactant concentration	$[\text{mol}\cdot\text{m}^{-3}]$
C_w	Mean heat capacity of the reactor	$[\text{J}\cdot\text{K}^{-1}]$
d	Stirrer diameter	$[\text{m}]$
D	Reactor diameter	$[\text{m}]$
d_w	Thickness of the reactor wall	$[\text{m}]$
E_a	Activation energy	$[\text{J}\cdot\text{mol}^{-1}]$
Fr	Froude number: $N^2 d g^{-1}$, ratio of inertial forces to gravitational forces	$[-]$
g	Gravitational constant	$[9.8094 \text{ m}\cdot\text{s}^{-2} \text{ at } 48.5^\circ \text{ (Switzerland)}]$
h	Height	$[\text{m}]$
h_j	Outside heat transfer coefficient	$[\text{W}\cdot\text{m}^{-2}\cdot\text{K}^{-1}]$
h_r	Internal heat transfer coefficient	$[\text{W}\cdot\text{m}^{-2}\cdot\text{K}^{-1}]$
I	Integral controller parameter	$[\text{s}]$
k	Rate constant	$[\text{mol}^{1-n}\cdot\text{m}^{3(n-1)}\cdot\text{s}^{-1}]$
K	Proportional controller gain	$[-]$
m	Mass	$[\text{kg}]$
\dot{m}	Mass flow rate	$[\text{kg}\cdot\text{s}^{-1}]$
n	Order of reaction	$[-]$
N	Stirrer revolution speed	$[\text{s}^{-1}]$
Ne	Power number	$[-]$
Nu	Nusselt number: $h_j D \lambda^{-1}$, ratio of total heat transfer to conductive heat transfer	$[-]$
p_1 to p_3	Identified parameters of the heat transfer model	$[p_1: \text{W}\cdot\text{m}^{-2}\cdot\text{K}^{-2}, p_2: \text{W}\cdot\text{m}^{-2}\cdot\text{K}^{-1}, p_3: -]$
P	Product	$[-]$
Pr	Prandtl number: $\mu C_p' \lambda^{-1}$, ratio of momentum diffusivity to thermal diffusivity	$[-]$
q	Heat release rate	$[\text{W}]$

q'	Specific heat release rate	$[\text{W}\cdot\text{kg}^{-1}]$
Q	Heat	$[\text{J}]$
r	Reaction rate	$[\text{mol}\cdot\text{m}^{-3}\cdot\text{s}^{-1}]$
R	Ideal gas constant	$[8.3145 \text{ J}\cdot\text{mol}^{-1}\cdot\text{K}^{-1}]$
R_1 to R_9	Industrial reactors	$[-]$
Re	Reynolds number: $N d^2 \rho \mu^{-1}$, ratio of inertial forces to viscous forces	$[-]$
s^*	Local temperature sensitivity	$[\text{K}]$
t	Time	$[\text{s}]$
T	Temperature	$[\text{K}]$
T^*	Maximum temperature in the sensitivity analysis	$[\text{K}]$
U	Overall heat transfer coefficient	$[\text{W}\cdot\text{m}^{-2}\cdot\text{K}^{-1}]$
V	Volume	$[\text{m}^3]$
wt	Weight	$[\text{kg}]$
X	Conversion	$[-]$
\mathcal{X}	Vessel number	$[-]$

Greek symbols

α	Constant of proportionality	$[\text{W}\cdot\text{K}^{-1}]$
β	Slope of the Wilson plot	$[\text{m}^2\cdot\text{K}\cdot\text{W}^{-1}]$
γ	Reaction mixture number	$[\text{W}\cdot\text{m}^{-2}\cdot\text{K}^{-1}]$
ΔH	Enthalpy	$[\text{J}\cdot\text{mol}^{-1}]$
$\Delta H'$	Specific enthalpy	$[\text{J}\cdot\text{kg}^{-1}]$
Δt	Time difference	$[\text{s}]$
ΔT	Temperature difference	$[\text{K}]$
λ	Thermal conductivity	$[\text{W}\cdot\text{m}^{-1}\cdot\text{K}^{-1}]$
μ	Dynamic viscosity	$[\text{kg}\cdot\text{m}^{-1}\cdot\text{s}^{-1}]$, habitually expressed in Pa·s or cP
ρ	Density	$[\text{kg}\cdot\text{m}^{-3}]$
τ	Time constant	$[\text{s}]$
φ	Resistance to heat transfer due to apparatus	$[\text{m}^2\cdot\text{K}\cdot\text{W}^{-1}]$
Φ	Dimensionless parameter characterizing the model under consideration	$[-]$

Subscripts

0	Initial	$[-]$
a	Corrected jacket	$[-]$
accu	Accumulation	$[-]$
ad	Adiabatic	$[-]$
air	Air	$[-]$
amb	Ambient	$[-]$
b	Boiling	$[-]$
bottom	Bottom	$[-]$

c	Cooling	[-]
C	Cold	[-]
cal	Calibration	[-]
<i>cf</i>	Cooling failure	[-]
dos	Dosing	[-]
ex	Exchange	[-]
ext	External	[-]
f	Final	[-]
fus	Fusion	[-]
h	Heating	[-]
H	Hot	[-]
i	<i>i</i> th component	[-]
in	Inlet	[-]
j	Jacket	[-]
l	Laboratory	[-]
lat	Lateral	[-]
loss	Losses	[-]
m	Mean	[-]
max	Maximum	[-]
min	Minimum	[-]
mix	Mixing	[-]
out	Outlet	[-]
p	Plant	[-]
r	Reaction mixture	[-]
R	Reactant	[-]
reflux	Reflux	[-]
rx	Reaction	[-]
safe	Safe	[-]
set	Setpoint	[-]
side	Side	[-]
st	Stirrer	[-]
th	Thermal	[-]
tot	Total	[-]
vap	Vaporisation	[-]
vort	Vortex	[-]
w	Reactor wall	[-]

Superscripts

indus	Industrial Reactor	[-]
on-line	On-line	[-]
RC1	Reaction Calorimeter	[-]
T	Temperature	[K]

Abbreviations

AISI	American Iron and Steel Institute	[–]
ARC [®]	Accelerating Rate Calorimeter	[–]
ATR	Attenuated Total Reflection	[–]
AZF	AZote de France	[–]
CFD	Computational Fluid Dynamics	[–]
CEFIC	European Chemical Industry Council	[–]
COM	Component Object Model	[–]
CPU	Central Processing Unit usage	[%]
DSC [®]	Differential Scanning Calorimeter	[–]
DIN	Deutsches Institut für Normung	[–]
DTA	Differential Thermal Analysis	[–]
EKF	Extended Kalman Filter	[–]
EPFL	Ecole Polytechnique Fédérale de Lausanne	[–]
EPROM	Erasable Programmable Read-Only Memory	[–]
ESCS	Expertenkommission für Sicherheit in der Chemischen Industrie der Schweiz	[–]
GC	Gas Chromatography	[–]
HC	Hastelloy Calibration probe	[–]
HWS	Heat Wait Search method	[–]
IP	Internet Protocol	[–]
IR	Infra Red	[–]
ISD	Inherently Safer Design	[–]
MTSR	Maximum achievable Temperature due to the Synthesis Reaction	[K]
NIST	National Institute of Standards and Technology	[–]
NNs	Neural Networks	[–]
ODE	Ordinary Differential Equations	[–]
PB	Proportional Band	[–]
PCI	Peripheral Component Interconnect	[–]
PE	Petroleum Ether	[–]
Progr	Programmed	[–]
PTFE	PolyTetraFluoroEthylene	[–]
QFS	Quick onset, Fair conversion and Smooth temperature profile	[–]
R&D	Research & Development	[–]
RAM	Random Access Memory	[–]
RC1 [®]	Reaction Calorimeter commercialised by Mettler Toledo	[–]
ROI	Return On Investment	[€]
rpm	Rate Per Minute	[1/60 s ^{–1}]
rx	Reaction	[–]
SR	Serial Release	[–]
TC	Temperature Control	[–]
TCP	Transmission Control Protocol	[–]
TMR _{ad}	Time to Maximum Rate under ADiabatic conditions	[s]
TOC	Temperature Oscillation Calorimetry	[–]

TT	Temperature Transmitter	[-]
VBA	Visual Basic	[-]
VDI	Verein Deutscher Ingenieure	[-]
WinRC ALR	WINDows Reaction Calorimeter Automated Laboratory Reactor evaluation software	[-]

Chapter 1

INTRODUCTION

1.1 General situation

The chemical industry today is completely different from the chemical industry of twenty-five years ago. The situation it has to face at present time consists in [1]:

- exchanging information with a network of partners, suppliers and customers
- high business complexity in a fast moving market
- very short product life-cycles and the requirement of rapid delivery
- constant innovation in products, technologies and quality
- price pressure due to global competition and cyclical markets.

In today competitive environment, one of the key issues for fine chemical companies is to reach the market with new products as quickly as possible. Speed, accuracy and cost all affect the way products are designed and the rate at which they can be introduced into the market. Total costs however will further be influenced by the required manpower, the costs for generating exposure data, expenses for administering the procedures, loss of market/investment, impact on intellectual property, flexibility and time-to-market. Downstream users of chemicals may face market restrictions, generation of exposure data, testing costs, effects from the phasing out of substances, including R&D costs to find substitutes for chemical substances that are not registered, reformulation of preparations and possible component-type approval [2].

As regards costs, the key parameter is the return on investment (ROI). On that score, we are on the horns of a dilemma: companies and departments make investments for long(er) term gains but when it comes to personal productivity, individuals tend to look at the shorter term, i.e. no project chemist ever wants to go into negative ROI, on a personal basis [3]. If the biggest major change in the way we do chemistry may involve the widespread application of computational chemistry, there is a natural unwillingness of the individuals to take this change responsibility. Plotting ROI vs. time brings to the situation depicted in Fig. 1.1.

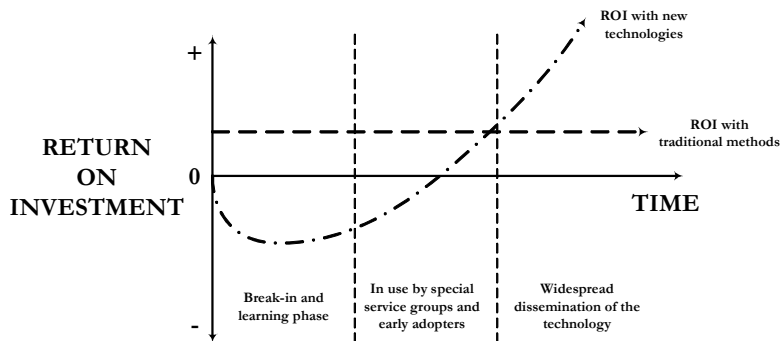


Figure 1.1: Return on technology investment vs. time (after [3]).

To summarise, the fine chemical and pharmaceutical industry is under pressure because of [4]:

- escalating cost of drug development
- deteriorating industry image
- price controls, importation and reference pricing
- increase competition
- patent expirations.

1.2 Process development

1.2.1 Basic concepts

This work deals with one of the steps that may influence the rate at which innovative products can be introduced into the market: the process development. Process development is commonly seen as a segment of the chain that links a new process concept with its commercial exploitation. The tasks in the process development are executed more or less in parallel in different parts of the development organisation and efficient information generation and exchange and technology transfer are of the greatest importance [5]. In the start-up phase, dynamic models are used in the plant for the operator training and to assist the decision making in «what if» situations like:

- malfunctioning of feeding system causing improper reactant ratios
- overdosing active reactant
- reduced heat and/or mass transfer
- breakdown of mixing or cooling system.

Deduced scenarios are of course intimately related to the process equipment. Process plants for carrying out chemical reactions are used in several industrial fields, for example the chemical, pharmaceutical or biological industry. They are either purpose built for a specific chemical reaction or designed as multi-purpose plants. Multi-purpose plants are especially suited for customer specific productions or for industrial fields with fast changing production lines and products. Therefore, multi-purpose plants are often operated discontinuously and either the multi-purpose plant and/or the chemical reaction have to be adapted. The Swiss chemical industry, which consists essentially in fine chemical products, utilises most often batch or semi-batch reactors operating discontinuously. Therefore, chemical engineers, in their everyday work, rather adapt the process recipe to the equipment than they design the most suitable reactor for a given synthesis.

When speaking about process development of batch or semi-batch operations, one of the most important aspects is the scale-up. Traditionally, it involves scaling-up from laboratory equipment through mini-plants to full scale commercial operation with magnitude factors of typically 10^4 . However, the economic environment implicates more product changeovers and large scale-up that more and more tend to avoid pilot-plant tests. Furthermore, as Bonvin says [6]: «In order to meet safety and environmental requirements, numerous experimental tests that rely on widely-varying conditions are performed in the *laboratory*. The appropriate use of available laboratory data to facilitate large scale-up represents a promising industrial opportunity as well as a considerable challenge». For this reason, new apparatus or methodologies facilitating the taking into consideration of important factors (like product quality, safety, environment and economic impacts) sound very appealing to chemical companies. Ideally, it is important that new technologies reduce uncertainties as much as possible in earlier stages where experiments are done on a small

scale in relatively cheap flexible equipment rather than in later stages with lesser flexible and more expensive equipment. This strategy is in line with the adage «make your mistakes on a small scale and reap your profits on a large scale». The main issue with this approach, however, is that basic decisions concerning the process design must be made at a time when the knowledge of the process is only superficial [7].

In conclusion, the ability to efficiently and quickly integrate such powerful features into existing processes is crucial to an industry where time-to-market can mean the difference between success and failure. Therefore, all actors of the fine chemical industry, primarily small and medium size companies with limited technical resources, will be interested in a specific development methodology.

1.2.2 Computational tools

In several years, an industrial revolution has appeared with the emergence of computers. Computational tools, which can be considered as software tools, are relatively cheap means to obtain information, as compared to the process development units that represent the hardware tools [8]. One use of computational tools is the kinetic modelling. On that score, enormous efforts and improvements have been achieved in the last two decades. Kinetic models that are based on elementary reactions offer the best accuracy and reliability. Moreover, the knowledge of a specific elementary reaction can be re-used for completely different operating conditions and in different species mixtures. In contrast, more approximate methods have parameters determined strictly by fitting to experimental measurements and have very limited applicability. Although global reaction expressions can be included in detailed kinetic mechanisms, more fundamental expressions provide more accuracy and extensibility. The procedure is generally first to identify the kinetic parameters of the reactions at laboratory scale, either by classical analysis of samples or by on-line methods, and second to simulate production conditions [9].

However, the other side of the coin is that the success of this approach entirely relies on the quality of the kinetic model and hence on the quality of measurements data. Moreover, the number of products of the chemical industry is rather large: the order of magnitude is 10^5 . The number of reactions involved is of the same order of magnitude. If all kinetic-relevant data of reactions were determined experimentally, many man-years of work would be necessary [10].

1.2.3 Safety aspects

Major accidents in chemical industry have occurred world-wide. The 1984 gas leak in Bhopal, India, was a terrible tragedy which understandably continues to evoke strong emotions even 21 years later. In Europe, the Seveso accident in 1976 in particular prompted the adoption of legislation aimed at the prevention and control of such accidents. The Seveso II directive applies to some thousands

industrial establishments where dangerous substances are present in quantities exceeding the thresholds in the directive. As regards land use planning, the accidents in Enschede (firework, Netherlands) and Toulouse (AZF, France) prompted again the need to maintain appropriate distances between Seveso establishments and residential areas.

Since then, process development and risk assessment are more closely interconnected. Process hazard analysis and the preparation of an operating procedure, however, are time-consuming tasks in the development of industrial processes. Risk assessment proceeds in five steps:

- look for the hazards
- decide who might be harmed, and how
- evaluate the risks arising from the hazards and decide whether existing precautions are adequate or more should be done
- record the findings
- review the assessment from time to time and revise it if necessary.

Focusing on step three and on chemical processes, risks are related to reactivities and to toxic properties of the chemicals involved. However, undesired reactions or poorly controlled desired reactions may lead to thermal runaways. For this purpose, runaway scenarios have been developed. The goal is to obtain an educated estimate on the quantities characterising the potential runaway. The basic questions are [11]:

- Can the process temperature be controlled by the cooling system?
- Which temperature can be reached after runaway of the desired reaction, assuming adiabatic conditions for a cooling failure (this temperature is termed the Maximum achievable Temperature due to the Synthesis Reaction (*MTSR*))?
- Which temperature can be reached after runaway of the decomposition?
- What is the most critical instant for a cooling failure to happen?
- How fast is the runaway of the desired reaction?
- How fast is the runaway of the decomposition starting at *MTSR*?

For information of the desired reaction, reaction calorimetry is an appropriate chemical engineering tool. It allows a chemical reaction to be run under conditions representative of a specific process. The specific heat evolution rates measured as a function of the process time can be directly used in a heat balance consideration of the operational plant [12].

1.3 Aim of the thesis

Finally, a successful process development is achieved if the concordance, between laboratory and plant scales, of the three main time constants is respected:

- *reaction* time constant
- full scale equipment *dynamics* time constant
- *mixing* time constant.

In this thesis, only the first two items will be discussed, of course also related to safety aspects. The reaction time constant may be determined at laboratory scale using the data provided by a reaction calorimeter, in our case the RC1[®] commercialised by Mettler Toledo. Thermal characteristics of the reaction like heat production rate, necessary cooling power, reactant accumulation, etc., are fundamental for safe reactor operation and process design. However, an industrial chemical reactor not only behaves according to the kinetics of the reaction but also to the dynamics of its temperature control system. Scale-up to the large capacity industrial reactor may be limited because the control is performed indirectly via the heat transferred between the fluid circulating in the jacket and the reactant mixture. The transfer area to volume ratio decreases as the size of the reactor increases, leading to serious limitations of the heat transfer capacity of the jacket. Additionally, many problems occur due to the thermal inertia (long time constant) of the jacket wall [13]. Moreover, reaction enthalpies, kinetic parameters and hence product selectivity and global safety are known to be temperature-dependent. Therefore, only the combination of both reactions kinetics and reactor dynamics allows describing and predicting the behaviour of an industrial reactor with respect to productivity, selectivity and safety. Currently, commercialised calorimeters, and among them the RC1[®], enable for an ideal control of the temperature even for very exothermic reactions. But they do not allow identifying the effect of the temperature control dynamics of full scale equipment. In this work, we would like to develop a «scale-down» methodology allowing to reproduce the exact temperature course of an industrial reactor at laboratory scale, and this, without explicit knowledge of the reaction kinetics.

Thus, the objectives of this thesis are:

- elaborate a specific methodology for process development in the fine chemical industry
- develop a laboratory tool allowing reducing the number of large scale experiments
- reduce development time for chemical processes.

By so doing, the new way to use the reaction calorimeter RC1[®] will allow simulating the thermal behaviour of plant reactors, resulting in a better understanding of full scale production issues, in terms of productivity and quality. Moreover, the assessment of safety scenarios will be more accurate, first because the starting temperature in case of a cooling failure corresponds to that of

plant conditions and second because the reaction enthalpy, the heat production rate and the thermal accumulation also more correctly reflect full scale reality. It is thus the goal of this work to develop a tool that helps to eliminate most of costly late development changes and leads to breakthrough improvements in quality, safety and time-to-market.

Chapter 2

PRELIMINARIES

2.1 Reaction calorimetry

2.1.1 Introduction

Every process liberating or consuming a finite amount of energy, calorimetry is useful in potentially characterizing any chemical and also physical proceeding. Moreover, heat evolution is a definite, reproducible, and directly measurable characteristic of a chemical reaction. Reaction calorimetry has the advantage that the heat release rate of reaction (q_{rx}) is directly proportional to the rate of reaction. This allows easy access to basic kinetic and thermodynamic data of chemical reactions (heat of reaction, reaction rate and conversion). Calorimetry not only provides information on the chemical reaction process itself, but also on reactor parameters necessary for safe reactor operation and process design:

- global reaction kinetics
- heat production rate
- necessary cooling power
- reactant accumulation
- temperature rise under adiabatic conditions (ΔT_{ad})
- heat-transfer coefficients for scale-up.

However, calorimetry is a nonselective method. It is impossible to distinguish between parallel chemical reactions with heat generation and simultaneous enthalpic processes within the system such as phase transition, crystallisation, mixing or dissolution.

- Modes of operation

In calorimetry, one distinguishes mainly between four modes of operation:

- *Isothermal*: a system condition in which the temperature is kept constant. This implies that potential temperature variations are compensated by sufficient heat exchange with the environment of the system.
- *Adiabatic*: a system condition in which no heat is exchanged between the system, including the sample container, and its environment.
- *Isoperibolic*: a system condition in which the surroundings temperature is held constant, while the measuring device is allowed to have a different temperature.
- *Dynamic* (scan rate): a system condition in which the temperature of the sample is increased at a known and usually constant rate.

Another mode of operation, combining the isothermal, adiabatic and dynamic ones is the *Heat Wait Search* (HWS): an experimental technique in which a substance is heated step by step until very slow decomposition of the substance is detected. The experimental apparatus then becomes adiabatic and the course of the decomposition is tracked.

2.1.2 Heat balance and principles of measurement

There is no generally accepted classification of calorimeters. The attempt to classify all calorimeters in detail leads to a lack of clarity and insignificance in practice. Thus, many authors have published overviews of calorimetry [14-18]. They differ in that they are based either on the measurement principle, on the mode of operation, or on the principle of construction. Based on the classification of Regenass [16], it is possible to distinguish between two different categories: *heat accumulation* and *heat flow* methods.

In the *heat accumulation* method, the effect (e.g. an increase or decrease in temperature) of the heat to be measured is not minimized by any compensation, but leads to a temperature change in the sample and the calorimeter substance with which the sample is thermally connected. This temperature change is the parameter to be measured. It is proportional to the amount of heat exchanged between the sample and the calorimeter itself used as a heat sink. Adiabatic and most of the isoperibolic instruments use this method. To quote the main ones (Fig. 2.1): the Accelerating

Rate Calorimeter (ARC[®]) allows a sample to undergo thermal decomposition due to self-heating while recording the time-temperature-pressure relationships of the runaway process; the calorimeters SEDEX[®] (can be also classified in the heat flow calorimeters depending on the mode of operation) and SIKAREX[®].

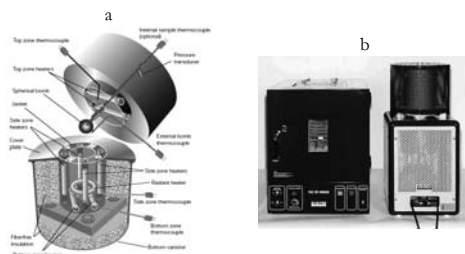


Figure 2.1: Examples of heat accumulation calorimeters. a: Columbia Scientific Industries ARC[®] [19]; b: Systag's SEDEX[®] and SIKAREX[®] [20].

In the *heat flow* method, the heat to be measured is determined by the power (heat flow rate) required to maintain the sample under isothermal conditions or for the sample to follow a temperature profile defined beforehand. However, as the heat is measured with the heat flow, temperature gradients are always present in calorimetric measuring systems, so that a strictly isothermal state cannot be reached. This accumulated heat is a major cause of uncertainty and error because it depends on the derivative of the reactor temperature. Heat flow calorimeters can be divided into four subgroups (see Fig. 2.2):

- *Heat transfer* calorimeters: the generated heat is measured by means of the temperature difference between reactor and jacket.
- *Heat balance* calorimeters: the generated heat is determined by the total heat balance of the heating/cooling liquid circulating through the jacket.
- *Heat compensation* calorimeters: the generated heat is measured by the electrical power required to maintain isothermal conditions, while the jacket fluid temperature is fixed, with $T_j < T_r$.
- *Peltier type* calorimeters: the generated heat is determined by the required voltage applied to Peltier elements to maintain isothermal conditions, while the jacket fluid temperature is fixed, with $T_j > T_r$ or $T_j < T_r$, depending on the polarity of the power supplied to the Peltier junction.

Note that the Differential Scanning Calorimeter (DSC[®]) also belongs to the *heat flow* calorimeters. Two containers or supports with sample and reference sample are set with temperature sensors to measure the temperature difference between the specimens.

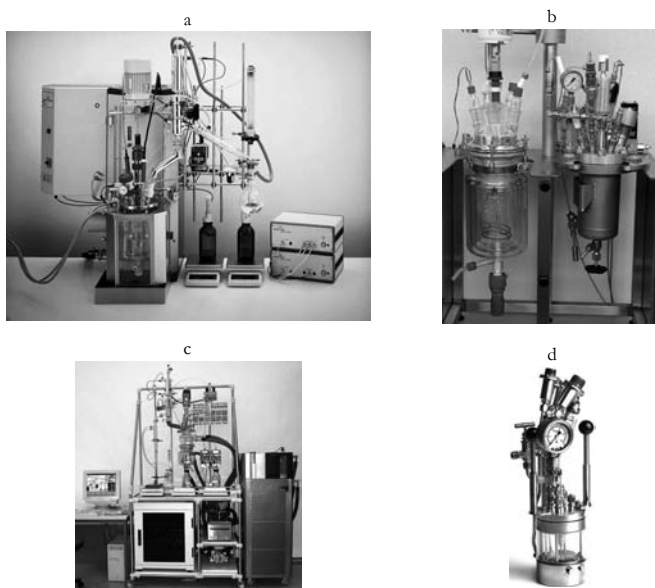


Figure 2.2: Examples of heat flow calorimeters. a: Mettler Toledo's RC1[®] [21] (heat transfer); b: HEL's Simular[®] [22] (heat compensation); c: Systag's Syscalo[®] [23] (heat balance); d: ChemiSens's CPA 202[®] [24] (Peltier elements).

2.1.3 Short historical reminder of heat flow calorimetry

Calorimetry has already been studied for a long time. Shortly after the introduction of the concept of heat by Black in 1760, Lavoisier and Laplace published the first example of use of calorimetry by investigating the heat released by a living mouse in an ice calorimeter. The lack of generally satisfying classification of calorimeters, due to the many characteristic features, such as calorimeters compensating for the thermal effects, measuring temperature differences in time or in space, makes the description of the calorimetry history also a difficult task. Focusing on heat flow calorimetry makes it easier. Its roots lie in differential thermal analysis (DTA) [25]. It was systematically developed in the second quarter of the 19th century by Tian [26] and Calvet [27]. Based on these works, heat flow calorimeters specially designed for the investigation of the kinetics of industrial reactions were built from the 1960's in almost every major company such as Monsanto [28], BASF [29], Ciba [30, 31], Sandoz [32], Roche [33] or Bayer [34].

Calorimetric works within Ciba started around 1965 and more intensely as a consequence of a plant runaway in 1969. It simultaneously focused on heat balance and on heat transfer systems. After several trials to determine what kind of temperature control was appropriate, and after giving up the heat balance method, Regenass and co-workers [35] could develop a «Bench Scale Calorimeter» (Fig. 2.3). The first commercially available type was the Ciba-Geigy BSC-81 in 1981, which became lately the famous RC1® after Mettler acquired a license on this calorimeter.

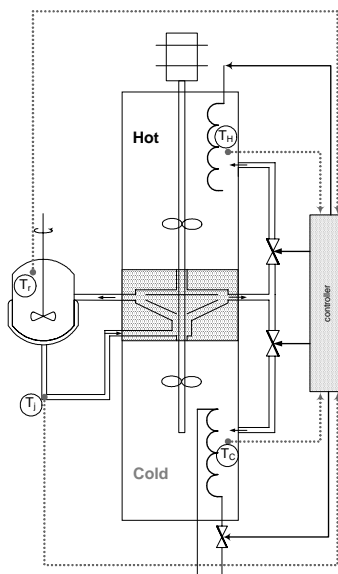


Figure 2.3: Schematic representation of the BSC-75 model. The controller records the temperatures of reaction mixture (T_R), jacket (T_J), hot (T_H) and cold (T_C) sources and adjusts the valves opening in consequence.

Thereby, applications of reaction calorimetry have been explored by both industrial and academic scientists covering the areas of process safety, process development, and basic research.

Interesting reviews on heat flow calorimetry can be consulted in the publications of Regenass [36], Karlsen and Villadsen [37] or Landau [15].

2.1.4 Safety aspects and reaction calorimetry

- Relating heat flow and kinetics

Stoessel [38] reminds the three essential questions in the design of thermally safe (semi-)batch reactors:

- Can the heat of reaction be removed by the cooling system?
- What temperature can be reached in case of a cooling failure?
- May a secondary decomposition reaction be triggered?

To answer these questions, thermodynamic data, kinetic parameters and physical properties of the reactants together with reactor conditions are required. Since the heat flow is closely related to the kinetics, the measurement of the heat flux serves as a direct indicator of the reaction rate. For this reason, reaction calorimetry became a broadly used method in process safety. In the review by Landau [15], a very simple illustration explains this concept. Consider a first order irreversible reaction given as:



The rate of this reaction, r , is directly proportional to the rate of heat evolution, q_{rx} :

$$q_{rx} = r \cdot V \cdot (-\Delta H_r) \quad (2.2)$$

Equation 2.2 clearly describes the relationship between the heat flow and the reaction rate. The rate expression, assuming mass action kinetics, is given by:

$$r = dC_R / dt = -k \cdot C_R \quad (2.3)$$

Substituting Eq. 2.3 into Eq. 2.2 leads to:

$$q_{rx} = -k \cdot C_R \cdot V \cdot (-\Delta H_r) \quad (2.4)$$

Initially, the heat flow is given as:

$$q_{rx,0} = -k \cdot C_{R,0} \cdot V \cdot (-\Delta H_r) \quad (2.5)$$

Dividing Eq. 2.4 by Eq. 2.5 yields:

$$q_{rx} / q_{rx,0} = C_R / C_{R,0} \quad (2.6)$$

The result of Eq. 2.6, valid for simple first order reactions, shows, after integration of Eq. 2.3 followed by combination with Eq. 2.6, how heat flow is related to the kinetics:

$$C_R / C_{R,0} = e^{-kt} = q_{rc} / q_{rc,0} \quad (2.7)$$

This approach can be applied to any kinetic model, however, it sometimes does not yield an analytical result, and must be numerically evaluated to extract kinetic parameters from the heat flow data.

Use and extension of the non-invasive (temperature measurements only) nature of reaction calorimetry as a tool for monitoring reactions has been abundantly published [33, 39-42].

- Runaway scenarios

Although the major objective of the chemical industries will always remain releasing benefits, safety aspects gained importance during the last two decades. Since the 1984 gas relief in Bhopal, India, there have been improvements in process safety and emergency response. Within months of the disaster, chemical companies and trade associations put together new process safety programs and set higher safety standards. This tragedy gave new impetus to a concept developed by Kletz called «Inherently Safer Design» (ISD) [43, 44], in which chemical plants are designed to reduce risk through use of fundamentally safer systems in the manufacturing process. Four paths lead to ISD: *minimise* or *intensify* (use smaller quantities of hazardous chemicals or increase reaction efficiency), *substitute* (replace a hazardous chemical with a safer one), *moderate* (shift to less hazardous processes and chemicals), *simplify* (design facilities to eliminate unnecessary complexity). Assessment of runaway scenarios becomes natural in keeping with this concept. Moreover, risk analysis allows a better understanding of the process and consequently helps to reduce costs. Finally, the conclusion of the risk assessment should always provide information on which to base decisions. Risk is usually defined as the combination of two fundamental concepts:

$$Risk = Severity \cdot Probability \quad (2.8)$$

Four different situations can occur [45]:

- *High* severity, *high* probability: intolerable, may contravene good practice, the law or moral codes.
- *Low* severity, *low* probability: tolerable, the risks we live with day-by-day, but still needs to be managed.
- *High* severity, *low* probability: where risk management has traditionally focused; requires robust risk management.
- *Low* severity, *high* probability: often not given enough attention, although capable of causing significant loss over prolonged periods.

In order to assess the risk of batch and semi-batch operations, different methods can be considered. In the past, an important source of safety knowledge has been to learn from the incidents themselves. Today, risk analysis based on some basic properties and approximate data tend fortunately to replace the incidents as a source of information. The goal is to determine the conditions under which the process should be performed to guarantee that, in case of a cooling breakdown, the risks remain within acceptable limits.

The perhaps most exhaustive method to determine the *severity* of a runaway is the one proposed by Gygax in 1988 [12] and extended by Stoessel [11]. It introduces the concept of *MTSR*, «Maximum Temperature due to the Synthesis Reaction»:

$$T_{gf}(t) = T_r(t) + (1 - X_{th}(t)) \cdot \Delta T_{ad} = T_r(t) + (1 - X_{th}(t)) \cdot \frac{(-\Delta H_r) \cdot C_{R,0}}{\rho \cdot C_p^r} \quad (2.9)$$

$$MTSR = \left[T_{gf}(t) \right]_{\max}$$

with $T_{gf}(t)$ and ΔT_{ad} the temperature reached in case of a cooling failure and the temperature rise under adiabatic conditions respectively. According to this equation, the *MTSR* is therefore the maximum temperature that can be reached by the desired synthesis reaction when carried out under adiabatic conditions. Eq. 2.9 is given for a semi-batch reactor; for a batch process, the *MTSR* is directly calculated by setting the thermal conversion $X_{th}(t)$ to zero, since the most critical moment for a cooling failure to happen is, in the case of normal n -th order reactions, at the beginning of the reaction. One part of the scenario assessment is to determine when the most critical moment for a cooling failure occurs, i.e. when $T_{gf}(t)$ is maximal and thermal stability minimum [46]. As Eq. 2.9 proves it, it greatly depends on the degree of reagents accumulation in the process and can be controlled in case of a semi-batch operation by the feed rate [47-50].

The measurement of the heat flux being related to the reaction rate (cf. Eq. 2.2), reaction calorimetry is the appropriate tool for determining the *MTSR*. For example, in order to find the degree of accumulation at time t , $1 - X_{th}(t)$, the heat evolution curve is sufficient:

$$1 - X_{th}(t) = X_{acc}(t) = 1 - \frac{\int_0^t q_{rc} \cdot dt}{\int_0^\infty q_{rc} \cdot dt} \quad (2.10)$$

Another key concept is to know the needed time, given an initial temperature often set as *MTSR*, for a secondary decomposition reaction to be triggered. This time is a parameter to evaluate the *probability* of the runaway. For this purpose, Gygax [12] took again the notion of time to maximum rate under adiabatic conditions, initially developed by Semenov [51], and reintroduced by Townsend and Tou [52]:

$$TMR_{ad} = \frac{C_p' \cdot R \cdot T_0^2}{q_0 \cdot E_a} \quad (2.11)$$

This formula was established for zero order reactions but can also be used for other orders, as long as the influence of concentration on reaction rate can be neglected. This approximation is particularly valid for fast and very exothermic reactions.

The isothermal mode of DSC[®] provides an easy way to measure the kinetic parameters used in the TMR_{ad} formula: a set of isothermal experiments is run at different temperatures. The neperian logarithms of the maximum heat release rate of the autocatalytic decomposition, determined on each thermogram, are plotted as a function of the inverse temperature in an Arrhenius diagram. From this diagram, a linear fit allows the calculation of the heat release rate for every temperature. As for it, the activation energy is calculated by:

$$E_a = \frac{R \cdot \ln\left(\frac{q_2'}{q_1'}\right)}{\frac{1}{T_1} - \frac{1}{T_2}} \quad (2.12)$$

with q_1' and q_2' the maximum heat release rates obtained during the isothermal DSC[®] measurements at temperatures T_1 and T_2 respectively. Using this energy of activation and the specific heat capacity, the TMR_{ad} can be estimated according to Eq. 2.11.

The risk scenario can then be assessed based on the following table:

Table 2.1: Criteria for the severity and probability assessments, derived from [11].

Criteria	Severity	Probability
High	$\Delta T_{ad} > 200$ °K or T_b surpassed	$TMR_{ad} < 8$ h
Medium	50 °K $< \Delta T_{ad} < 200$ °K	8 h $< TMR_{ad} < 24$ h
Low	$\Delta T_{ad} < 50$ °K	$TMR_{ad} > 24$ h

Many authors have published papers related to safety and chemical processes. Concerning the present scope of interest, a few ones can be cited: Fierz et al. [53] give one of the first example of combining reaction calorimeter data and safety aspects; Alos et al. [54, 55] focus on parametric sensitivity criterion to predict thermal runaway in batch and semi-batch reactors respectively; Nomen et al. [56] investigate the relation between calorimetric measurements and risk assessment; in his work, Leggett [57] points out that «the understanding of the reactive nature of chemical

processing operations is the first step to accomplish the reduction of risks» and illustrates how isothermal differential scanning and adiabatic calorimetry can lead to essential data, whereas Regenass [58], Stoessel et al. [59] as well as the ESCIS [45] give a complete review of the tools and methodologies to assess thermal risks.

2.1.5 Process development and scale-up

Most of the pharmaceutical and fine chemical reactions are appreciably exothermic. Therefore, they must be well apprehended before conducted on plant scale. In a typical industrial vessel, most of the reaction heat is evacuated by the jacket fluid. To ensure that the heat release rate never exceeds that of the heat removal, the best processing strategy has to be found. As reaction calorimeters provide data of the instantaneous rate on heat release, they can be used to determine the macro-kinetic parameters and hence to develop a heat flow model [60]. This model can then simulate vessels of any volume. Hence, reaction calorimetry found many applications in process development, too. The iterative methodology in scale-up analysis includes experimental considerations, development of heat flow models and simulation of large-scale vessels, but still many rules of thumb. The heat production rate, the enthalpy of the reaction as well as the specific heat capacity of the reaction mass, determined from calorimetric data, are independent on the size of the vessel. However, the heating/cooling capacities differ from laboratory to plant scale.

Choudhury et al. [61], summarising the original work of Bürli [62], show how to estimate the cooling power of the plant reactor by scaling-up the U -value based on reaction calorimetry measurements. The overall resistance of the heat transfer between the reaction mixture and the cooling liquid, $1/U$, is the sum of three elements in series¹ (see Fig. 2.4):

$$\frac{1}{U} = \frac{1}{h_r} + \frac{d_w}{\lambda_w} + \frac{1}{h_j} = \frac{1}{h_r} + \varphi \quad (2.13)$$

The internal heat transfer coefficient h_r can be evaluated at laboratory scale in a reaction calorimeter using the Wilson method [63]. The data required for the Wilson method can be obtained from calorimetric calibrations at various stirrer speeds in isothermal mode (see Fig. 2.5).

-
1. U : depends on the reactor contents and on the rate of agitation; is temperature dependent for a given reaction mixture.
 h_r : depends on the physical and chemical properties of the reaction mixture; can be influenced by the stirrer speed and its diameter; is also temperature dependent.
 h_j : depends on the physical and chemical properties of the heat carrier liquid and on its velocity; for a given flow rate is a weak function of temperature.
 φ : depends on the reactor itself and on the heat exchange system; depends only on temperature if the flow rate of the heat carrier liquid is constant.

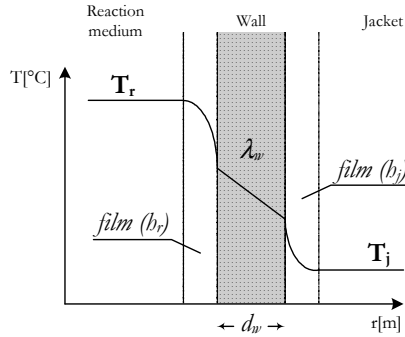


Figure 2.4: Schematic representation of the steady-state temperatures profile and heat transfer resistance in series in an agitated jacketed reactor.

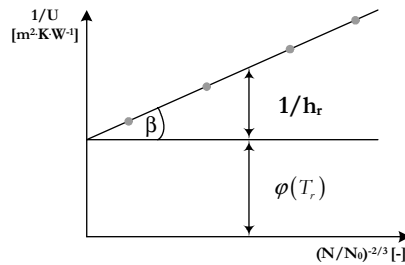


Figure 2.5: Determination of the internal heat transfer coefficient, h_r , by means of the Wilson plot. The gray points represent the experimental values of $1/U$ at different stirrer revolution speeds. A trend drawn through these points enables to determine the h_r and $\phi(T_r)$ values.

From the dimensionless description of the forced heat transfer given by Chilton [64], Uhl & Gray [65] proposed the following dependency based on the ratio of the stirrer revolution speed N and an arbitrary reference speed N_0 :

$$\frac{1}{h_r} = \beta \cdot \left(\frac{N}{N_0} \right)^{-2/3} \quad (2.14)$$

Finally, providing similar geometry between laboratory and plant vessels, the heat transfer coefficient of the reaction mixture inside the plant vessel, $h_{r,p}$, is calculated from the laboratory reactor data obtained at the same temperature with:

$$h_{r,p} = h_{r,l} \cdot \left(\frac{d_p}{d_l} \right)^{1/3} \cdot \left(\frac{N_p}{N_l} \right)^{2/3} \cdot \left(\frac{\mu_{r,p}}{\mu_{w,p}} \right)^{0.14} \quad (2.15)$$

Unfortunately, the Wilson method is based on semi-empirical relations. The estimation or measurement of the maximum cooling capacity of the plant reactor as well as pilot experiments to verify mixing effects remain necessary. To this end, Lake [66] described a simple manner to obtain both approximate cooling capacities and heat transfer coefficients of jacketed vessels, by cooling down a known volume of water or suitable liquid at the maximum rate. On the other hand Kumpinsky [67] proposed a method for the determination of the overall heat transfer coefficient, based on transient tests in which the temperature of the vessel responds to a change in jacket temperature.

The use of reaction calorimetry in combination with simulation tools for process development investigations is nowadays gaining importance because of increasing computational capacity. However, modelling requires assumptions that keep it from fully replacing experiments. Moreover, the models need input data that only pilot studies can provide. Only a few examples deal with scale-up and simulation, probably because details of processes are usually regarded as confidential by manufacturers. As an example, Landau et al. [68] developed in 1994 both heat flow and kinetic models from calorimetric measurements. These were then used to simulate the heat transfer of a production batch and semi-batch processes. The influences of changes in reactor geometry, agitation and mass transfer when switching from the laboratory settings to the production reactors have been assumed to be minor compared with heat-transfer problems. However, this assumption can of course not be generalised. Two years later, Bollyn et al. [69] combined reaction calorimetry and reactor simulation for scaling-up a highly exothermic oxidation reaction. The reaction model was derived from reaction calorimetry data and incorporated in a process model, which was then used to simulate production conditions. Once again, availability of production vessel data was inevitable, particularly its cooling capacity.

2.1.6 On-line monitoring of chemical reactions

With reaction calorimetry, rates of reaction or conversion of reactants can be determined quasi-instantaneously and continuously with a high degree of resolution. This makes reaction calorimetry an ideal tool for real-time feedback control of chemical composition during the course of reaction. On-line heat balance or heat flow calorimetry allows the efficient control of batch and semi-batch reactors and the determination of the best time profiles of temperature, feeding rates and concentrations.

A great part of the works being published on on-line monitoring deals with polymerisation reactions. The reason is that most polymerisation reactions, especially radical ones, are strongly exothermic. Since the heat flow is not constant but follows the kinetics, calorimetric measurements are a very valuable and simple method to characterise a reactor and to control the reaction.

Moreover, since monomer accumulation can be detected by a decrease of the heat release rate, on-line reaction calorimetry can rapidly detect and correct it by reducing or even stopping reagent addition. In other words, the control of molecular weight distribution or the monitoring of emulsion polymerisation can be done by evaluating on-line the energy balance from calorimetric data. The most extensive article dealing with this theme is probably that of de Buruaga et al. [70]. The authors used a Mettler Toledo RC1[®] reaction calorimeter with an external computer to solve on-line the mass and energy balances. From this evaluation, the monomer flow rate was adjusted every 5 s by means of a PI algorithm.

Recently, more sophisticated techniques were developed. They can be divided into two parts: *state and parameter estimation* and *measurement devices*.

The state and parameter estimation relies on process models to predict the system behaviour to future disturbances. Several publications deserve special mention: apart from the original work of De Vallière [71]: the publications of Wilson et al. [72], that assesses the industrial-scale feasibility of an on-line estimator, and of Krämer & Gesthuisen [73], that describes the way to simultaneously estimate the heat of reaction and the heat transfer coefficient with the help of extended Kalman filtering (EKF). However, it would seem that the scope of use of EKF is rather limited: the first authors cast serious doubt on the usefulness of on-line estimation in industrial situations, compared to simple open-loop prediction, whereas the second ones point out that for small laboratory scale reactors, with high jacket flow rates, the state observer will not correctly work due to measurement limitations, i.e., too large a system noise.

The measurement devices part uses spectroscopic methods (IR, IR-ATR or Raman) to monitor the performance and estimate on-line the concentrations. As said previously, calorimetry measures a sum of all reactions and other heat flows during a (semi-)batch run. Detailed information about the conversion of the process reaction is only possible if additional measurements are available. Analytical methods such as spectroscopy or gas chromatography can provide this kind of information. In 2001, Ubrich et al. [74] combined spectroscopic measurements and reaction calorimetry to optimise the feed rate of a semi-batch reaction under the constraint that the maximum attainable temperature in case of a cooling failure never exceeds a safe value. In a recent publication, Hergeth et al. [75] compared different methods to keep track of emulsion and suspension polymerisation reactions. They suggested that calorimetry, combined with near infrared or Raman spectroscopy, shows the highest potential for on-line applications. In 2005, Zogg et al. [76] developed a new estimation algorithm that allows a simultaneous evaluation of on-line measured infrared and calorimetric data to determine kinetic and thermodynamic parameters. It is able to identify several reaction parameters, such as reaction enthalpies, rate constants, activation energies as well as reaction orders in a single step. Their work showed the importance to use a combined algorithm in order to obtain the optimal reaction parameters, whereas separate calorimetric and spectroscopic evaluations lead to significantly different solutions.

2.1.7 Scale-down

There is a need for scaling at two independent occasions in industrial production: when a new process is scaled-up and when an existing process is subject to modifications. Furthermore, in fine chemical industry, a new process is often conducted in an already existing plant vessel. Therefore, the main problem consists in optimising the production path with respect to productivity, selectivity and safety, under the constraint of a more or less fixed reactor design. To detect problems early in the future production reactor, low cost small scale trials (targeted experiments) and best mimicking compartment would be particularly adapted. However, examples of this approach in the literature are rare. Probably, several scale-down approaches have been studied and used in industry, but never published because of confidential reasons. The unique published contribution is that of Kupr & Hub [77], who worked at that time for Sandoz. They had perfectly understood that the changes of physical conditions between laboratory and production reactors remained so far neglected. Indeed, for an efficient scale-up, the kinetic of the reaction needed to be known. However, this is a time consuming requirement in contradiction with today's mandatory short time-to-market periods. Instead of a theoretical calculation, they limited the heat supply of a 1 L reaction calorimeter so that the conditions of the large reactor could be apprehended. For that purpose, the heating/cooling capacity was modified by limiting the heat transfer area in the reactor mantle. With the help of a moving pipe in the overflow container (see position f, Fig. 2.6), the heat carrier liquid level was adjusted to the desired height. The criterion was that the product of the overall heat transfer coefficient with the heat transfer area per volume of reaction mass should be the same in laboratory and production plants. The invaluable advantage is that the knowledge of the reaction kinetic was no more a prerequisite.

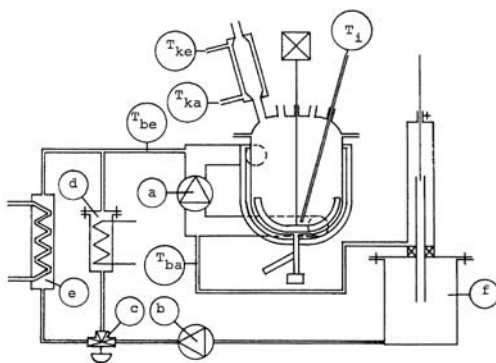


Figure 2.6: Reaction calorimeter according to Kupr & Hub [77]. a: centrifugal pump; b: gear pump; c: control valve; d: flow heating; e: heat exchanger; f: overflow container; $T_{be} = T_{j,in}$; $T_{ba} = T_{j,out}$; $T_i = T_p$; $T_{ke} = T_{refluc,in}$; $T_{ka} = T_{refluc,out}$

Unfortunately, it seems that the project did not arouse the expected interest. It was by that time abandoned and according to this bibliographic overview never cited or copied.

2.1.8 Current trend

As the complexity and hence the costs of the pharmaceutical and fine chemical products are incessantly growing, usually only very small quantities are at disposal for calorimetric measurements, typically in the order of several tens of grams. Therefore, the recently commercialised calorimeters have the tendency to offer smaller recipient volumes. Even though the flexibility of the latter is lower, especially for reactions under reflux or gas production evaluations, the development of very sensitive devices allows to obtain precise values of reaction and phase change enthalpies or of heats of mixing. Moreover, this type of systems is faster thanks to a simple handling and cheaper, as small quantities of products are staked. For all these reasons, the main manufacturers propose at least one small scale calorimeter in their products range. Fig. 2.7 presents some of them.

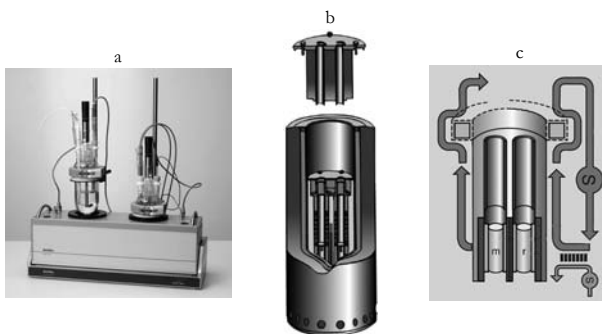


Figure 2.7: Examples of calorimeters with small sample volumes. a: Mettler Toledo MultiMax's[®] with 250 mL reactors (versions with 50, 20 or 10 mL also exist); b: Setaram Calvet C80[®] (measurement cell volume of 12.5 mL); c: Setaram MicroDSC III[®] (maximal sample volume of 850 μL).

The research has of course preceded this trend toward miniaturisation and numerous publications deal with microcalorimeters, with volumes of several μL . For example, Schneider et al. [78] developed a microreactor, with a volume of less than 1 μL , combined with a commercial microcalorimeter device. This system can characterise very fast and exothermic reactions, for which

the required isothermal conditions are difficult to maintain in the existing calorimeters. The specific heat release rate measured during their study reached $160'000 \text{ [W}\cdot\text{kg}^{-1}]$ (!) but nevertheless, the conditions remained completely isothermal. The global kinetics of the reaction as well as its activation energy, yet unknown, were determined.

2.2 Heating/Cooling reactor designs

In order to heat or cool process substances, different heating/cooling systems are set up in the fine chemical industries. The attainable temperatures, heat injection or removal as well as the controllability (process safety) are the determinant parameters to consider when starting the operations.

Heating systems use warm water, superheated water (under pressure), steam or other heat carriers. Among other utility fluids, oils are mostly used: organic, polyglycols, mineral and silicone oils (like Diphenyl, Marlotherm, Syltherm, Baysilon, etc.). The heating can also be eventually obtained from an electrical resistance placed in a tube that directly plunges in the reaction mass. However, this system tends to be abandoned because it can lead to very high surface temperatures. *Cooling systems* use factory water, brine (H_2O & NaCl (-20°C) or H_2O & CaCl_2 (-40°C)), mixtures of alcohol and water or other cool carriers (e.g. oil). Ice is sometimes directly poured in the mixture that needs to be cooled. Ice is interesting because of its heat capacity and above all its latent heat of fusion ($\Delta H_{fus}' = 320 \text{ [kJ}\cdot\text{kg}^{-1}]$, all the same). In this case, needless to mention that the reaction mass is diluted and has to be compatible with water. Note that of course most of the set up systems combine heating and cooling devices.

In the following chapters, the most commonly applied systems for agitated vessels will be emphasised.

2.2.1 Example A

- Heat carrier: steam; cool carrier: factory water

The most frequent heat carrier is steam. This steam, with a pressure of e.g. 6 bar, is introduced at the top of the half pipe coils or the jacketed vessel. During its way, the steam has to condense, for the heat of condensation being the greatest part of the energy contained in steam. The condensate is then discharged at the bottom in a drainer (see Fig. 2.8). At start up, it is necessary to exhaust the air from the coils or the jacket, because air decreases the heat transfer. The condensate temperature

depends on the steam pressure and can be adjusted with the help of a pressure reducer. The regulation can be set either by the inlet or outlet temperature. However, for temperatures higher than 200 °C, the pipe system, the valves, and hence the costs become rapidly weighty since pressure increases above 30 bar.

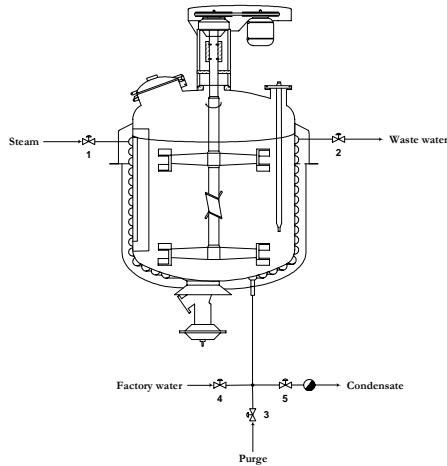


Figure 2.8: Heating/cooling system with steam and factory water.

Factory water is of course the most standard and simple cool carrier. Compared with steam, the system is reversed: water is introduced into the coils *from the bottom*, respectively the jacket, and discharged *on the top*. The quantity of cool water has to be adjusted or regulated, so that on one hand the outlet temperature does not exceed 45 °C (to prevent fouling) and that on the other hand no water is wasted. The passage from steam to water and inversely is performed with the following valve functioning pattern:

Table 2.2: Valves positioning for example A (Fig. 2.8).

Mode	1	2	3	4	5
<i>Heating</i>	Regulate	Closed	Closed	Closed	Open
<i>Purge</i>	Closed	Open	Open	Closed	Closed
<i>Cooling</i>	Closed	Open	Closed	Regulate	Closed

- Heat carrier: steam; cool carrier: brine

When factory water does not suffice to attain the end process temperature (typically $< 10\text{ }^{\circ}\text{C}$), brine or a mixture of alcohol/water is employed (see Fig. 2.9). These liquids are cooled with the help of a compression refrigerating machine.

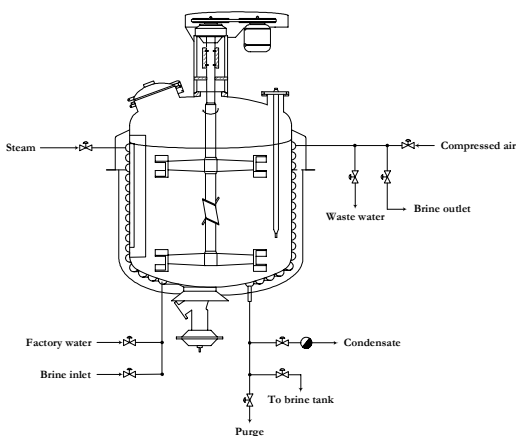


Figure 2.9: Heating/cooling system with factory water and brine cooling.

When passing from factory water to brine and inversely, the cooling system needs to be completely purged to avoid mixing of the two cool carriers (brine could dilute with water and consequently freeze the cooling device). During emptying, attention has to be paid to avoid that brine, respectively alcohol/water mixture get into the waste water network (wastage and environmental discharge).

2.2.2 Example B

- Heat carrier: warm water, superheated water

With this system, the coils or jacket, expansion vessel and associated piping are filled with water. The water is pumped in loop and heated by supply with steam through a mixing nozzle (see Fig. 2.10). During this process, the volume of the circulating water as well as that of the condensate increase, the excess of water is then exhausted via the expansion vessel (overflow pipe). With this system (without pressure), the process substances can be heated up to a maximal temperature of about $90\text{ }^{\circ}\text{C}$.

If temperatures greater than 90 °C have to be reached, the whole heating system is set under pressure (increase of the boiling point). In addition, the overflow of the expansion vessel is closed and the surplus water is exhausted by a steam trap (with float) or by a level regulation. According to the steam pressure and/or condensate temperature, such a technique is adapted for a large temperature range (e.g. at 9 bar up to 170 °C).

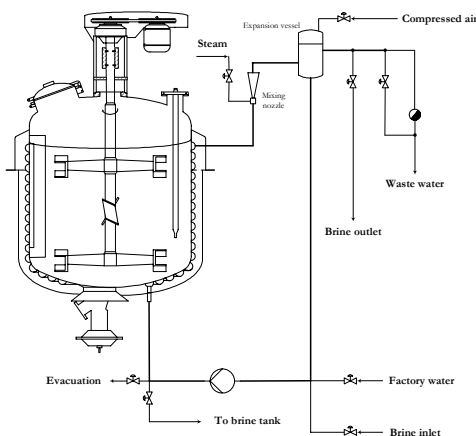


Figure 2.10: Heating/cooling system with warm and superheated water.

Note that for such heating systems, no water has to be taken from the piping. Indeed, during expansion an immediate and violent steam build-up could arise.

- Cool carrier: factory water, brine or alcohol/water mixture

During cooling with water, the latter is fed in loop into the coils, respectively the jacket, and the expansion vessel (with overflow pipe). If brine or a mixture of alcohol/water is used as cool carrier, the system must be previously emptied (see example A).

2.2.3 Example C

If, for safety reasons (e.g. process materials dangerously reacting with water), no water may be used as a heating/cooling agent, or if a larger temperature range is wished, a secondary circulation is used (see Fig. 2.11). In these, an inert organic heat transfer liquid is warmed up, respectively cooled down. The liquid is pumped in closed loop to a heat or a cool exchanger, depending on the required temperature. Its advantage is its great flexibility: it permits a direct transition from heating to cooling and inversely (no idle time). However, the investment is more important.

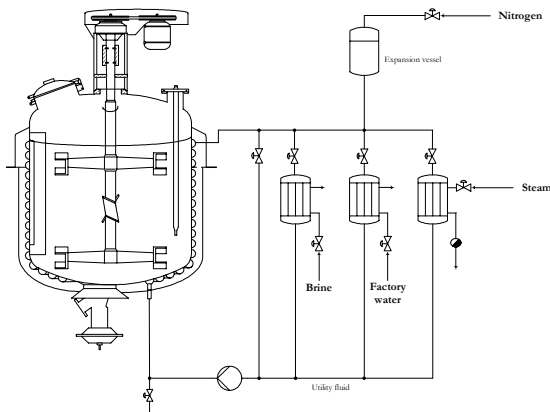


Figure 2.11: Heating/cooling system with secondary circulation.

2.3 Process dynamics and control

2.3.1 Historical background [79]

Most of the chemical processing plants were run essentially manually prior to the 1940s. Only the most elementary types of controllers were used. Many operators were needed to keep watch on the many variables in the plant. In the 1940s and early 1950s, it became soon uneconomical and often technically impossible to run plants without automatic control devices. At this stage rule-of-thumb guides and experience were the only design techniques. In the 1960s chemical engineers began to apply dynamic analysis and control theory to chemical process. The concept of examining the many parts of a complex plant together as a single unit, with all interactions included, and devising ways to control the entire plant is called *systems engineering*. The rapid rise in energy prices in the 1970s provided additional needs for effective control systems. So the challenges to the process control engineer have continued to grow over the years. In recent years, the performance requirements for process plants have become increasingly difficult to satisfy because of the trend toward larger, more flexible and highly integrated plants with smaller capacities between the various processing units. In fact, without process control it would not be possible to operate most modern processes safely and profitably, while satisfying plant quality standards.

2.3.2 Classification of control strategies

Control strategies can mainly be categorised in *feedback control* and *feedforward control* strategies.

In feedback control, the process variable to be controlled is measured and used to adjust another process variable which can be manipulated. It is important to make a distinction between *negative feedback* and *positive feedback* [80]. Negative feedback refers to the desirable situation where the corrective action taken by the controller tends to move the controlled variable toward the setpoint. A simple and practical example is a room thermostat (and actually any thermostat). When the temperature in a heated room reaches a certain upper limit, the room heating is switched off so that the temperature begins to fall. When the temperature drops to a lower limit, the heating is switched on again. Provided that the limits are close to each other, a steady room temperature is maintained. In the case of positive feedback, the system will even increase the change of the variable. The negative feedback loop tends to slow down a process, while the positive feedback loop tends to speed it up. Positive feedback is used in certain situations where rapid change is desired.

The majority of the fine chemical plant reactors take advantage of the feedback control strategy to control either the inner or jacket temperatures.

In feedforward control, the controlled variable is *not* measured. In other words, feedback control is reactive; feedforward control is pro-active. Feedforward control can respond more quickly to known kinds of disturbances, but is ineffective with novel disturbances. Feedback control deals with any deviation from the desired system behaviour, but requires the system to respond to the disturbance in order to notice the deviation. A feedforward system can be illustrated by the cruise control in a car [81]. Imagine the car has a mean of sensing the slope of the road it is travelling on. On encountering an uphill stretch of road, the 5° nose-up attitude of the car causes the throttle to be opened to a predetermined corresponding amount. The car does not have to slow down at all for the correction to come into play.

2.3.3 Parametric sensitivity

The temperature control of a reaction provides one of the easiest ways to ensure that the three key parameters productivity, selectivity and safety remain within fixed operability boundaries. These boundaries are most of the time not easy to determine and may be very parameter sensitive. Since 1956 and the work of Bilous and Amundson [82], the parametric sensitivity of temperature has been abundantly studied. Barkelew, in 1959, was the first to exploit this concept for batch reactors and later for adiabatic ones [83, 84]. In 1982, Morbidelli and Varma analysed the sensitivity behaviour of a tubular reactor [85] and two years later, of a fixed-bed catalytic reactor for the case of n -th order irreversible reactions [86]. Developing the sensitivity analysis, they proposed a numerical procedure to calculate sensitivities [87]. The local temperature sensitivity, s_{Φ}^* , is defined as:

$$s_{\Phi}^*(X) = \frac{dT^*(X)}{d\Phi} \quad (2.16)$$

with T^* denoting the maximum temperature, X the conversion and Φ an independent dimensionless parameter characterising the model under consideration, e.g. the Semenov number, the heat of reaction, the reaction order, the activation energy or the initial temperature. The critical condition for parametric sensitivity or runaway is defined when s_{Φ}^* is maximum. This criterion is called generalised since the maximum temperature becomes simultaneously sensitive to small changes of any of the model parameters.

In 1992, Haldar and Rao were the first to give experimental results for batch [88] and semi-batch [89] reactors. Several years later, Alos et al. [54, 55] applied the local temperature sensitivity criterion to isoperibolic-constant jacket temperature semi-batch reactors. Their results showed that the criterion discerns between non-ignition and thermal runaway regions. However, it is not able to differentiate between the runaway and the QFS¹ regions, because in both cases, the reactor is ignited.

2.3.4 P, I, D control²

It is well known that chemical reactors dynamics are highly nonlinear and time varying. However, the reactor temperature input-output behaviour exhibits a relatively small time delay so that in most of the existing approaches, the plant can be modelled as a first- or second-order system [90]. Therefore, the control problem can be handled using one of the three basic feedback controllers: proportional (P), integral (I), derivative (D) or a combination of them, which are able to accommodate the plant dynamics variations over the whole operating range [91]. Fig. 2.12 is a block diagram for a feedback controller. In practice, PI and PID controllers represent the majority of the industrial control systems. These controllers are commonly tuned by means of the operator know-how or using the well known Ziegler and Nichols method [92]. Since then, several authors have attempted to improve the tuning of PID controllers. In 1995, Voda and Landau [93] proposed an auto-calibrated PID control, whereas in 1996 Miklvcova et al. [91] developed a combined controller including an auto-tuning and an auto-calibrated PID controller. For the Mettler Toledo reaction calorimeter, which uses two PI controllers within a cascade controller, Ubrich [94] gives some standard P and PI values as well as examples of how to define the optimal P value.

-
1. Quick onset, Fair conversion and Smooth temperature profile; observed when the reactor temperature curve approaches the target temperature rather rapidly.
 2. This notation is used to mean that the three controller configurations P, PI & PID can be employed.

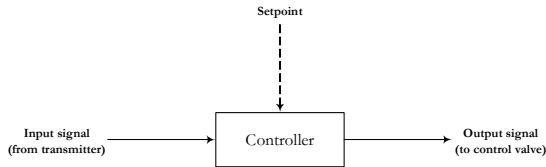


Figure 2.12: Schematic representation of a feedback controller.

Some proportional controllers, especially older models, have a proportional band setting instead of a controller gain. The proportional band PB (in %) is defined as:

$$PB = \frac{100\%}{K} \quad (2.17)$$

This definition applies only if K , the gain, is dimensionless. Note that a small (narrow) proportional band corresponds to a large controller gain, while a large (wide) PB value implies a small value of K . Fig. 2.13 shows a proportional band setting of 5 %. In this example, a small change in temperature provides a large change in output. If the weighting is too small for the process dynamics, oscillations will occur and will not settle at setpoint. Typically, flow or pressure controllers have a much larger proportional setting due to a possible narrower measurement range and a faster process reaction to a change in the control output.

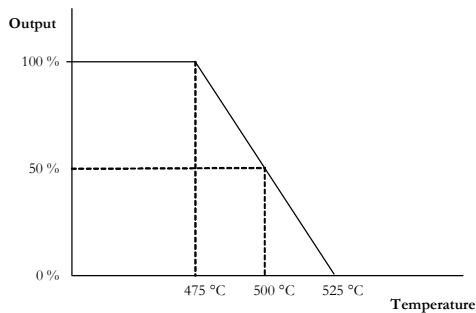


Figure 2.13: Example of a proportional band controller. Setpoint = 500 °C. Measurement range = 0-1000 °C. 5 % PB = 5 % of 1000 °C = 50 °C. 100 % output at 475 °C. 0 % output at 525 °C.

Integral control action is widely used because it provides an important practical advantage: the elimination of offset. While the elimination of offset is usually an important control objective, the simple integral controller is seldom used by itself because a consequent control action only comes into play after the error has persisted for some time. Consequently, integral control action is normally employed in conjunction with proportional control as the popular proportional-integral (PI) controller.

However, an inherent disadvantage of integral control action is a phenomenon known as *reset windup*. It typically occurs when a PI or PID controller encounters a sustained error, for example, during the start-up of a batch process or after a large setpoint change. It can also occur as a consequence of a large sustained load disturbance that is beyond the range of the manipulated variable. Fig. 2.14 shows a classic response to a step change in setpoint when a PI controller is used. The large overshoot occurs because the integral term continues to increase until the error signal changes sign at $t = t_1$. The integral term begins to decrease only after that point.

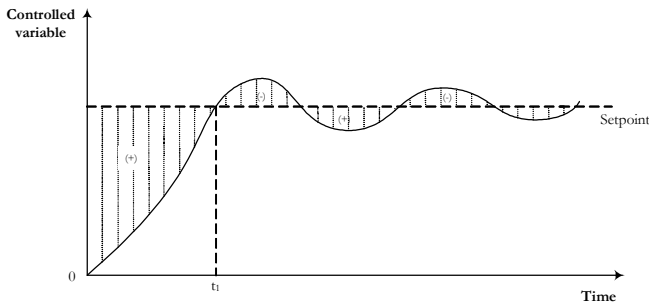


Figure 2.14: Reset windup during a setpoint change, inspired by Seborg et al. [95]. The integrated error corresponds to the dashed area.

Clearly, it is undesirable to have the integral term continuing to build up after the controller output saturates since the controller is already doing all it can to reduce the error. Fortunately, commercial controllers are available which provide *antireset windup* to reduce reset windup by temporarily halting the integral control action whenever the controller output saturates.

2.3.5 Cascade control

A disadvantage of conventional feedback control is that corrective action for disturbances does not begin until after the controlled variable deviates from the setpoint. An alternative approach which improves the dynamic response to load changes is the use of a secondary measurement point and a secondary feedback controller, the so-called cascade control. This method has two aims:

- to eliminate the effects of disturbances
- to improve the dynamic performance of the control loop

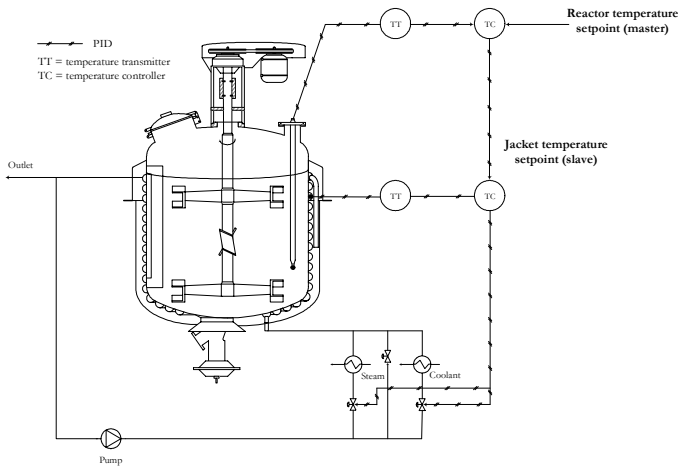


Figure 2.15: Cascade control of a chemical reactor.

Fig. 2.15 illustrates a common system where cascade control is used. Note that the two feedback control loops are nested, with the *secondary control loop* (slave) located inside the *primary control loop* (master). Seborg et al. [95] well describe the advantage of this controller: «The simplest control strategy would handle disturbances (such as reactant feed temperature or composition) by adjusting a control valve on the steam or coolant temperature. However, for example, an increase in the inlet cooling water temperature may cause unsatisfactory performance. The resulting increase in the reactor temperature, due to a reduction in heat removal rate, may occur slowly. The cascade control approach measures the jacket temperature, compares it to the setpoint, and uses the resulting error signal as the input to a controller for the cooling water, thus maintaining the heat removal rate from the reactor at a constant level.» For example, the reaction calorimeter RC1[®] uses a cascade control loop to maintain the reaction mixture temperature.

2.3.6 Advanced control systems

- Lyapunov exponents

Chapter 2.3.3 (page 29) showed that for certain operating conditions, the behaviour of reactors becomes very sensitive to small variations in the inlet conditions. This sensitivity to initial conditions is a well-known characteristic of chaotic phenomena. Chaos arises from the exponential growth of an infinitesimal perturbation. This exponential instability is characterised by the

spectrum of a mathematical tool called the «Lyapunov exponents». The Lyapunov exponents measure the average attraction of an invariant set. In particular, they measure the feasibility to predict the behaviour of the system by quantifying the average rate of convergence or divergence of nearby trajectories. A positive exponent implies divergence, a negative one convergence and a zero exponent indicates the temporally continuous nature of a flow. Consequently a system with positive exponents has positive entropy, in that trajectories that are initially close together move apart over time. The more positive the exponent, the faster they move apart.

To obtain the Lyapunov exponents from a system with known differential equations, one needs to [96]:

- calculate the Jacobian from the differential equations
- calculate the eigenvalues of the Jacobian
- average over n steps to obtain Lyapunov exponents.

If differential equations are not known, which is often the case in real world situations, the exponents must be calculated from a time series of experimental data, which is a more complex problem. Notably, in 1994, Strozzi et al. used Lyapunov exponents to calculate the parametric sensitivity of batch [97] and later of semi-batch reactors [98].

- Neural networks

Neural networks (NNs) are based on the architecture of the mammalian brains. They are composed of simple elements operating in parallel. Rather than using a digital model, in which all computations manipulate zeros and ones, a neural network works by creating connections between processing elements, the computer equivalent of neurons. Commonly neural networks are adjusted, or trained, so that a particular input leads to a specific target output (see Fig. 2.16). The network is adjusted, based on a comparison of the output and the target, until the network output matches the target. Batch training of a network proceeds by imposing weight and bias changes based on an entire set of input vectors. There is an extensive variety of neural networks being studied or used in practice. However, the most widely used is back-propagation [99].

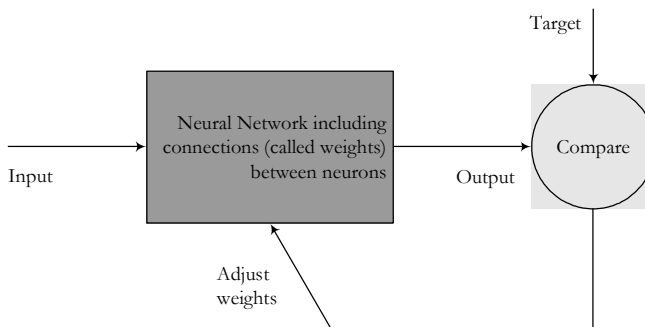


Figure 2.16: Schematic representation of neural networks (after [100]).

In the field of chemical engineering and particularly in temperature control, neural networks have generated a great interest in the last fifteen years: first, they may result in a better processing of problems with a large amount of data; second, a neural network can be used directly as a controller: it computes the control variable to be applied to the process.

The first paper dealing with neural network as a tool for temperature control is that of Zaldivar et al. [101], in 1992. They discussed the use of NNs for the adaptive control of temperature in a jacketed vessel in which an exothermic reaction took place. The classical temperature control algorithm of the Mettler Toledo RC1[®] reaction calorimeter has been substituted by a multilayer neural network interacting with the simulator of the RC1[®]. The authors concluded that neural networks could be able to predict the behaviour of non-linear systems, such as those found in batch and semi-batch processes. The co-workers also published more recent applications of neural networks in chemical engineering [102-104].

Cabassud's group from Toulouse also worked on NNs and their application in temperature control. In 1995, they presented the implementation of networks for the control of a semi-batch pilot-plant reactor equipped with a monofluid heating/cooling system [105, 106] and a year later for a batch process [107]. Conceptually, at time t , the network inputs correspond to the available information on the reactor, i.e. past and present temperatures and control variables. The neural model computes the reactor temperature at the next sampling time. The authors concluded that NNs could be very useful in industrial cases where the complexity of the dynamic model is such that it is impossible to be run on-line.

2.4 Thermal reaction engineering

Once a specified heating/cooling system and an efficient temperature control have been chosen for a given industrial reactor, one can concentrate on the thermal course of a chemical reaction. It is often the only degree of freedom at chemical engineers' disposal in order to fulfil the quality and safety requirements. Mainly, four different thermal strategies can be applied. They are briefly described below.

2.4.1 Isothermal control: $T_r = \text{const}(t)$

- Isothermal at boiling point

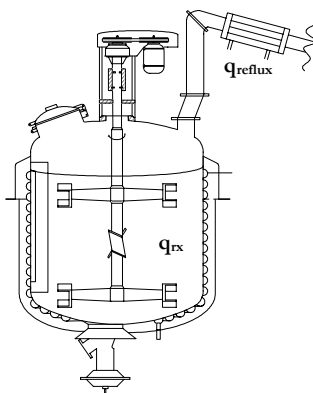


Figure 2.17: Isothermal reaction at boiling point.

• Characteristics

With this system, the temperature is held constant at the boiling point of the reaction medium. The heat excess is removed by a condenser, the liquid flowing back in the medium (Fig. 2.17).

- $T_r = T_b$ self-regulating at constant pressure.
- Boiling power proportional to heat excess.
- Efficient heat removal in the condenser.

• Advantages and disadvantages:

- + inherent temperature limit, well defined
- + efficient cooling power per m^2 (the condenser can be dimensioned independently of the

geometry of the reactor)

- + low-cost system (no temperature regulation needed)
- reaction temperature and system pressure are coupled (if a reaction can not be performed at the boiling point, it is possible to apply a partial vacuum to decrease it and even though work under reflux).

- Isothermal without boiling

With this system, isothermal conditions are guaranteed with the help of temperature measurement of reaction mass, external heating/cooling source and unit control (see Fig. 2.18). The latter adapts the valves opening of coolant or steam by using a conventional P, I, D system. Therefore, the system has to be previously tuned, which can be a very time consuming stage.

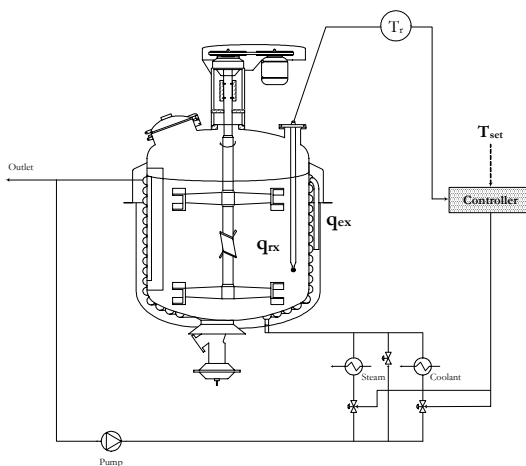


Figure 2.18: Isothermal reaction at $T_r \neq T_b$.

• Needed:

- high power thermostat
- fast control unit
- good heat transfer carrier with a large utilisation range.

• Advantages and disadvantages:

- + T_r is not dependent on the boiling temperature, but is user-defined
- + easily modifiable in adiabatic or isoperibolic conditions thanks to the unit control
- expensive and complicated compared with isothermal at boiling point

- eventually insufficiently isotherm if heating/cooling capacity too low.

2.4.2 Isoperibolic control: $T_j = \text{const}(t)$

With this system, as a matter of fact less and less used as it, only the jacket temperature is controlled and held constant with the help of a control unit. This means that the surrounding temperature of the reaction mass does not vary over time. Compared with the previous mode, the tuning is easier and faster.

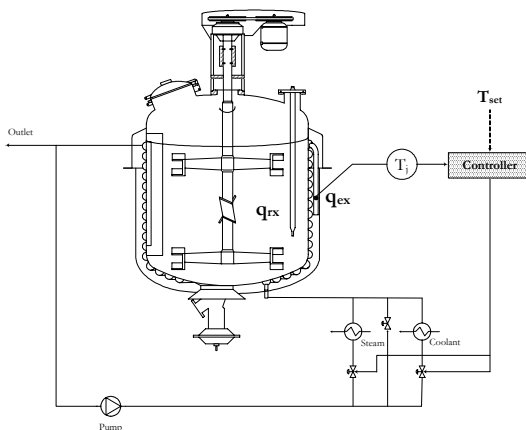


Figure 2.19: Reaction under isoperibolic conditions.

- *Ways of achievement:*
 - thermostatic double mantle (see Fig. 2.19)
 - oil or water bath
 - poorly or not isolated in the ambient air with temperature considered as constant.
- *Key parameter:*
 - The time constant of heat exchange, τ_r , gives an indication of the time needed to heat or cool the reactor (for more details, see also p. 72):

$$\tau_r = \frac{m_r \cdot C_{p_r}}{U \cdot A_{tot}} \quad (2.18)$$

2.4.3 Adiabatic control: $q_{\text{ex}} = 0$

- Adiabatic reaction

With this way of performing a reaction, the temperature of the environment is the same as the one of the reaction mass. This means that both T_r and T_j have to be measured, unless the reactor is perfectly isolated. It goes without saying that for elementary safety reasons, it is necessary to estimate the order of magnitude of exothermic effects beforehand by means of isothermal experiments or other methods.

- *Are adiabatic:*

- isolated reactors, with ideally no heat exchange
- large reactors, with a small heat exchange area per volume of reaction ratio
- fast reactions, for which the accumulated heat cannot be removed.

- *Advantage:*

+ Conversion is thermally measurable:

$$X = \frac{T(X(t)) - T(X_0)}{\Delta T_{ad}} \quad (2.19)$$

- Adiabatic regulation

With this mode T_r follows the reaction profile. T_j is adjusted so that heat generated by the reaction is conserved within the system (see Fig. 2.20). In addition, the heat absorbed by the inserts should be compensated by the control system. This allows the adiabatic profile of a reaction to be investigated. It should be mentioned that this type of regulation is especially used in reaction calorimetry rather than at industrial scale.

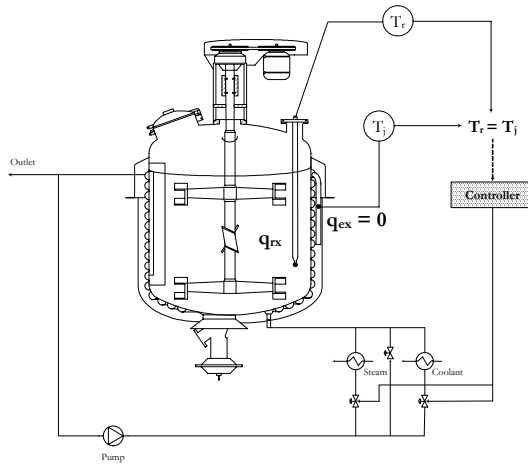


Figure 2.20: Reaction under adiabatic conditions.

- *Criterion:*

- $T_j - T_r = 0$: the jacket temperature follows that of reaction mass, thus behaving as an insulated vessel.

- *Needed:*

- high power thermostat
- fast control unit for T_j to rapidly adapts itself.

- *Advantage and disadvantages:*

- + easily modifiable in isothermal, isoperibolic or even temperature programmed
- expensive and complicated
- unstable control unit (risk of runaway), thus seldom used.

2.4.4 Programmed temperature control: $T_{set} = \text{Progr}(t)$

This system is the most complicated one, but also the most versatile one (in fact, with this type of system, all the previous modes are accessible without further modifications). The setpoint temperature corresponds to a predefined function of time (see Fig. 2.21). Sometimes, polytropic conditions are achieved: the reactor is heated up at a temperature lower than that of reaction; it is

then run under adiabatic conditions; finally, the cooling is started up to stabilise the temperature at the desired level. By doing so, energy is saved because it is the heat of reaction that allows to attain the process temperature. Moreover, for batch reactions, the cooling capacity is not oversized since the low temperature at the beginning of reaction diminishes the heat production rate.

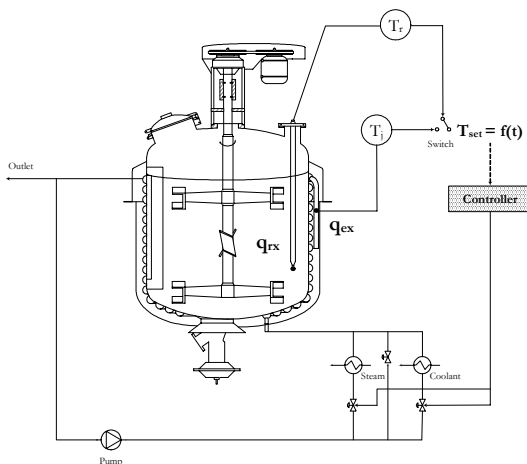


Figure 2.21: Reaction under programmed temperature conditions.

• *Needed:*

- high power thermostat
- fast control unit
- good heat transfer carrier.

• *Characteristics:*

- direct temperature control: T_r -mode (control of reaction medium temperature)
- indirect temperature control: T_j -mode (control of jacket temperature).

• *Advantage:*

- + T_r is adaptable to the conversion that takes place, if combined with on-line analytical technics.

Chapter 3

MODELLING OF INDUSTRIAL REACTORS DYNAMICS

3.1 Aims and strategy

Due to *cultural* and *historical* reasons, reactor sizes, types and heat exchange systems found in the pharmaceutical and fine chemical companies are very eclectic. Therefore, with the goal to be as general as possible, the dynamic behaviour of a large choice of different reactors was modelled. They mainly differ in sizes, materials and control systems. Even if sophisticated methods for the control and optimisation of batch and semi-batch reactors exist, such as the use of extended Kalman filters for parameters estimation, the approach utilised here bases its argument only on classical heat balance equations. There are two reasons: first, for most of the industrial reactors, for which time constants are normally in the order of several minutes or even hours, the use of closed-loop identification tools instead of simple open-loop prediction is not inevitably justified [72]; second, the role of the dynamics identification used here is rather to predict and optimise the thermal behaviour at laboratory scale than to update on-line the control strategy.

Besides, the use of classical heat balance equations is a more general approach. Thus, the same methodology of dynamics identification could be applied to the whole set of reactors studied. Moreover, even if the more elaborated techniques described above have clearly demonstrated their efficiency, examples of their implementation on production reactors remain scarce. The reason is that the industrial environment is always careful and prefers to keep using well-established techniques as long as the advantages of new methods are not clearly demonstrated. Indeed, a new process usually becomes profitable several weeks or even months after its installation, first because

granted investments need to be written off and second because the staff has to grow familiar with it. Therefore, it is often not compatible with the today's short term profits vision. Thus, as this thesis deals with applied research and as it was always intended to commercialise the developed products, it seemed that the use of conventional and largely widespread heat balance equations was relevant. Therefore, the experimental work was limited to the identification of two models: the most simple and most frequently used one with an overall heat transfer coefficient and the second one, that describes the jacket temperature dynamics.

The experiments performed to characterise the heat transfer dynamics should also be simple and applicable to all industrial reactors. The reasons are also two-fold: as mentioned previously, the purpose is to develop an easy and fast methodology, but also because of the short time available to conduct the experiments. Indeed, the current competition is such that a production reactor remains rarely unemployed. It was then decided to realise simple heating/cooling experiments with a set mass of liquid with known physical and chemical properties (see § 3.3, p. 56 for the experimental part).

The next chapter describes in details the equations and the identification employed. After that, the results for the nine studied industrial reactors are presented.

3.2 Modelling - general equations

3.2.1 Mass balance

The amount of product remaining constant and no reaction taking place during the performed experiments, the mass balance is trivial because there is no variation. The only side effect that could have been taken into account is the solvent evaporation at high temperature. However, since reactors were always equipped with condensers and since in any case temperature always remained at least 20 °C below boiling point, solvent evaporation has been neglected.

3.2.2 Heat balance - Reactor temperature

Heat can be exchanged in a reaction mixture by various mechanisms. The general equation describing the energy balance over a reactor is:

$$\left(\sum_i m_i \cdot C_{p_i}' + C_w \right) \cdot \frac{dT_r}{dt} = q_{rc} + q_{ds} + q_{mix} + q_{st} + q_{ex} + q_{loss} + q_{reflux} \quad (3.1)$$

For the experimental simulation of the dynamic behaviour of industrial reactors, since no reaction (q_{rx}) and no dosing (q_{dos}) take place, no mixing (q_{mix}) and no reflux (q_{reflux}) powers are produced, Eq. 3.1 was then simplified as follows:

$$\left(m_r \cdot C_{p_r}'(T_r) + C_w\right) \cdot \frac{dT_r}{dt} = q_{ex} + q_{st} + q_{loss} \quad (3.2)$$

The next sections present a detailed description of each term of Eq. 3.2 as well as the potential difficulties that can be encountered during their evaluation.

- m_r

m_r is the mass of liquid that is introduced in the reactor. Most of the time it has been weighed, but sometimes also calculated from the measured volume. At the end of each experiment, the remaining amount was weighed again. The losses (due principally to evaporation) were at the most equal to 0.7 % of total mass. m_r can therefore be considered as constant and measured very accurately.

- C_{p_r}'

The specific heat capacity is known to depend on the temperature. To this end, various bibliographic sources were used:

- VDI Wärmeatlas [108]
- McGraw-Hill Handbook [109]
- NIST standard reference database [110]
- Aspen Properties[®] [111]
- Component Plus[®] [112]
- Internal data bank from diverse chemical companies

A polynomial fit (4th order) through the data given for different temperatures allows to obtain $C_{p_r}' = f(T_r)$.

- C_w

The mean heat capacity of the reactor corresponds to:

$$\sum_i m_w^i \cdot C_{p_w}^i \quad (3.3)$$

i.e. the product of the mass and the specific heat capacity of the i th element that follows the evolution of T_r . $C_{p_w}^i$ can easily be found in the literature for the known material(s) of the reactor contents [108]. On the contrary, m_w^i is much more difficult to evaluate. For the simulation, this parameter was assumed to be the result of two contributions:

- The mass of the reactor wall that is wetted by the utility fluid. This mass is the product of the maximum heat exchange area (given by the manufacturer) and the wall thickness, plus the total coil, respectively jacket, mass in contact with the reactor. It is considered as constant since the utility fluid always flows inside the entire coil or jacket.
- The sum of the various masses of inserts that plunge into the reaction mixture (such as stirrer, temperature probe, baffles). It depends on the mass of liquid introduced and for a given mass on the stirrer revolution speed. The dependency on the temperature has been neglected. Only a visual evaluation allows the determination of these masses. Although accuracy is moderate (the liquid reaches a certain height of the stirrer, but it is not exactly known to what percentage of the total mass it corresponds), the value is small compared with the wetted mass of the reactor (10 % at the most).

Note that this total wetted mass is much smaller than the total mass of the reactor, particularly for large vessels. For example, for a 630 L reactor, it corresponds to solely 17 %. Note also that the larger the reactor, the smaller the contribution of the reactor itself, C_m , to the total heat capacity (reactor and reaction mixture). As an indication, it represents 16 % for a 40 L reactor, 2 % for a 630 L reactor, and 0.7 % for a 25 m³ reactor, all of them full of water.

- dT/dt

The temperature variation of the reactor content, as well as the jacket inlet, and sometimes outlet, temperatures are followed by Pt-100 probes. Their tolerance was studied for one industrial reactor and ± 1 % of the measuring range was given by the manufacturer, which corresponds to a precision of ± 3 °C. However, at the time of their last calibration, their effective error was less than ± 1 °C. This precision was assumed to be the same for other reactors. Moreover, $T_{j,in/out}$ may be measured several meters away from the exact inlet or outlet jacket point. A simple losses evaluation between these two points allows saying that the possible difference can be neglected.

The sampling time is either chosen by the user or set automatically. It usually ranges between 5 and 30 seconds.

- q_{st}

In the agitation field, the power supplied by the stirrer to the reaction mixture is calculated with the power equation [61, 113]:

$$q_{st}(T_r) = Ne \cdot \rho_r(T_r) \cdot N^3 \cdot d^5 \quad (3.4)$$

The power number Ne depends on the geometry, the Reynolds (Re) and Froude (Fr) numbers. Generally, the effect of the Froude number is negligible in the case of fully baffled vessels (no vortices). Fundamentally, three different types of flow, expressed by the Reynolds number, are distinguished:

- $Re < 10$: laminar flow, Ne is proportional to Re^{-1}
- $10 < Re < 10^4$: transition range
- $Re > 10^4$: turbulent flow, where the power number stays constant, i.e. independently of variations of the Reynolds number

Note that all experiments were conducted under turbulent conditions, so that Ne was only dependent on the stirrer type. However, it is important to keep in mind that q_{st} can appreciably vary. In water: for an impeller with diameter of 25 cm and stirrer revolution speed of 80 rpm, $q_{st} = 0.5$ W, whereas for an Intermig[®], diameter 70 cm and 170 rpm, $q_{st} = 2'500$ W, and for a Mig[®], diameter 1.9 m and 50 rpm, $q_{st} = 7'900$ W.

Table 3.1 summarises the features of the most common stirrers (see page 49 for a description of parameter C):

Table 3.1: Nusselt & Newton constants of various mixing designs [17, 113-116].


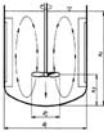




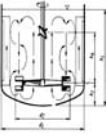

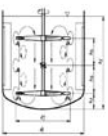

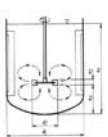

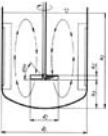

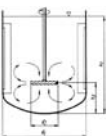

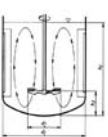

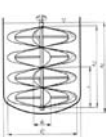
Stirrer type	Scheme	Flows	C [-]	Ne turbulent [-]	Features & typical uses
Propeller			0.54 ^[114, 117] 0.46 ^[116]	0.35 (3 blades) 0.85 (5 blades)	Is an axial-flow stirrer. Acceleration of the liquid takes place at the propeller level. Is typically used for low- to medium-viscosity media, preferably with three blades.
Impeller		Not available	0.33	0.20	Stirring device with three curved stirring arms arranged at an angle. The stirring action depends upon a radial flow, which is reversed axially by the arrangement of the stirrer close to the bottom. Application: homogenising
Anchor			0.36	0.35	This close-clearance stirrer has a stirrer to vessel diameter ratio between 0.9 and 0.98. Its main function is to reduce the thickness of the highly viscous boundary layer at the vessel wall, intensifying heat transfer.

Table 3.1: Nusselt & Newton constants of various mixing designs [17, 113-116].

Stirrer type	Scheme	Flows	C [-]	Ne turbulent [-]	Features & typical uses
Intermig [®]			0.54 (2 stages)	0.65 (2 stages)	For low to medium product viscosities. Homogeneous dissipation of introduced energy. High axial flow velocities, therefore increased heat transfer and reduced scaling at vessel wall.
Mig [®]			0.42 (2 stages) 0.46 (3 stages)	0.55 (2 stages)	Successful as a suspension stirrer in vessels up to 3000 m ³ . Has two blades of opposed blade angle on a single radial arm. Provide excellent blending of highly viscous media.
Flat-blade disk turbine			0.54 ^[71, 114, 117] 0.87 ^[116]	4.60 (6 blades)	Is a typical example of a radial-flow stirrer. The turbine's actual mixing effect occurs predominantly in the shear zone of the radially emerging jet. Is frequently used for gassing applications.
Pitched-blade disk turbine			0.53 ^[117] 0.61 ^[116]	0.60 (4 broad blades) 1.2 (6 narrow blades) 2.0 (6 broad blades)	Compared with the propeller, the flow pattern induced has a stronger radial component. This stirrer is capable of handling media with viscosities up to 50'000 mPa's and can thus be used in both the laminar and the turbulent flow range.
Disperser disk			Not found	0.20	Exerts high local shear forces due to the special tooth shape. Highly concentrated energy dissipation. Suitable for non-Newtonian media in combination with an axial pumping impeller.
Interprop [®]			0.52	Not found	Intensified axial impulse by increase of the impeller blades' angle of attack. Performs exceptionally well in blending applications and ones calling for efficient heat transfer.
Helical-ribbon			0.52	Only laminar flow	For extremely high viscosities (laminar flow regime) High specific torques can be introduced. Adaptable for the process/product (many different shapes, angles and pitches are possible).

- q_{ex}

The power transferred to or from the utility fluid, q_{ex} , can be calculated by two different approaches [16]:

- the so-called «heat balance» approach:

$$q_{ex} = U \cdot A_{lat} \cdot \Delta T_m \quad (3.5)$$

- the so-called «heat flow» approach:

$$q_{ex} = \dot{m}_j \cdot C p_j' \cdot (T_{j,in} - T_{j,out}) \quad (3.6)$$

In the present work, the first equation has been employed, since the second one requires the measurement of the mass flow rate of heat carrier fluid, which was available only for the two smallest industrial reactors. The various terms of Eq. 3.5 are shortly described below.

- U

The overall resistance of the heat transfer between the reaction medium and the cooling liquid, $1/U$, is the sum of three elements (see also Fig. 2.4, p. 19):

$$\frac{1}{U} = \frac{1}{h_r} + \frac{d_w}{\lambda_w} + \frac{1}{h_j} = \frac{1}{h_r} + \varphi \quad (3.7)$$

The heat transfer coefficient due to the reaction mixture, h_r , is calculated by combining the Nusselt correlation and the Nusselt number. As for the heat transfer of a fluid flowing in a pipe, there exists a correlation between the Nusselt, Prandtl and Reynolds criteria that applies to stirred tank reactors [64]:

$$Nu = C \cdot Re^{2/3} \cdot Pr^{1/3} \cdot \left(\frac{\mu_r}{\mu_w} \right)^{0.14} \quad (3.8)$$

The last term of Eq. 3.8, which is the ratio of the dynamic viscosities, can generally be neglected for media with low viscosity. Substituting the definitions of the Nusselt, Prandtl and Reynolds numbers into Eq. 3.8 leads to:

$$h_r(T_r) = C \cdot \underbrace{\frac{N^{2/3} \cdot d^{4/3}}{D \cdot g^{1/3}}}_{\text{technical data of the reactor}} \cdot \underbrace{\sqrt[3]{\frac{\rho_r(T_r)^2 \cdot \lambda_r(T_r)^2 \cdot C p_r'(T_r) \cdot g}{\mu_r(T_r)}}}_{\text{physical and chemical data of the reaction mass}} = \gamma \cdot \gamma \quad (3.9)$$

As for C_p , $\rho(T_p)$, $\lambda(T_p)$ and $\mu(T_p)$ are obtained from a polynomial fit (4th order) of the literature values. The parameter C depends on the stirrer type as shown in Table 3.1, p. 47.

The resistance of the reactor wall is easily calculated, knowing its thickness and its thermal conductivity. The following table indexes the main materials found in fine chemical industries.

Table 3.2: Density and thermal conductivity of various materials [108].

Type	DIN norm	AISI norm	ρ at 20 °C[kg m ⁻³]	λ at 20 °C[W m ⁻¹ K ⁻¹]
Steel	1.0425	-	7'850	55
Stainless steel	1.4301	304	7'900	14.9
Stainless steel	1.4306	304 L	7'900	16.9
Stainless steel	1.4401	316	7'950	15.3
Stainless steel	1.4435	316 L	7'950	15.3
Stainless steel	1.4571	316 Ti	7'980	13.0
Enamel	-	-	2'300 to 2'500	0.9 to 1.2
Glass	-	-	2'500 to 2'800	0.8 to 1.2

The external film coefficient h_j is in the core of the whole identification methodology. Although, as for h_p , some correlations exist [113], they are valid only for the same class of reactor (geometry, type of coils or double mantle, etc.). It has therefore been decided to take an empirical model and then to identify, by means of a least-square fit, the parameters p_1 and p_2 of this model:

$$h_j(T_j) = p_1 \cdot T_j + p_2 \quad (3.10)$$

This model is simple. Indeed, it is not relevant to identify more than two parameters when relative great uncertainties are associated with Eq. 3.2 and when less than ten experiments are conducted in the same reactor.

Note that this simple equation is used in simulation programs such as Visimix[®] [118], BatchReactor[®] [112] as well as in de Vallière's thesis [71]. Moreover, the plot of the Nusselt correlation (Eq. 3.9) with respect to temperature is close to linear between 5 to 95 °C.

$$\bullet A_{lat}$$

The heat exchange area is the sum of three contributions:

$$A_{lat} = A_{bottom} + A_{side} + A_{roft} \quad (3.11)$$

When the stirrer is idle, A_{lat} can easily be determined: the area of the bottom depends on the geometry of the reactor and is generally given by the manufacturer or can be calculated with the formula of a revolution corpse (see Fig. 3.1):

$$A_{bottom} = 2 \cdot \pi \cdot \int_{x_1}^{x_2} f(x) \cdot \sqrt{1 + f'(x)^2} dx \quad (3.12)$$

with $f(x)$ describing the form of the base (flat, spherical, torispherical, conical, toriconical, ellipsoidal or hemispherical).

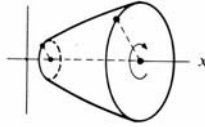


Figure 3.1: Revolution corpse turning around its axis.

The remaining side area depends on the mass of reaction medium introduced at time t , its density, which is function of the temperature, and on the reactor diameter.

The prediction of the increase in heat exchange area due to vortex formation was subject to intense research. Several models exist [117, 119, 120], but all of them predict only the vortex depth or volume, and not the liquid level increase at the reactor wall.

An easy-to-use equation, based on the law of conservation of energy, gives a first estimate:

$$h_{vort} = \frac{N^2 \cdot D^2}{8 \cdot g} \quad (3.13)$$

And hence:

$$A_{vort} = \pi \cdot D \cdot h_{vort} \quad (3.14)$$

This correlation is valid only for Newtonian fluids with no vertical or radial velocity. However, experimental results have shown that the increase of heat exchange area is dependent on the liquid volume, type of agitator and physical and chemical properties of the reaction mixture.

A more elaborate equation, according to Uhl & Gray [65], includes the Froude number, which describes the ratio of inertial to gravitational forces, and a function $g(V_p)$ that depends on the volume of the reaction mixture, V_p , and the total reactor volume, V_{tot} :

$$\mathcal{A}_{vort} = C_1 \cdot Re^{C_2} \cdot Fr^{C_3} \cdot N^2 \cdot g(V_r) \quad (3.15)$$

$$g(V_r) = \left(\frac{V_{in} - V_r}{V_{in}} \right)^{C_4}$$

Zaldivar [121] proposes to fit the experimental data in order to find C_1 to C_4 . However, for the experiments performed during this thesis work, this approach could not be used because it would have necessitated the handling of different fluids and stirrers, the modification of the liquid volume, the temperature and the stirrer revolution speed. And as said previously, the time at disposal to perform these experiments was very short.

Another alternative to calculate the vortex formation is to use dedicated software such as Visimix[®] [118]. Unfortunately, this solution is not the panacea:

- All reactor shapes are not included in the software's library. Included configurations can not be completely defined by the user: e.g. conical bottom with cone angle limited to 60 °.
- All stirrer types are not included in the software's library. Included types can not be completely defined by the user: e.g. number of stages depending on the liquid level.

In conclusion, in our experience nothing can fully replace experimental evaluations to determine the increase of heat exchange due to vortex formation. This remark is especially true for complex configurations such as multi stages agitators, for which all equations and correlations described above give lower h_{vort} than they actually are.

- ΔT_m

The driving force of the heat transfer, the temperature difference between the reaction mixture and the utility fluid, ΔT_m , is computed by the following formulae:

- logarithmic mean:

$$\Delta T_m = \frac{(T_{j,in} - T_r) - (T_{j,out} - T_r)}{\ln \left(\frac{T_{j,in} - T_r}{T_{j,out} - T_r} \right)} \quad (3.16)$$

- arithmetic mean:

$$\Delta T_m = T_j - T_r \quad (3.17)$$

with $T_j = (T_{j,in} + T_{j,out})/2$.

- q_{loss}

The heat losses depend on the temperature difference between the system and the surroundings, and also on the system isolation. It can therefore be evaluated using the same approach as for the heat transfer between the jacket and the reaction medium:

$$q_{\text{loss}} = U_{\text{loss}} \cdot A_{\text{loss}} \cdot (T_{\text{amb}} - T_r) \quad (3.18)$$

U_{loss} is evaluated by using the same approach as for Eq. 3.7 by replacing h_j by the outside heat transfer coefficient for air [108]:

$$h_{j,\text{air}} = 8 + 0.04 \cdot (T_w - T_{\text{amb}}) \quad (3.19)$$

For reactor R₇ (see § 3.7, p. 69), q_{loss} was evaluated using an experiment with the coils emptied. The stirrer was switched on and the temperature evolution recorded. At 115 rpm, the temperature of the 6'300 kg of water introduced increased by 2.1 °C within 12 h, which corresponds to an average power of ~1'280 W; at this stirring velocity, the average power released by the agitator is, according to Eq. 3.4, of ~1'954 W. Thus, the losses amounted to ~674 W. By carrying out the same calculation for the two other stirrer speeds employed, the losses amounted to ~352 W and ~379 W at 20 and 65 rpm respectively. The tendency was explained by the increase of heat transfer surface at high stirrer revolution speed. Finally, the average value of 470 W was used in the equations. It is important to compare it with that exchanged through the coils, q_{ex} . The latter can reach, during the heating and when the difference in temperature between utility fluid and water was maximum, an approximate value of 300'000 W. That confirms, if needs be, that for reactors of this size, the losses could be neglected.

3.2.3 Heat balance - Jacket temperature

The jacket temperature has also its own dynamics that depends on the heating/cooling device employed, on the temperature controller and on the physical and chemical properties of the heat carrier fluid. This temperature appearing in the heat transfer model (see Eqs. 3.10-3.16-3.17), it is necessary to take it into account in order to completely characterise the heat transfer dynamics. In fine chemical, pharmaceutical or polymer industry, most of the industrial reactors are thermally controlled by changing the inlet temperature of an intermediate fluid flowing inside the jacket surrounding the reactor. As a whole, the major difference between set up systems is the direct or indirect heating/cooling (see § 2.2, p. 24). Once again, for both cultural and historical reasons, Swiss fine chemical companies use different strategies to control the jacket temperature. The

cascade controller is probably the most common one: the temperature adjustment for the indirect system is performed measuring the inner reactor and outlet fluid temperatures using two feedback control loops. Moreover, most of the systems are able to work at either controlled internal temperature (T_r -mode) or controlled external temperature (T_j -mode).

A complete description of the jacket dynamics would include two more equations:

$$m_j \cdot C_{p_j} \cdot \frac{dT_j}{dt} = \dot{m}_j \cdot C_{p_j} \cdot (T_{j,in} - T_{j,out}) - U \cdot A_{int} \cdot \Delta T_m + q_{loss} \quad (3.20)$$

in order to compute T_j and:

$$m_{j,in} \cdot C_{p_j} \cdot \frac{dT_{j,in}}{dt} = q_{excl} + q_{loss} \quad (3.21)$$

in order to compute $T_{j,in}$. $m_{j,in}$ and q_{excl} are the mass of utility fluid heated or cooled inside the heat exchanger and the power provided by the power device (electrical element, steam, cold water, brine,...) respectively.

The output values of the controller, the valves position of the heating/cooling device and above all the mass flow rate of utility fluid being very rarely recorded, and in order to use the same type of equations for all industrial reactors studied, the evolution of the jacket temperature T_j was modelled as two consecutive first-order systems. Two orders are necessary because all studied reactors have a PB controller (see p. 31 for a description of a PB). Fig. 3.2 shows the response of the jacket temperature to two setpoint changes. When the actual jacket temperature is far enough from its setpoint, the controller output is at its maximum value, implying a faster heating or cooling; then, when approaching the setpoint, the temperature evolution acts like a first order model.

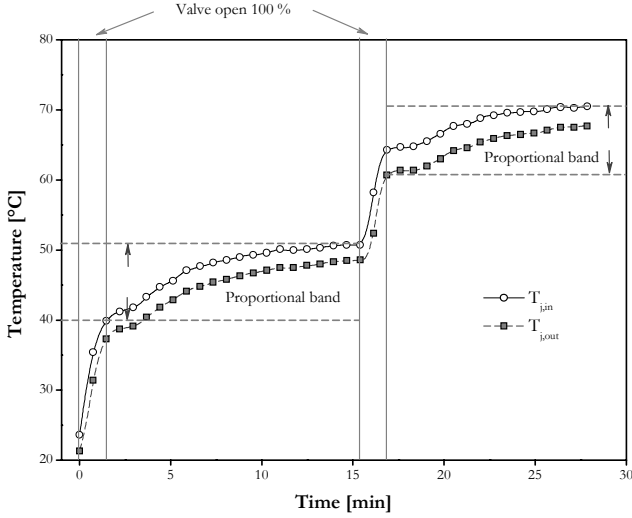


Figure 3.2: Example of a proportional band of a cascade controller installed on a 630 L reactor, in T_j -mode. From t_0 to $t = 16$ min, $T_{j,set} = 50$ °C, then $T_{j,set} = 70$ °C. The two vertical bands represent zones where the steam valve is completely open, meaning that the controller output saturates.

Therefore, the dynamics of the jacket temperature has been modelled as:

- during the heating process:

$$\begin{aligned} \text{if } |T_j - T_{j,set}| > p_3 \cdot (T_{j,set} - T_{j,0}) \text{ then } \frac{dT_j}{dt} &= \frac{T_{j,max} - T_j}{\tau_b} \\ \text{else } \frac{dT_j}{dt} &= \frac{T_{j,set} - T_j}{\tau_b} \end{aligned} \quad (3.22)$$

- during the cooling process:

$$\begin{aligned} \text{if } |T_j - T_{j,set}| > p_3 \cdot (T_{j,0} - T_{j,set}) \text{ then } \frac{dT_j}{dt} &= \frac{T_{j,min} - T_j}{\tau_c} \\ \text{else } \frac{dT_j}{dt} &= \frac{T_{j,set} - T_j}{\tau_c} \end{aligned} \quad (3.23)$$

3.3 Experimental part

3.3.1 Standard experiments

Nine industrial reactors have been characterised. The next chapters will describe them in details. However, the procedure employed was the same for all of them. It consisted in special types of heating/cooling experiments allowing the dynamic identification of the heat exchange system. The jacket or vessel content temperature was forced by requesting a step change of the setpoint. Once a measured mass (corresponding to a reactor filling of one third) of an inert liquid with known physical and chemical properties was introduced in the reactor, a complete heating and cooling cycle was performed under agitation and total reflux. Working in T_r -mode (internal temperature controlled), and after a stabilisation phase at low temperature, the setpoint was modified to a temperature about 20 °C below the boiling point of the liquid, followed by about 1 h stabilisation phase at high temperature. Then, the setpoint was changed to a value about 20 °C higher than the fusion point, again followed by about 1 h stabilisation phase, this time at low temperature. This cycle was repeated with the same amount of liquid, with at least one different stirrer revolution speed. Afterwards, the amount of liquid was modified twice (to a filling level of 2/3 and 3/3) and every time, the same heating/cooling cycle was performed as previously described. If the T_r -mode was not available, which was the case for the first series of reactors, the setpoint was set during one cycle to the maximum, respectively minimum possible jacket temperatures the heat transfer system could reach.

This leads to six to nine experiments (according to the number of different stirrer speeds). They allow to characterise the heat transfer between jacket and reaction mixture. A supplementary experiment, called «stair-shape» because of its distinguishing appearance, enables the description of the jacket temperature dynamics. With the industrial reactor being completely filled and working in T_j -mode (jacket temperature controlled), the setpoint is changed in steps of ± 20 °C from the lowest to the highest temperature defined in the previous section. For each setpoint, a ~ 1 h stabilisation phase was observed. Note that this experiment was performed at only one stirrer revolution speed.

During all experiments, the inside reactor temperature (T_r), the jacket inlet ($T_{j,in}$) and, if available, outlet ($T_{j,out}$) temperatures, the stirrer revolution speed (N) as well as the reactor pressure were recorded and registered.

The whole series of experiments performed in the various industrial reactors are given in the appendix A.2, p. 165.

3.3.2 Parameters identification of the dynamic model

The aforementioned complete model, Eqs. 3.2-3.19 and Eqs. 3.22-3.23, was implemented in Madonna[®] [122] and the various parameters of the model ($p_1, p_2, p_3, T_{j,max}, T_{j,min}, \tau_h$ and τ_d) were identified by means of a least-square fit over the measured temperatures using a stiff ODEsolver. An example is given in the appendix A.1, p. 163. The calculation time for a tolerance of 0.001 using a Dell[®] Laptop PC (Intel[®] Pentium[®] M, 1.7 MHz, 768 MB of RAM) is approximately 3 min.

Note that the identification does not consist in finding seven parameters to fit one curve, which will undoubtedly generate parameters correlations. First, for each reactor, the complete set of heating/cooling curves was evaluated simultaneously. Second, p_1 and p_2 appear only in the T_r curve (see Eq. 3.10, p. 50), whereas $p_3, T_{j,max}$ and τ_h come into play only in the heating phase of the *jacket* temperature, and $p_3, T_{j,min}$ and τ_c only in the cooling phase of T_j (see Eqs. 3.22-3.23, p. 55).

3.4 First set of reactors - 40 & 49 L

3.4.1 Features and experiments

The smallest reactors characterised during this study, R₁ and R₂, have the following features:

Table 3.3: Characteristics of industrial reactors R₁ & R₂.

Property	R ₁	R ₂
Nominal volume [L]	40	49
Material	stainless steel	glass + enamel
Reactor diameter [m]	0.40	0.40
Type of stirrer	anchor	impeller
Stirrer diameter [m]	0.35	0.25
Baffles	1	1
Wall thickness [mm]	6.0	13.2 (with enamel)
Working mode	only T_j	only T_j
Utility fluid	oil (Syltherm XLT)	oil (Syltherm XLT)
Shape of bottom	torispherical	torispherical
Heating	thermostat (Huber [®])	thermostat (Huber [®])
Cooling	cryostat (Huber [®])	cryostat (Huber [®])

For these two reactors that can work only in T_f -mode, both water and toluene were used as solvents for the characterisation of the heat transfer dynamics. Moreover, the same kind of heating/cooling cycles described in the previous chapter were applied. During a heating period ($T_{j,set} = 150\text{ }^\circ\text{C}$) and a cooling period ($T_{j,set} = -10\text{ }^\circ\text{C}$ for water and $-50\text{ }^\circ\text{C}$ for toluene) the liquid was heated and then cooled between around 10 and $70\text{ }^\circ\text{C}$ for water and between around -30 and $90\text{ }^\circ\text{C}$ for toluene. Three different masses of liquid and for each of them three different agitator speeds were used. A «stair-shape» experiment with jacket setpoint jumps of $\pm 20\text{ }^\circ\text{C}$ for both water and toluene completed the set of experiments. Tables A.1 & A.2 (see appendix) summarise all performed experiments.

3.4.2 Experimental results

Figs. 3.3 & 3.4 represent typical examples of curves recorded in reactor R_2 . Note that reactor R_1 exhibits comparable results.

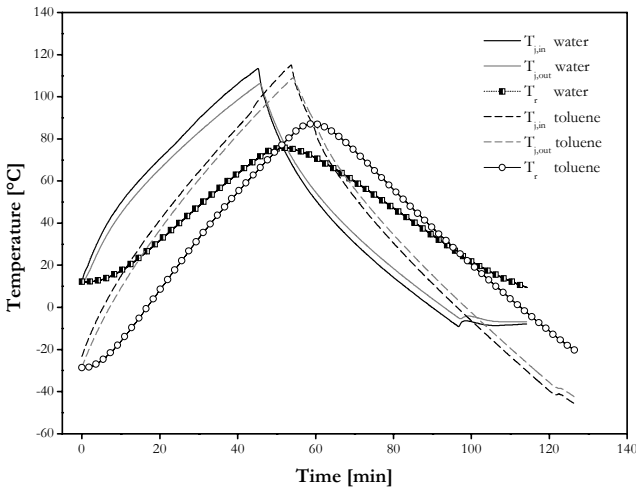


Figure 3.3: Typical heating/cooling curves obtained with reactor R_2 . Lines: jacket inlet and outlet temperatures; ■: recorded temperature of water (15 kg, 240 rpm); ○: recorded temperature of toluene (12 kg, 240 rpm).

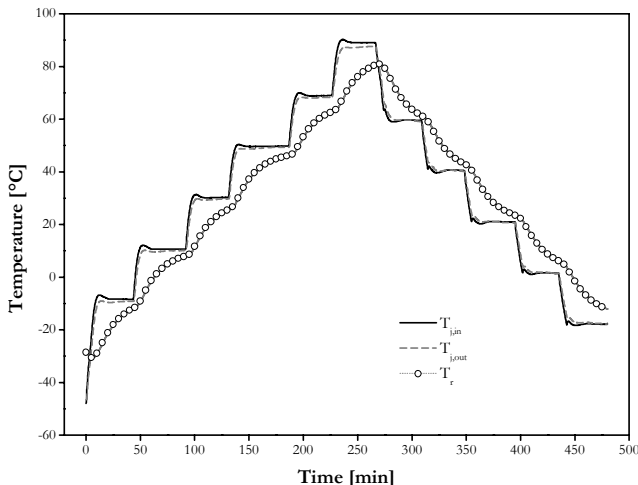


Figure 3.4: Example of a «stair-shape» experiment obtained with reactor R_2 . Lines: jacket inlet and outlet temperatures; \circ : recorded temperature of toluene (27 kg, 80 rpm).

Even if their nominal volumes are small, their heating/cooling dynamics are rather slow. Reactor R_2 heats and cools water at mean rates of 1.3 and 1.1 $^{\circ}\text{C}\cdot\text{min}^{-1}$ respectively and toluene at mean rates of 2.0 and 1.7 $^{\circ}\text{C}\cdot\text{min}^{-1}$. This is not due to the material of the reactor itself or the stirrer, but rather from the installed heating/cooling device: a Huber Unistat[®] thermostat/cryostat with a power of ~ 5.2 kW with oil circulating in loop. Compared to heat exchangers with steam or brine, the available power is much lower. It should also be stated that the mean temperature difference between inlet and outlet jacket temperatures is around 4 $^{\circ}\text{C}$, confirming, if necessary, that the liquid flow rate was sufficiently high and could not be questioned. Note that, as Fig. 3.3 shows, neither the 150 $^{\circ}\text{C}$ setpoint for heating nor the -50 $^{\circ}\text{C}$ setpoint for cooling were attained.

3.4.3 Modelling

The increase in heat transfer area due to the vortex formation has been evaluated visually. Despite the small nominal volumes of these reactors, this parameter was not primordial as for the second set of reactors (see § 3.5.2, p. 64) because of the stirrers configuration (only one stage) and their relatively small diameters. The procedure reaching heat balance was described in § 3.2. However, as it can be seen on Fig. 3.4, the jacket temperature reaches its setpoint in a rather abrupt manner. Consequently, Eqs. 3.22 & 3.23 were slightly modified:

- during the heating:

$$\begin{aligned} \text{if } |T_j - T_{j, \text{set}}| > p_3 \cdot (T_{j, \text{set}} - T_{j, 0}) \text{ then } \frac{dT_j}{dt} &= \frac{T_{j, \text{max}} - T_j}{\tau_b} \\ \text{else } \frac{dT_j}{dt} &= 0 \end{aligned} \quad (3.24)$$

- during the cooling:

$$\begin{aligned} \text{if } |T_j - T_{j, \text{set}}| > p_3 \cdot (T_{j, 0} - T_{j, \text{set}}) \text{ then } \frac{dT_j}{dt} &= \frac{T_{j, \text{min}} - T_j}{\tau_c} \\ \text{else } \frac{dT_j}{dt} &= 0 \end{aligned} \quad (3.25)$$

Surprisingly, the parameter p_l (see Eq. 3.10) identified for reactor R_2 was negative and close to zero ($-0.2 \text{ [W}\cdot\text{m}^{-2}\cdot\text{K}^{-2}]$). At first sight, there is no reason for p_l to be negative because this would mean that the jacket heat transfer would decrease with temperature. As a higher temperature decreases the film thickness because of lower viscosity, the heat transfer resistance is reduced. At the same time, the higher temperature induced a lower mass flow rate of the heat exchange fluid (see Fig. 3.5). Therefore, one can state positively that the effect of the mass flow rate on h_j is slightly higher than that of the temperature, or at least that they compensate each other. Thus, for R_2 , p_l was set to zero.

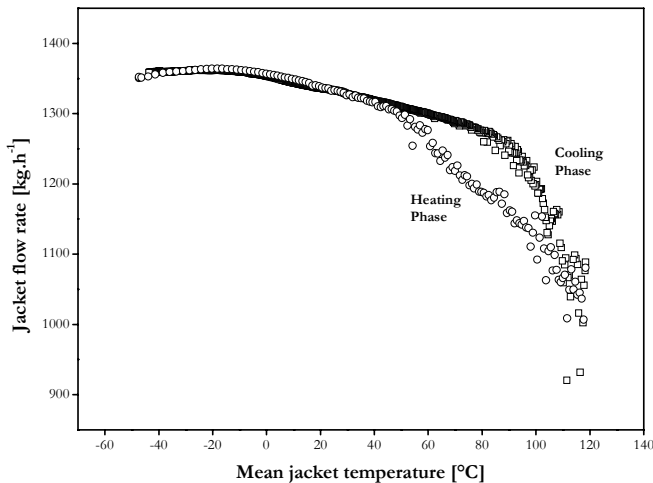


Figure 3.5: Mass flow rate of the heat transfer fluid as a function of the mean jacket temperature.
Example presented: reactor R₂ filled with 27 kg of toluene and 160 rpm.

Table A.10 (see appendix) indexes the identified parameters for these two industrial reactors.

3.4.4 Results

R₁ and R₂ having almost the size of kilo-laboratory reactors, their modelling was subject to small deviations. The neglected secondary effects, mainly the heat losses due to evaporation of the solvent and the cold droplets flowing back in the mixture, lead to small disturbances (see Fig. 3.6a). Therefore the larger the reactor and/or the more fluid quantity introduced, the better modelled the experimental data. However, the reactors being filled at least up to 2/3 during normal production, the model can be considered sufficiently precise.

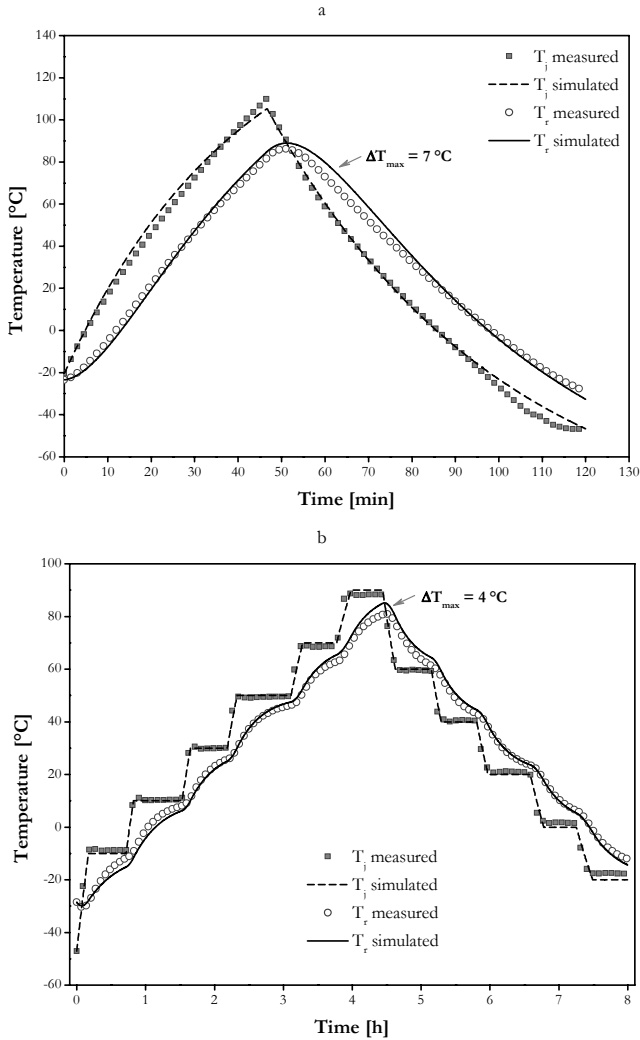


Figure 3.6: Validation of the complete heat balance model for reactor R₂. a: 4 kg of toluene, stirrer revolution speed 120 rpm; b: 30 kg of toluene, 80 rpm, «stair-shape» experiment. For improved clarity, not all experimental points are shown.

Modelling in Fig. 3.6b also exhibits its greatest deviation at high temperature. Even if the temperature was about 20 °C below the boiling point, the high ratio of gas/liquid exchange area to volume was such that evaporation probably already took place. Still, the mean temperature difference of 1.6 °C between the model and the experiment remains reasonable.

3.5 Second set of reactors - 250 to 630 L

3.5.1 Features and experiments

Table 3.4 lists the main features of the second set of industrial reactors characterised, R₃ to R₅:

Table 3.4: Characteristics of reactors R₃, R₄ and R₅.

Property	R ₃	R ₄	R ₅
Nominal volume [L]	250	630	630
Material	stainless steel	stainless steel	stainless steel
Reactor diameter [m]	0.70	1.00	1.00
Type of stirrer	3 stages Intermig [®]	3 stages Intermig [®]	3 stages Intermig [®]
Stirrer diameter [m]	2 x 0.35 / 1 x 0.25	3 x 0.70	2 x 0.50 / 1 x 0.30
Baffles	2	2	2
Wall thickness [mm]	5	5	5
Working modes	T_r or T_j	T_r or T_j	T_r or T_j
Utility fluid	H ₂ O / ethylene glycol	H ₂ O / ethylene glycol	H ₂ O / ethylene glycol
Shape of bottom	conical	torispherical	conical
Heating (indirect)	steam 12 bar	steam 12 bar	steam 12 bar
Cooling (indirect)	cold water / brine	cold water / brine	cold water / brine

As for reactors R₁ and R₂, both water and toluene were used as solvents and the same kind of experiments were performed. Tables A.3-A.4 & A.5 (see appendix) outline them. Note that even if these reactors offer T_r - and T_j -modes, experiments were conducted in T_j -mode.

3.5.2 Modelling

For this set of reactors, the vortex formation due to stirring was rapidly found to be a crucial parameter because, when identified separately, p_1 and p_2 were excessively high for small masses and fast stirrer revolution speeds. This suggested a compensation for the vortex to keep the same $U\mathcal{A}$ coefficient. After unfruitful trials with Visimix[®] [118], it became evident that vortex formation needed to be visually estimated, using agitator and baffles as points of reference. Fig. 3.7 shows that vortex exhibits strong discontinuities and can contribute to more than 70 % of the total heat transfer area. Thus, even with the reactor filled only to one third, with a fast stirrer revolution speed the area becomes comparable to that of the full reactor. For 200 kg, the vortex height stays low until 100 rpm and then rises to become even greater than for 300 kg. This typical behaviour appears when the liquid level reaches the blades of one stirrer stage, the liquid being splashed on the reactor wall. Note that for 600 kg the total available heat exchange area is already used without agitation. Therefore, vortex formation does not play a role anymore.

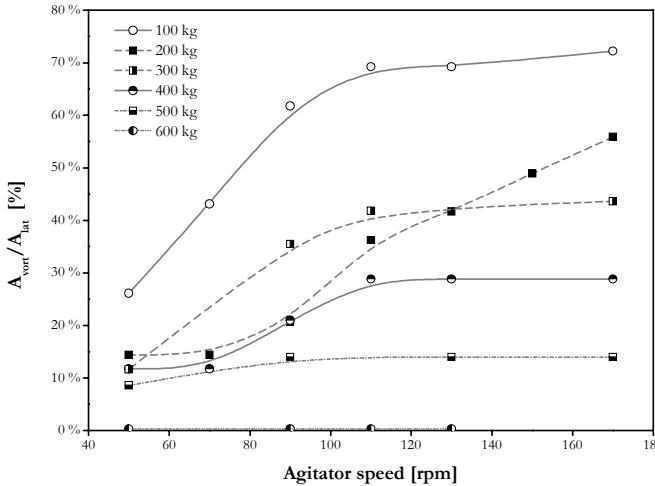


Figure 3.7: Vortex contribution, corresponding to the ratio A_{vort}/A_{tot} to the overall heat transfer area for reactor R_4 filled with water. The lines are only represented to visually suggest the trend.

The parameters identified are listed in Table A.10 (see appendix).

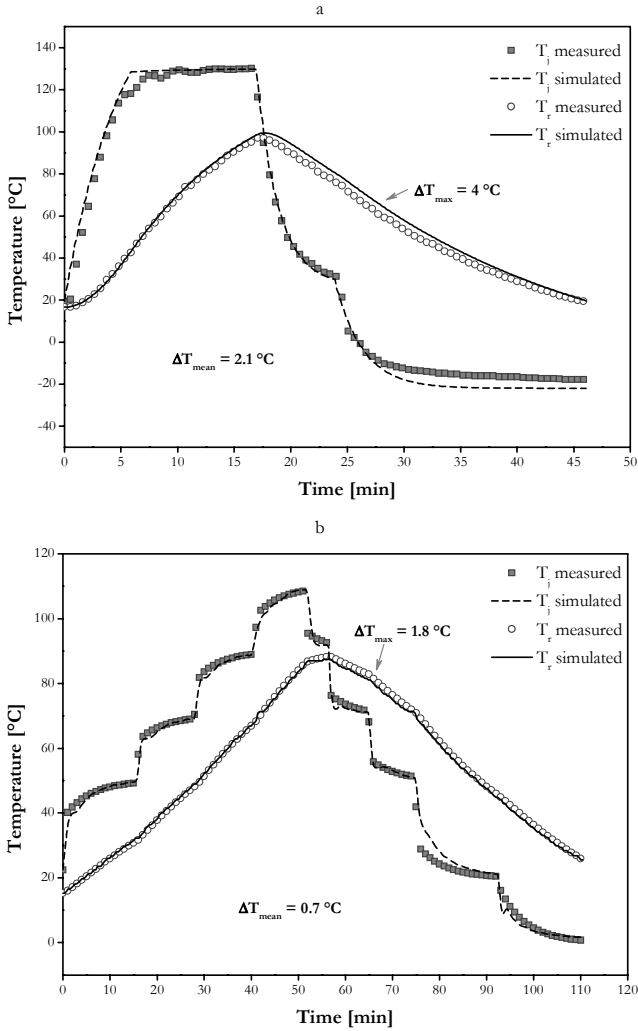


Figure 3.8: Validation of the complete heat balance model for reactor R₃ & R₄. a: R₃, 240 kg of water, stirrer revolution speed 100 rpm; b: R₄, 600 kg of water, ■: recorded jacket temperature; ○: recorded water temperature. For improved clarity, not all experimental points are shown.

Fig. 3.8 represents typical heating/cooling curves recorded experimentally with this set of industrial reactors as well as their corresponding modelling. It is obvious that their dynamics is very fast compared to their sizes. Reactors R_4 and R_5 heat and cool with an average rate of about $4 [^{\circ}\text{C}\cdot\text{min}^{-1}]$, whereas R_3 nearly attains $6 [^{\circ}\text{C}\cdot\text{min}^{-1}]$ for toluene! Fig. 3.8a shows the characteristic break of the transition in cooling mode: if the jacket temperature is lower than 30°C and the setpoint lower than 20°C , then brine is used as an indirect cooling agent instead of cold water.

Once again, the smaller the reactor, the greater the modelling deviation. Fig. 3.8a represents the worst case, with a maximum temperature deviation of 4°C . Nevertheless, the 2°C average modelling deviation remains reasonable, and this for an experiment with an extremely fast temperature change. For normal operations, i.e. during ideally isothermal conditions, the change of reaction medium temperature remains in a range of several degrees. In this case, the modelling would be undoubtedly more precise. For the 630 L reactors, accuracy is much higher with an average temperature difference of less than 1°C . Similarly to the first set, maximal deviation occurs at high temperature, probably due to slight evaporation.

3.6 Third set of reactor - 4 m^3

Table 3.5 lists the main features of the 4 m^3 industrial reactor R_6 and Table A.6 (see appendix) summarises the performed experiments.

Table 3.5: Characteristics of reactor R_6 .

Property	R_6
Nominal volume [L]	4000
Material	stainless steel + enamel
Reactor diameter [m]	1.76
Type of stirrer	anchor
Stirrer diameter [m]	1.63
Baffles	-
Wall thickness [mm]	18.8 ± 1.3
Working modes	T_r or T_j
Utility fluid	oil
Shape of bottom	torispherical
Heating (indirect)	steam 6 bar
Cooling (indirect)	cold water

Examples of heating and cooling experiments are shown in Fig. 3.9. For the modelling of this reactor, only T_r was simulated, while T_j was recorded, and corresponds to the mean value between inlet and outlet temperatures.

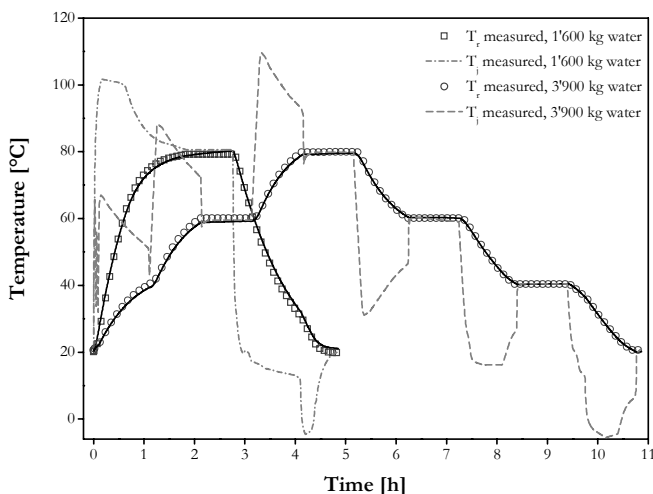


Figure 3.9: Validation of the complete heat balance model for reactor R_6 . \square : recorded reactor temperature T_r for 1'600 kg of water, stirrer revolution speed 33 rpm; \circ : recorded T_r for 3'900 kg of water, 33 rpm, «stair-shape» experiment; dot and dash lines: recorded jacket temperatures; solid lines: simulated temperatures.

These experiments also revealed the high efficiency of the installed PID cascade controller. As shown in Fig. 3.9, the inner temperature setpoint is reached without overshooting. Even the jacket temperature, that exhibits a faster response and which controls the inner temperature, does not oscillate. This means that, with such a device, the various thermal parameters of a reaction can be tuned very precisely. This feature is particularly important in terms of quality, reproducibility and safety. For example, the crystals size of a product is highly dependent on the temperature profile during the crystallization phase and is often subject to deviations between various batch runs. Based on the performed heating/cooling experiments, this problem should be easily overcome in reactor R_6 .

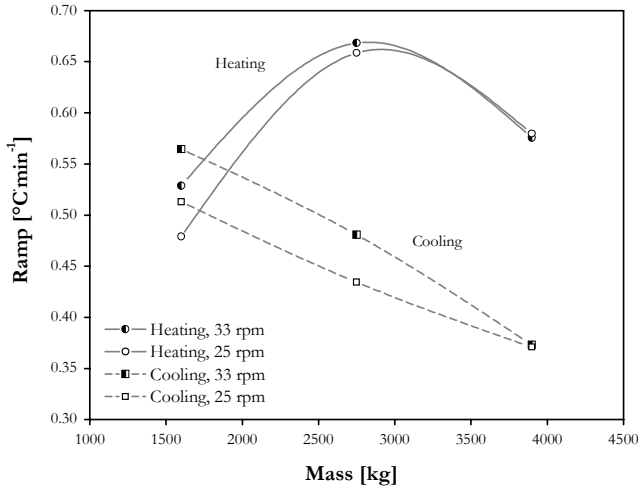


Figure 3.10: Mean ramps for the heating/cooling of reactor R_6 filled with water. ●: heating, stirrer revolution speed 33 rpm; ○: heating, 25 rpm; ■: cooling, 33 rpm; □: cooling, 25 rpm.

An overview of the heating/cooling ramps is given in Fig. 3.10. Heating appears to be clearly faster than cooling except for the experiments with 1600 kg of water. For this amount, the jacket temperature was limited to 100 °C because of previous reaction needed this characteristic. Without this limitation, heating is about 1.5 times faster than cooling. This can be explained by the greater heat transfer driving force, ΔT_m (see Eq. 3.5), during heating. As a general rule, the faster the agitation speed, the greater the reached ramp. However, the difference is decreasing with the mass, reflecting the more important vortex formation with small quantities of liquid. When the reactor is full, the difference is negligible because the whole heat exchanger surface is covered and the vortex has no effect anymore on the heat exchange area. It also indicates that the heat transfer is not limited by the inner resistance.

From the identified model, it is possible to calculate the various heat transfer resistances (h_r^{-1} , h_w^{-1} and h_j^{-1}) as well as the global heat transfer coefficient U as a function of the temperature and stirrer speed. It appears (see Fig. 3.11b) that the main heat transfer resistance is that of the vessel wall. This is not surprising: the reactor is built with a layer of enamel, its thermal conductivity being low (1.16 [W·m⁻¹·K⁻¹]). It confirms that the hydrodynamic flow was always turbulent and that the inner film thickness very small. For the outside film, the resistance is also lower than that of the wall because the flow is sufficiently high. This situation should be globally the same for organic compounds, even if the inner resistance is higher. One can therefore state positively that, solely from the thermal point of view, it is not necessary to work with stirrer speeds higher than 25 rpm (corresponding to 60 % of the maximal speed) when the reactor is filled with more than the 2/3.

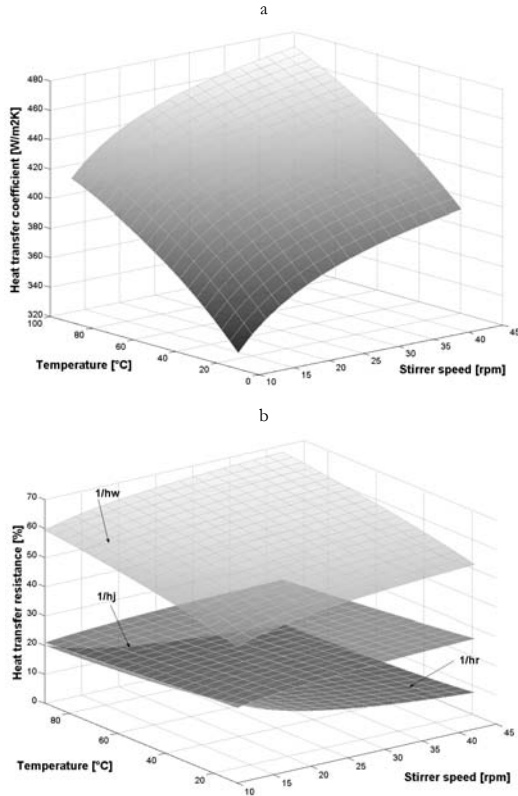


Figure 3.11: a: global heat transfer coefficient U ; b: contribution of the various heat transfer resistances to the global heat transfer resistance for reactor R_6 , as a function of the temperature and stirrer revolution speed.

3.7 Fourth set of reactors - 6.3 to 25 m³

3.7.1 Experiments and modelling

Table 3.6 lists the main features of the industrial reactors R_7 (6.3 m³), R_8 (16 m³) and R_9 (25 m³) and Tables A.7 to A.9 (see again appendix) summarise the performed heating/cooling experiments.

Table 3.6: Characteristics of reactor R₇ to R₉.

Property	R ₇	R ₈	R ₉
Nominal volume [L]	6'300	16'000	25'000
Material	stainless steel + enamel	stainless steel	stainless steel
Reactor diameter [m]	2	2.8	3.0
Type of stirrer	GlasLock®	3 stages Mig®	3 stages Mig®
Stirrer diameter [m]	0.85	3 x 1.8	1.9
Baffles	1	3	3
Wall thickness [mm]	24.0 + 1.6	12.0	12.0
Working modes	T_r or T_j	T_r or T_j	T_r or T_j
Shape of bottom	torispherical	torispherical	torispherical
Heating (direct)	steam 6 bar	steam 6 bar	steam 6 bar
Cooling (direct)	cold water	cold water	cold water

For the modelling of these reactors, as for reactor R₆, only T_r was simulated. In fact, when simulating the recorded jacket temperatures, namely that of the inlet, the reactor thermal evolution could not give satisfactory results. It turned out that the simulated response of T_r consecutive to a change of T_j was too fast. This can be intuitively understood: the mean jacket temperature of the whole coils is changed with a time delay of several minutes with the inlet temperature. This depends of course on the flow of heat carrier fluid and on coils volume (these two parameters being unknown), but also on the filling ratio of the reactor itself. Indeed, the fuller the reactor, the larger the heat exchanged and thus the greater the temperature difference between jacket inlet and outlet. Finally, based on least-square fits, the used shift was 3, 4 and 5 minutes for the reactor filled with 1/3, 2/3 and 3/3 respectively.

The identification of the thermal dynamics of reactor R₈ was slightly modified compared to all other reactors. The most striking feature of this reactor is that the heating is three times faster than the cooling, while this ratio is normally about two, or even less. In fact, heating being direct, the main reason comes from the latent heat of vaporisation. Besides, the inlet jacket temperature regularly reached 140 °C. Hence, and for this reactor only, the heat balance (see Eq. 3.2, p. 45) was modified by introducing the latent power for jacket temperatures higher than 100 °C:

$$\left(m_r \cdot C_{p_r}'(T_r) + C_w\right) \cdot \frac{dT_r}{dt} = q_{ec} + q_{st} + q_{loss} + q_{vap} \quad (3.26)$$

with q_{vap} the power due to the latent heat of vaporisation of steam at 6 bar, i.e. 2'755 [kJ·kg⁻¹] [123].

3.7.2 Results

Fig. 3.12 represents typical heating/cooling experiments conducted within reactor R₉ (25 m³) with water and methanol, as well as their respective simulation. Note that the masses were measured on an electronic scale with a precision of about 5 kg. The indicated masses are therefore not accurate to the nearest kilo.

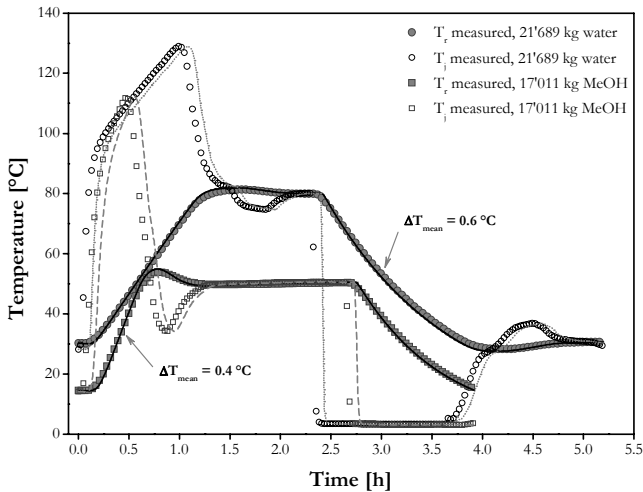


Figure 3.12: Validation of the complete heat balance model for reactor R₉. ■ & □: recorded T_r and T_j for 17'011 kg of methanol, stirrer revolution speed 55 rpm; ● & ○: recorded T_r and T_j for 21'689 kg of water, 23 rpm; dot and dash lines: simulated jacket temperatures; solid lines: simulated reactor temperatures. For more clarity, not all experimental points are shown.

Once the heat balance model has been identified, it is possible to calculate the various heat transfer resistances, as well as the global heat transfer coefficient U as function of temperature and stirrer revolution speed (see Fig. 3.13). It appears that for water, the main heat transfer resistance is that of the reactor wall, representing 60 to 80 % of the total resistance. This confirms that the heat flow inside the reactor was always turbulent and that the internal film, h_r^{-1} , was very thin. As observed for the external film, the heat flow being probably fast, its resistance is minor. With methanol, the situation is slightly different for slow stirrer speeds. In this case, the main heat transfer resistance is that of the internal film. This statement may certainly be generalised to most organic fluids and it is therefore recommended, from the thermal point of view, to work with stirrer speeds higher than 30 rpm to profit from a great heat transfer.

It is also possible to calculate the time constant of the reactor, τ_r , that gives an indication on the time needed to heat or cool the reactor:

$$\tau_r = \frac{m_r \cdot C_{p_r}}{U \cdot A_{tot}} \quad (3.27)$$

By putting T_0 the initial reactor temperature and T_j that of the jacket, we obtain the following expressions (assuming that the stirrer power compensates losses, which is normally the case for big reactors):

- temperature evolution as a function of time:

$$T_r = T_j + (T_0 - T_j) \cdot \exp\left(-t/\tau_r\right) \quad (3.28)$$

- time needed to reach T_r from T_0 with a jacket temperature T_j :

$$t = \tau_r \cdot \ln\left(\frac{T_0 - T_j}{T_r - T_j}\right) \quad (3.29)$$

- requisite jacket temperature to reach T_r from an initial temperature T_0 at a time t :

$$T_j = \frac{T - T_0 \cdot \exp\left(-t/\tau_r\right)}{1 - \exp\left(-t/\tau_r\right)} \quad (3.30)$$

Fig. 3.14 compares the R_0 time constants of water and methanol. It first shows that, for a given compound, they increase with the filling ratio, proving, if still necessary, that the increase of heat transfer area does not compensate for the mass increase. In spite of a smaller global heat transfer coefficient (see Fig. 3.13c), methanol time constants are lower than that of water because its heat capacity is lower (2.6 versus 4.2 [kJ·kg⁻¹·K⁻¹]). Note that time constant diminishes with temperature for water but increases for methanol. The fact that U varies more for water and the change in heat capacity with temperature explain this trend.

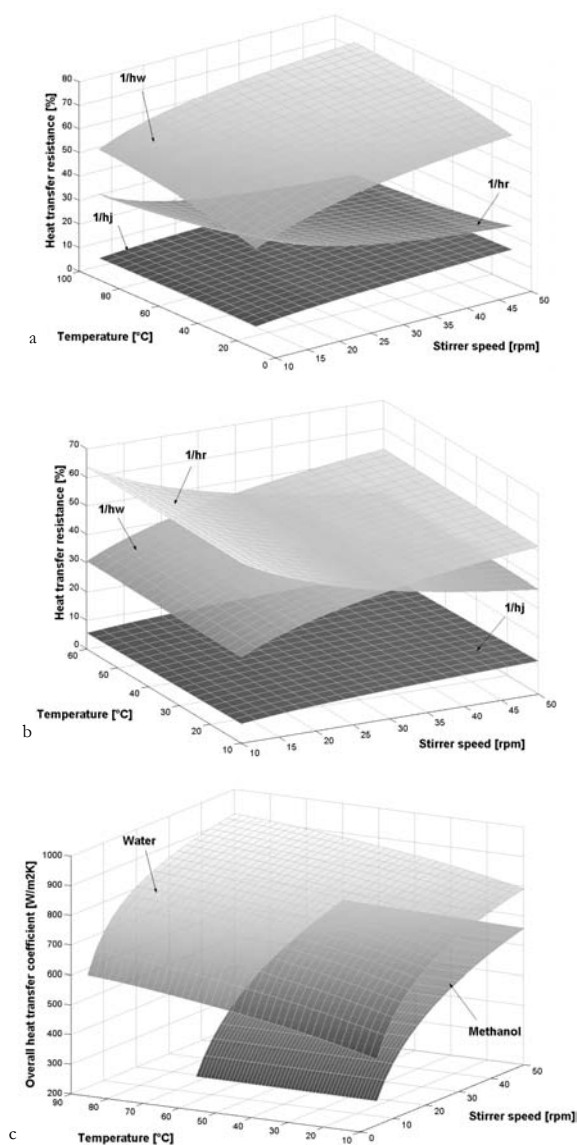


Figure 3.13: Contribution of the various heat transfer resistances to the global heat transfer for reactor R₀ filled with water (a) and methanol (b); c: comparison of overall heat transfer coefficients U for water and methanol.

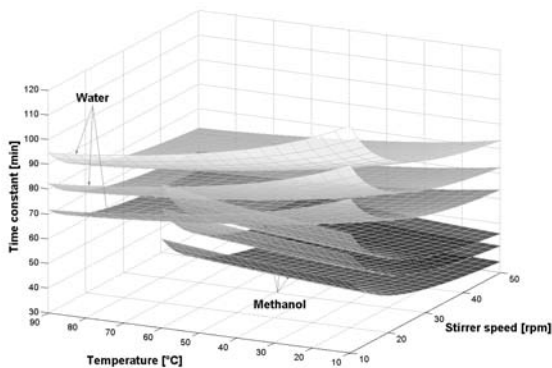


Figure 3.14: Comparison of water and methanol time constants (in minutes) for reactor R₀ as a function of temperature and stirrer revolution speed. For both solvents, time constants are calculated for three different masses corresponding to a reactor filling ratio of 1/3, 2/3 and 3/3.

3.8 Conclusions

The used heat balance equations allow a good description of the temperature evolution within the industrial reactors (see e.g. Fig. 3.8). Moreover, the treatment of the jacket dynamics as two first order dynamic systems allows to describe the temperature dynamics following a setpoint change. However, as reactors R₁ & R₂ have almost the size of kilo-laboratory reactors, their modelling was subject to small deviations. The neglected secondary effects, mainly the heat losses due to the solvent evaporation and cold droplets flowing back into the medium, lead to small disturbances (see Fig. 3.6). Therefore the larger the reactor and/or the more fluid quantity introduced, the better modelled the experimental data. Because reactors are filled at least up to 2/3 during normal production operations, the model is in this case sufficiently precise (mean temperature difference in the order of one degree).

Moreover, at the beginning of the model development, the importance of vortex formation was supposed to be negligible. In fact, this parameter was found to be crucial for reactors R₃, R₄ and R₅, due to their specific stirrer configuration: the power of the motor is very important and the three Intermig[®] stages allow a very efficient mixing. It has been shown that even if the reactor is

filled to one third and if the stirrer revolution speed is fast enough (i.e. at least 170 rpm) the real heat exchange area is comparable with that of the full reactor. Such a behaviour would not have been forecast by the simulation programs previously mentioned. Therefore, for this type of stirrer configuration, it appeared necessary to visually evaluate the vortex formation.

Despite these difficulties, the use of classical heat balance equations has proven to be sufficiently precise in order to identify the thermal behaviour of a very eclectic palette of plant reactors.

Once the complete model is identified, the thermal behaviour of industrial reactors can be numerically simulated during each stage of a manufacturing process: addition of a reagent during semi-batch operation, change of both jacket or reaction medium temperature setpoint, change of the stirrer revolution speed, etc. The continuation of the project consists in forecasting the thermal behaviour of industrial reactors during a chemical reaction run in a small scale device. More precisely, this temperature profile will be calculated using the identified reactor model and tracked on-line using a Mettler Toledo reaction calorimeter RC1[®]. By doing so, the various problems of quality, selectivity as well as safety consecutive to the transition from laboratory to production scale will be detected earlier and more accurately. However, the principle of the «scale-down» methodology has first to be developed, the RC1[®]-Excel communication mounted and a temperature control strategy applied. These are the themes the next chapter is dealing with.

Chapter 4

DEVELOPMENT OF THE SCALE-DOWN METHODOLOGY

4.1 Principle

Among others, reaction calorimetry has probably become the most popular tool to determine the conditions, under which a process should be performed to guarantee that, in case of a cooling breakdown, the risks remain under acceptable limits [42, 124]. Actually, it is the appropriate technique for the purpose of thermodynamic and kinetic analysis, often in combination with scale-up tasks. It can be used to carry out chemical reactions and processes or for determining the kinetics of a reaction and the thermodynamic properties of the reaction mixture. Most of these *laboratory* devices, and among them the Mettler Toledo reaction calorimeter RC1[®] used in this study, are quite versatile so that reactions can be carried out safely even under intense temperature and/or pressure conditions. Laboratory temperature controlling devices and laboratory heat-transfer units are characterised in that they are quite powerful and can control the temperature of reaction mixtures fast and accurately. In other words, their dynamics are almost ideal.

However, the temperature evolution of an *industrial* reactor reflects only partially the thermal characteristics of the chemical reaction. It also depends from another key parameter: the dynamics of the heating/cooling control system. Indeed, a process plant is much bigger than a laboratory device, with reaction vessel volumes ranging from a few litres up to several cubic meters. Due to their size and to the used materials it is almost impossible to build a process plant with an ideal dynamic temperature behaviour. To simulate the thermal behaviour of full-scale equipment at laboratory scale, it is therefore necessary to combine these two scopes: process dynamics and

calorimetric techniques. This is exactly the approach tackled here: on one hand, a library with all industrial reactors dynamically identified is available; on the other hand, the RC1[®] is used to perform chemical reactions at laboratory scale. The principle of the scale-down methodology is then the following:

- observe on-line the instantaneous heat production rate of a chemical reaction in the RC1[®]
- use this value in a numerical simulation model of the plant reactor dynamics
- deduce the evolution of the jacket and reaction mixture temperatures of the plant reactor model if this chemical reaction took place in it
- force the RC1[®] to track this temperature evolution and hence not to behave ideally anymore
- repeat the first four points during the entire course of the chemical reaction.

The next subchapters describe in details this methodology as well as the necessary developments brought to the commercialised RC1[®], particularly in its evaluation software.

4.2 Apparatus

The employed commercial reaction calorimeter in this thesis is the RC1[®]1, developed by Mettler Toledo. It is a bench scale calorimeter with a 2 L vessel that can approach industrial conditions.

The following equipment was used (see Fig. 4.1):

- RC1 classic with temperature range from -20 (with cryostat) to +200 °C
- standard AP01 2 L, glass, double mantle reactor, heat flow carrier: silicon oil
- 5 W glass and 25 W hastelloy calibration probes
- Pt-100 glass temperature sensor
- anchor and downward propeller glass stirrers
- RD10 dosing controller with measuring inputs (for measured value sensors), controllable outputs for peripheral control elements (pumps, valves) and microprocessor electronics, that communicate via a serial interface with the computer
- standard WinRC[®] ver. 7.11 (SR-6) and new WinRC ALR[®] ver. 7.5 (Revision 7.5.255, without calorimetric capabilities) evaluation software with two corresponding EPROM
- pump: ProMinent[®] beta4a 1602 with PTFE head and PTFE tubing

1. From now on, the registerserif will be omitted and the term «RC1» will be used with reference to the commercial Mettler Toledo reaction calorimeter RC1[®].

- balance: Mettler Toledo DeltaRange[®] PG5002-S, precision 0.01 g, max. 5.1 kg
- cryostat: Lauda Ultra-Kryomat[®] RUK 50 with temperatures from -50 to 100 °C, filled with 25 L of a solution of water/ethylene glycol 50:50
- computer: Dell[®] Desktop PC (Intel[®] Pentium[®] 4, 2.53 MHz, 512 MB of RAM).

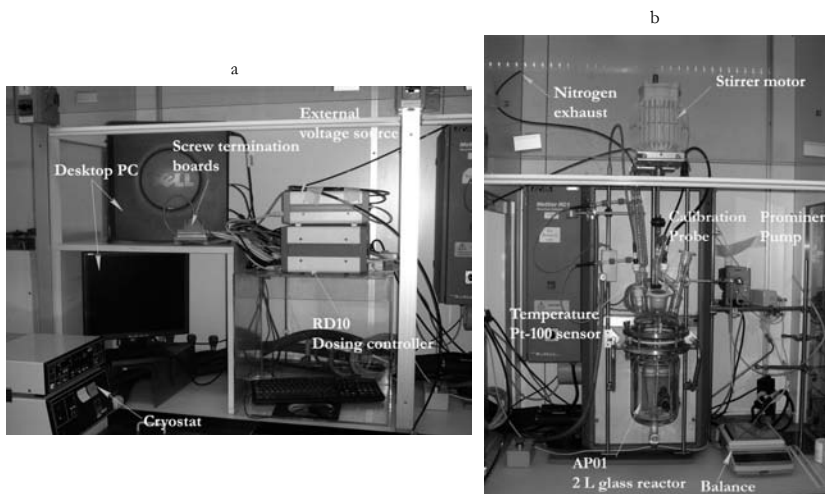


Figure 4.1: Used equipment. a: Desktop PC, RD10 dosing controller, cryostat, screw termination boards and external voltage source (see § 5.2, p. 96); b: RC1 calorimeter with AP01 2 L glass reactor, balance and dosing pump.

4.3 External data source communication

A new version of the evaluation software has been commercialised by Mettler Toledo: the WinRC ALR[®] ver. 7.5¹. Its main improvement is the addition of an «external data source» instrument that is able to transmit and receive on-line data (every 2 s at most). The communication between the RC1 and an external source (a computer in this case) is established with the help of an ActiveX constituent. Data are transferred in the form of strings via a TCP/IP connection. The

1. From now on, the registerserif will be omitted and the term «WinRC ALR» will be used with reference to the Mettler Toledo WinRC ALR[®] ver. 7.5 evaluation software.

exchanged data are organised into «arrays». On the RC1 side, these arrays data typically come from the various sensors and controllers (mainly T_r , T_j , T_{set} , m_r , N). Moreover, the new WinRC ALR software enables to control some parameters of the RC1 with the external data source. So, for example, T_r , T_j or N can be set by a value predefined or calculated within the external data source.

Any program able to use a Component Object Model¹, like for example Matlab [125], can be used as software interface. In this thesis we chose Microsoft Excel in combination with Visual Basic (VBA) for both their simplicity and their widespread use in industry. Excel is used to calculate the temperature evolution of plant scale reactors via their identified dynamics, whereas VBA is used for establishing the connection between the RC1 and Excel and for allowing the user to control parameters, mainly the temperature setpoint of the industrial reactor. The VBA window is given in Fig. 4.2:

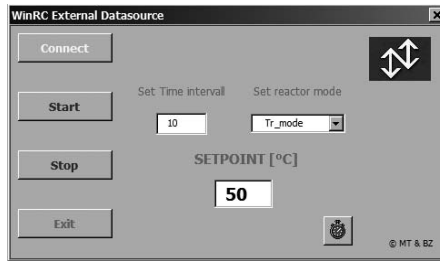


Figure 4.2: Visual Basic window used to establish the communication between Excel and the WinRC ALR software.

The VBA window comprises the following functions:

- **Connect** button: establishes the TCP/IP server side connection. WinRC ALR side is the client, Excel and its macros acting as the TCP/IP server.
- **Start** button: starts the collection and transmission of values from and to WinRC ALR; enables setting time interval.
- **Set time interval** textbox: sets the time interval, in seconds, between two timer events; is accessible on-line.
- **Set reactor mode** combobox: defines whether the reactor (T_r -mode) or jacket (T_j -mode) temperature of the industrial reactor is controlled; is accessible on-line.
- **Setpoint** textbox: sets the reactor or jacket setpoint temperature of the industrial reactor; is accessible on-line.
- **Stop** button: stops the collection and transmission of any values except from the

1. COM is a platform-independent, distributed, object-oriented system for creating binary software components that can interact with each other.

connection state.

- **Exit** button: terminates the communication and deletes the object.
- **Timer** event: at each timer event, user-defined data from the various calorimeter sensors are collected and sent to the k^{th} row in Excel; consecutively, data from the k^{th} Excel row are sent to the calorimeter. The row is then incremented, $k := k+1$.

4.4 Temperature control strategy

4.4.1 Context

The first tests performed with Excel and WinRC ALR were relatively basic. The goal was to verify that the communication between the two programs and the control of the RC1 by the external data source were accurate, robust and trustworthy. It consisted in reproducing within the RC1 a heating/cooling experiment recorded in an industrial reactor:

- prior to the experiment: filling in an Excel sheet with a predefined temperature profile
- running WinRC ALR software, RC1 being filled with a known amount of deionised water
- working in T_r -mode controlled by a variable, i.e. the RC1 contents (water in this case) was controlled by data coming from the Excel sheet
- sending values from Excel to WinRC ALR at regular intervals (typically 10 s), the latter being new RC1 setpoint temperatures.

Unfortunately, although the WinRC ALR and Excel communication worked perfectly well (for some experiments during more than 15 h), these first tests revealed two delay problems: first, when a new setpoint was sent from Excel to the RC1 software, the actual calorimeter value $T_{r,sel}$ took a certain time to reach the new setpoint; second, the T_r^{RC1} value did not reach $T_{r,sel}$ immediately. This resulted in a second delay, which is, of course, proportional to the requested temperature ramp (see Fig. 4.3). The first problem is inherent in the WinRC ALR software and hence inevitable. It is the so-called *segment time*, definitively set to 6 s. The second one is inherent to every dynamic system and results in a rather important difference. Moreover, based on experiments, it can be stated positively that:

- reducing the time interval between two transmitted setpoints does not improve the temperature difference by more than 0.2 °C, and makes Excel sheets and CPU usage uselessly cumbersome
- changing solvent quantity has only a minor effect and would not be applicable in practice
- changing stirrer revolution speed has an effect only for steep ramps, i.e. from 4 [°C min⁻¹]: for downward propeller, the temperature difference is reduced by 0.7 °C between

150 to 450 rpm

- delay also depends on the temperature of the RC1 cooling source.

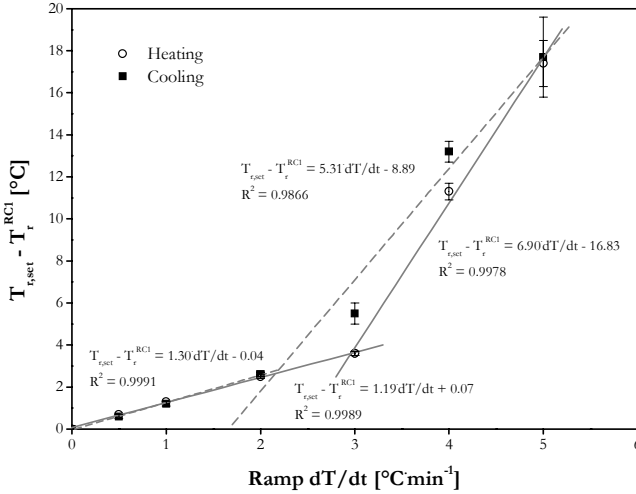


Figure 4.3: Comparison between setpoint and measured temperatures: $T_{r,set} - T_r^{RC1}$ as a function of the desired ramp. Error bars correspond to different stirrer revolution speeds (glass downward propeller 150 to 450 rpm). AP01 reactor filled with 1.60 kg of deionised water.

Finally, it seemed evident that in order to find a robust solution with fast temperature adjustment, working in T_j -mode was preferable.

4.4.2 PI controller

When the classical RC1¹ works in T_r -mode, any deviation from the temperature set value in the reactor is compensated by an appropriate correction of the jacket temperature through control algorithms. Fig. 4.4 shows the control loop used in the RC1 to maintain the reaction medium temperature. A first loop defines the set value of the jacket temperature ($T_{j,set}$) and a second loop controls the jacket temperature given by $T_{j,set}$ by means of a fast thermostating unit.

1. From now on, the terms «classical RC1» and «modified RC1» will refer to RC1 with standard WinRC ver. 7.11 and new WinRC ALR ver. 7.5 evaluation software respectively.

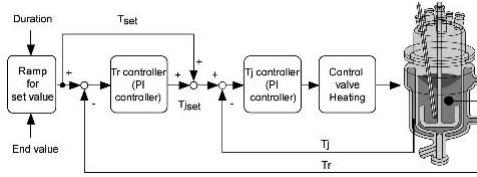


Figure 4.4: Temperature control representation in the RC1 [126].

The setpoint value of the jacket temperature is computed by the following expression:

$$T_{j,set} = T_{r,set} + K \cdot \left[(T_{r,set} - T_r) + \frac{1}{I} \cdot \int_0^t (T_{r,set} - T_r) \cdot dt \right] \quad (4.1)$$

where K stands for the proportional and I for the integral parameters of the temperature controller.

In our case, $T_{r,set}$ is the calculated industrial reactor temperature of the reaction medium (T_r^{indus}). Therefore, based on the classical RC1 control strategy, the following procedure is applied when working with the modified RC1:

- launch WinRC ALR and Excel concurrently
- use the VBA window to establish connection
- work with the modified RC1 in T_j -mode controlled by a variable setpoint
- calculate T_r^{indus} in the Excel sheet using the scale-down methodology (see § 4.5)
- calculate $T_{j,set}^{RC1}$ in the Excel sheet with:

$$T_{j,set}^{RC1} = T_r^{indus} + K \cdot \left[(T_r^{indus} - T_r^{RC1}) + \frac{1}{I} \cdot \int_0^t (T_r^{indus} - T_r^{RC1}) \cdot dt \right] \quad (4.2)$$

- send the calculated $T_{j,set}^{RC1}$ values to WinRC ALR, the latter being the RC1 jacket setpoints
- repeat the last three points every 10 s during the entire course of the experiment.

Parameters K and I have to be tuned to allow a fast temperature adaptation of the reaction mixture while avoiding oscillations consecutive to a too aggressive controller. Based on a least-square fit over classical RC1 results, K and I were set for water to 12 [-] and 0.0042 [s⁻¹] respectively. For organic solvents, K was reduced to 4 [-]. Moreover, the adjustment rules for PID controllers developed by Ziegler & Nichols [92] allow to determine the most adequate parameters.

As explained in § 2.3.4 (page 30), an inherent disadvantage of integral control action is the reset windup. To avoid it, the maximum output values of the PI controller were limited:

$$-15 \leq K \cdot (T_r^{indus} - T_r^{RC1}) \leq 15 \quad (4.3)$$

$$-200 \leq \int_0^t (T_r^{indus} - T_r^{RC1}) \cdot dt \leq 200 \quad (4.4)$$

meaning that $(T_{j,set}^{RC1} - T_r^{indus})$ can never exceed ± 25 °C for water and ± 18 °C for organic solvents. This is absolutely not an issue for normal operations (temperature ramps less than 3 [°C·min⁻¹]).

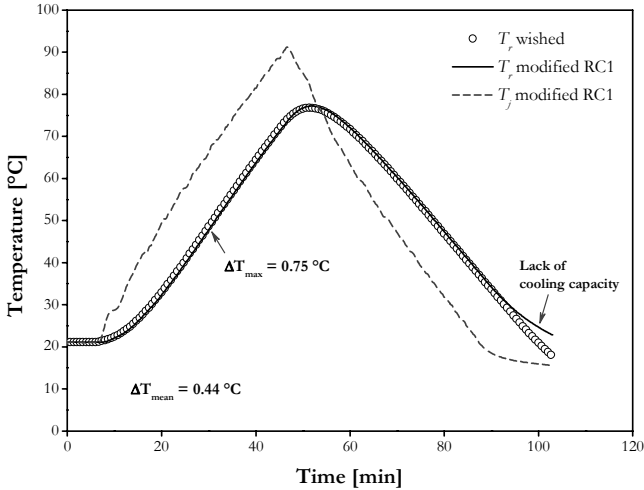


Figure 4.5: Reproduction of a temperature recorded in reactor R₂ (○). Modified RC1 filled with 1.670 kg of deionised water, anchor revolution speed 100 rpm, time interval between two transmitted data 10 s.

Fig. 4.5 shows the efficiency of the temperature control strategy with the PI controller. The recorded temperature of water (15 kg, stirrer revolution speed 80 rpm) in reactor R₂ was entered in an Excel sheet and sent to the modified RC1 at regular intervals, the latter working in T_j -mode. The mean temperature difference between the wished and actual T_r^{RC1} is only 0.44 °C, and this for a mean temperature ramp of 1.3 [°C·min⁻¹]. Below 30 °C, the temperature of the RC1 cooling agent (water at ~ 14 °C, the cryostat not having been installed yet) did not allow an efficient control anymore.

4.5 Scale-down methodology

So far it was shown that it is possible to describe the dynamic temperature behaviour of an industrial reactor, as a combination of heat balance equations and the dynamic evolution of its temperature controlling device. The complete mathematical model, describing this dynamics, will now be used to determine the temperature setpoints for controlling the reaction calorimeter RC1. By taking advantage of the features of the WinRC ALR evaluation software, combined with the temperature control strategy described above, the RC1 follows that setpoints and any reaction is carried out under temperature conditions resembling those of a plant reactor. The procedure of the scale-down strategy is schematically represented in Fig. 4.6. The initialisation phase takes place off-line, prior to the experiment, while the loop represented by the rest of the diagram is performed on-line every 10 s. The next sections describe the methodology step by step.

4.5.1 Initialisation phase

First of all, the reaction calorimeter has to be initialised and the already known parameters have to be fed into the program. Some of these are either *fixed* or *user-defined* and are related to the proportions and properties of the industrial reactor to be simulated. The fixed parameters are: reactor diameter D , stirrer diameter d , wall thickness d_w , thermal conductivity λ_w , mean heat capacity of the reactor C_w , stirrer constant C , power number Ne and the identified modelling parameters (see Table A.10, p. 169). The user-defined parameters are: experiment duration t_{∞} , initial mass of reaction medium $m_{r,0}$, stirrer revolution speed N , initial reaction mixture and jacket temperatures of the industrial reactor $T_{r,0}^{indus}$ and $T_{j,0}^{indus}$, and either reaction mixture setpoint temperature $T_{r,set}^{indus}$ or jacket setpoint temperature $T_{j,set}^{indus}$.

The heat balances having to be performed on-line while using the scale-down methodology, it is necessary to know some characteristics of the chemical reaction, starting from its specific heat capacity C_p' , the heat transfer capacity UA in the RC1, its produced or consumed heat Q_{rx} and until the heat losses q_{loss} . They are obtained by carrying out the reaction under isothermal conditions in the classical RC1. Moreover, these thermodynamic parameters and properties being temperature dependent, the reaction has to be carried out twice at different temperatures. Preferably, these two temperatures, T_1 and T_2 , should include the temperature domain in which the reaction is carried out using the scale-down methodology.

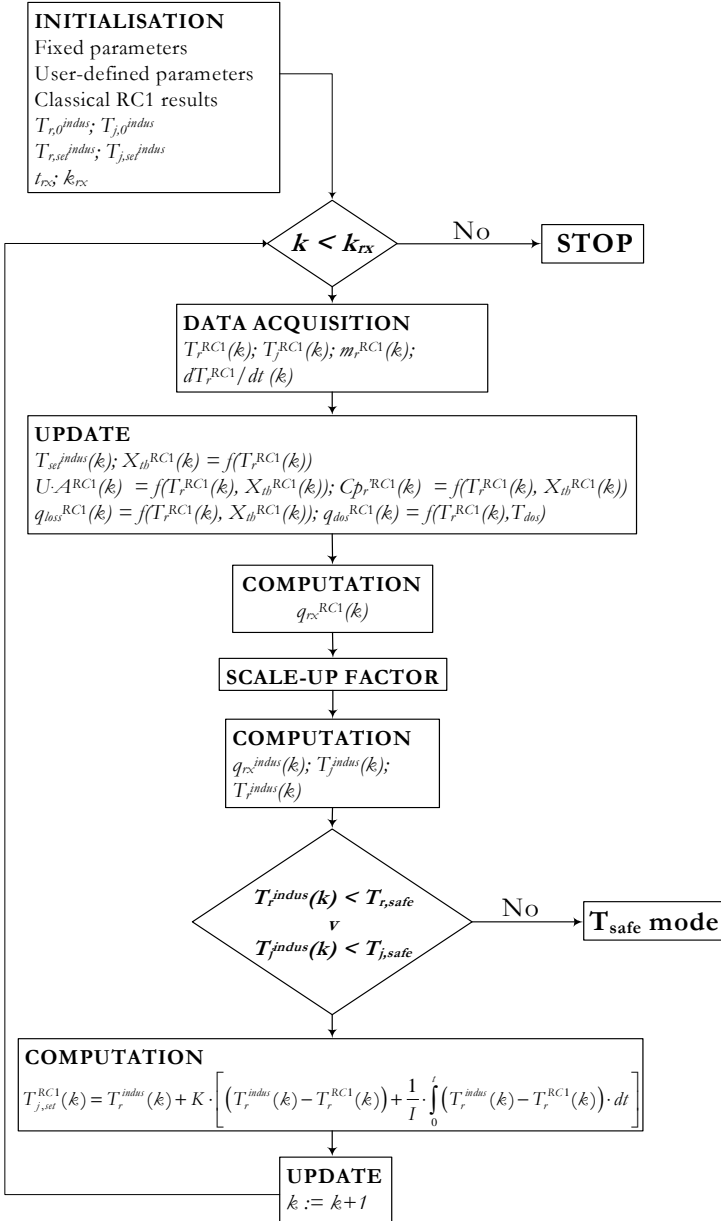


Figure 4.6: Structure of the program for implementing the scale-down strategy. k stands for the discrete expression of time, in this case an interval of 10 s.

4.5.2 Data acquisition

After the initialisation phase, the reaction is started in the modified RC1, while the jacket calorimeter temperature is controlled by a variable setpoint derived from the mathematical model. After a first time interval Δt , typically 10 s, corresponding to a timer event k , the values of the reaction mixture T_r^{RC1} and jacket T_j^{RC1} temperatures, the temperature evolution of reaction mixture dT_r^{RC1}/dt and the mass of the reaction mixture m_r^{RC1} are sent from WinRC ALR to the Excel sheet via the TCP/IP connection.

4.5.3 Update

The acquired values together with the reaction mixture or jacket temperature setpoint of the industrial reactor, the latter being modifiable on-line, are used to update the essential parameters for the heat balance: namely the thermal conversion X_{th}^{RC1} as a function of T_r^{RC1} , the heat transfer capacity UA^{RC1} , the specific heat capacity Cp_r^{RC1} , the power due to losses q_{loss}^{RC1} and the eventual power due to dosing q_{dos}^{RC1} (for semi-batch reactions), all function of both X_{th}^{RC1} and T_r^{RC1} . Note that the thermal conversion is equivalent to the chemical conversion for systems with a single reaction in which no additional thermal or physical effects (such as a mixing energy or crystallisation) are present [127]. From these values an on-line heat balance over the RC1 is computed allowing determining the instantaneous heat release rate of the reaction and, through integration, the thermal conversion. They are used for the numerical simulation of the industrial reactor dynamic behaviour. This is explained in details in the following:

$$- \mathbf{X}_{th}^{RC1}$$

The conversion is evaluated on-line while integrating the thermal signal. In this case, a rectangular approximation is justified by the small time interval:

$$X_{th}^{RC1}(k) = \frac{q_{rc}^{RC1}(k-1) \cdot \Delta t}{Q_{rc}^{RC1}} + X_{th}^{RC1}(k-1) \quad (4.5)$$

Eq. 4.5 clearly describes one of the great advantages of the developed method: *no* kinetic model is necessary. All the methodology is based only on the reading of temperature sensors and on heat balances. Recently, approaches combining reaction kinetics and numerical simulation became more popular [128-130]. However, kinetic determination typically involves expensive and time-consuming steps that are here avoided.

- $U \cdot A^{RC1}$

The procedure for evaluating $U \cdot A^{RC1}$ on-line as a function of both thermal conversion and temperature is given in Fig. 4.7. $U \cdot A$ values are determined *before* and *after* reaction at the time of the classical RC1 experiments. To do so, a known power is delivered by the calibration probe while no chemical reaction takes place, which is the case when only one reactant, eventually with an inert solvent, has been charged into the reactor and when the chemical reaction is complete or lower than the sensitivity of the apparatus (see also § 5.2.1, p. 96). After that, $U \cdot A^{RC1}$ is evaluated on-line with the help of a simple rule of three, i.e. a linear interpolation is performed on both temperature and conversion.

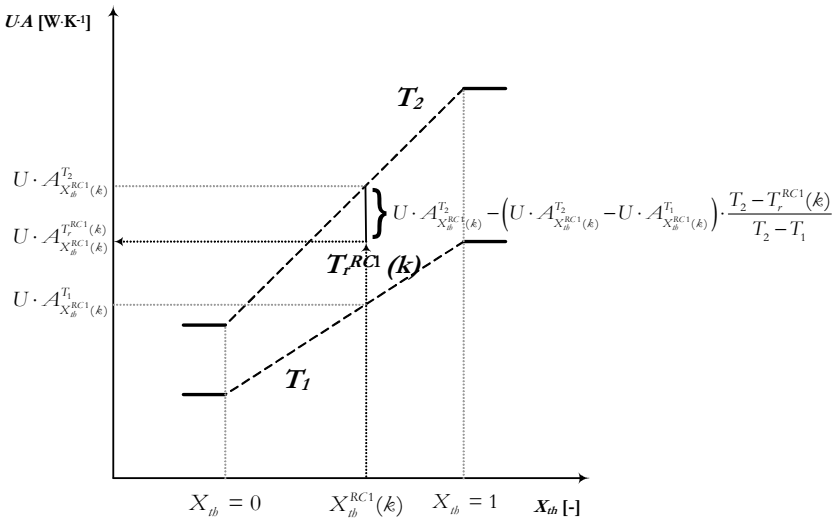


Figure 4.7: Procedure for evaluating on-line the heat transfer capacity UA as a function of both temperature and thermal conversion. In this example, $T_1 < T_2$.

- C_{Pr}^{RC1}

The specific heat capacity of the reaction medium is determined *before* and *after* reaction in the classical RC1 using temperature ramps (of typically 3 °C) at both T_1 and T_2 . Then, C_{Pr}^{RC1} is evaluated on-line using the same procedure as for $U \cdot A^{RC1}$.

- $q_{\text{loss}}^{\text{RC1}}$

When evaluating classical RC1 data, the losses provide the baseline for the heat flux, i.e. the values recorded without any heat released by chemical reaction. Therefore, they include all hypothetical side effects not taking into account in the heat balance, like mixing energy or evaporation, etc. For a given reactor, the heat losses mainly depend on the temperature difference between the reaction medium and the surroundings:

$$q_{\text{loss}}^{\text{RC1}}(k) = \alpha(k) \cdot (T_{\text{amb}} - T_r^{\text{RC1}}(k)) \quad (4.6)$$

with α a constant of proportionality, evaluated on-line using once again the procedure described above. Note that normally, heat losses due to evaporation of the reaction medium are proportional to its vapour pressure, hence exponentially proportional to the temperature. This can be considered to be the major contribution to heat losses when working at high temperature, i.e. close to the boiling point, or during reactions under reflux [131]. However, as experiments were always performed at temperatures relatively far away from the boiling point and hence never under reflux, this approach was not justified and would have made the model unnecessarily cumbersome.

- $q_{\text{dos}}^{\text{RC1}}$

$q_{\text{dos}}^{\text{RC1}}$, the power due to the temperature difference between the feed and the reaction medium for semi-batch operations, is calculated on-line using the following equation:

$$q_{\text{dos}}^{\text{RC1}}(k) = \frac{m_r^{\text{RC1}}(k) - m_r^{\text{RC1}}(k-1)}{\Delta t} \cdot C_{p_{\text{dos}}} \cdot (T_{\text{dos}} - T_r^{\text{RC1}}(k)) \quad (4.7)$$

Note that in Eqs. 4.6 & 4.7, the surrounding T_{amb} and feed T_{dos} temperatures are considered constant during the entire course of the experiment. Therefore, the specific heat capacity of the feed $C_{p_{\text{dos}}}$ is also constant.

4.5.4 Heat balance over the RC1

The acquired and updated parameter values are then used to compute a first heat balance on the RC1 itself in order to calculate the heat release rate of the chemical reaction following:

$$q_{\text{rx}}^{\text{RC1}}(k) = m_r^{\text{RC1}}(k) \cdot C_{p_r}^{\text{RC1}}(k) \cdot \frac{\Delta T_r^{\text{RC1}}(k)}{\Delta t} + U \cdot A \cdot (T_r^{\text{RC1}}(k) - T_a^{\text{RC1}}(k)) - q_{\text{dos}}^{\text{RC1}}(k) - q_{\text{loss}}^{\text{RC1}}(k) \quad (4.8)$$

with T_a^{RC1} representing the corrected jacket temperature: in a non isothermal operation of the RC1, the appreciable heat capacity of the reactor wall must be taken into account. Part of the heat flow from the oil into the reactor wall is used to heat/cool the wall and does not flow from the reactor wall into the reaction mass. The temperature across the wall depends on:

- the thermal conductivity and thickness of the reactor wall, i.e. its time constant
- the resistance of the oil film
- the resistance of the reaction mass film.

A mathematical model developed by Mettler Toledo, including these parameters, is used to calculate the temperature distribution in the reactor wall and gives an (imaginary) active jacket temperature that is designated T_a .

4.5.5 Scale-up factor

The scale-up factor simply relates to the ratio of the reaction mass in the RC1 to the hypothetical user-defined reaction mass in the industrial reactor:

$$\text{Scale-up factor} = \frac{m_r^{indus}(\kappa)}{m_r^{RC1}(\kappa)} \quad (4.9)$$

As the reaction processes are assumed to be the same in laboratory and plant conditions, this scale-up factor stays constant during the experiment.

4.5.6 Heat balance over the industrial reactor

The reaction thermal power calculated above is multiplied by the scale-up factor and the hypothetical change of the reaction mixture temperature of the industrial reactor during the time interval Δt is calculated similarly to Eq. 3.2 (see p. 45) by:

$$\Delta T_r^{indus}(\kappa) = \frac{q_{rx}^{indus}(\kappa) + q_{cs}^{indus}(\kappa) + q_{st}^{indus}(\kappa) + q_{loss}^{indus}(\kappa)}{(m_r^{indus}(\kappa) \cdot C_p^{indus}(\kappa) + C_w^{indus})} \cdot \Delta t \quad (4.10)$$

and thus:

$$T_r^{indus}(\kappa) = T_r^{indus}(\kappa - 1) + \Delta T_r^{indus}(\kappa) \quad (4.11)$$

Moreover, the hypothetical jacket temperature of the industrial reactor T_j^{indus} is also computed based on the identified mathematical model that describes its thermal dynamics.

These temperatures are then compared with safety margins set by the user, typically boiling temperatures, quality restrictions or even technical limitations.

4.5.7 Setpoint

When the calculated temperature setpoints remain within the preset safety margins, a new setpoint value for the jacket temperature of the reaction calorimeter, $T_{j,set}^{RC1}$, is computed from the calculated T_r^{indus} according to Eq. 4.2. This procedure allows the anticipation of the control dynamics of the reaction calorimeter. If the calculated temperature falls outside the permissible limits, then it triggers the safe mode: T_r^{RC1} is set to a safe temperature predefined by the user.

4.5.8 Reiteration

The routine of measuring temperatures, computing q_{rx}^{RC1} , scaling it up and determining a new jacket temperature setpoint for the reaction calorimeter is continued until the reaction has reached its end time defined by t_{rx} or has to be terminated because the preset safety margins have been reached.

4.5.9 Block diagram

Having specified the frame of the scale-down methodology, we now discuss how this control strategy could be implemented. A block diagram of the temperature control system of the RC1 is shown in Fig. 4.8, p. 93. It consists in a *negative feedback control* strategy. Note that this block diagram describes the flow of information within the control system. The control objective for the scale-down approach is to adjust the reaction mixture temperature of the RC1, T_r^{RC1} , to that calculated of the industrial reactor, T_r^{indus} , to be simulated.

If the controlled variable is indeed the RC1 temperature, the manipulated variable is the temperature *setpoint* of the industrial reactor ($T_{r,set}^{indus}$ or $T_{j,set}^{indus}$ for T_r - or T_j -mode respectively). This temperature is accessible on-line via the Visual Basic window, that establishes the external data source communication (see Fig. 4.2, p. 80). The sources of disturbance are first the heat transfer dynamics and second, in case of a chemical reaction, the heat production rate calculated on-line in the Excel sheet. They allow the calculation of T_r^{indus} , which is then compared to T_r^{RC1} .

At each timer event, the operation of the temperature control system can be summarised as follows:

- The *setpoint* temperature of the industrial reactor is read from the VB window and recorded in the Excel sheet.
- Simultaneously, the heat production rate inside the reaction calorimeter is evaluated via the procedure given by Eq. 4.8. After multiplication by the scale-up factor, $q_{rx}^{indus}(k)$ is computed in the Excel sheet.
- $T_{r,set}^{indus}(k)$, respectively $T_{j,set}^{indus}(k)$, and $q_{rx}^{indus}(k)$ serve to predict the temperature evolution of the industrial reactor, hence, $T_r^{indus}(k)$.

- $T_r^{indus}(k)$ is compared with $T_r^{RC1}(k)$ to calculate the error signal. The PI controller introduced in the Excel sheet allows then to calculate $T_{j,set}^{RC1}(k)$, according to Eq. 4.2, to control the reaction medium temperature.
- This jacket setpoint temperature is sent to the RC1 calorimeter via the external data source communication. Then, the RC1 *itself* controls the jacket temperature by means of its fast thermostating unit. This is obtained by a special PI controller that is not user defined.

The procedure is then repeated at the next timer event.

- Modes of operation

In the following sections, the possible modes of operation are briefly discussed.

• *In the absence of a chemical reaction*

The temperature of the industrial reactor is only influenced by $T_{r,set}^{indus}$, respectively $T_{j,set}^{indus}(k)$, and reflects the dynamic behaviour of the industrial reactor. $T_{r,set}^{indus}$, respectively $T_{j,set}^{indus}(k)$, can be predefined in the Excel sheet (see Fig. 4.5, p. 84) or adapted on-line via the VB window. This mode of operation allows to check if the PI parameters of the Excel controller are adequate.

• *In the presence of a chemical reaction*

The temperature of the industrial reactor is influenced by both $T_{r,set}^{indus}$, respectively $T_{j,set}^{indus}(k)$, and q_{rx}^{indus} . Note that once again, $T_{r,set}^{indus}$, respectively $T_{j,set}^{indus}(k)$, can be a value predefined in the Excel sheet or adapted on-line. If q_{rx}^{indus} is known from a previous experiment and assumed not to be temperature dependent, then $T_{r,set}^{indus}(k)$, respectively $T_{j,set}^{indus}(k)$, can be off-line optimised for $T_r^{indus}(k)$ to follow the desired profile. Then, deviations during the scale-down experiment will directly reflect the dependency of the heat production rate on temperature.

As the whole methodology is based on heat balances, the feed rate of the RC1 scale-down experiment, in case of a semi-batch reaction, has to be kept at the desired value for the laboratory and full scale equipment temperatures to be comparable. Therefore, $m_r^{RC1}(k)$ should also match industrial conditions. For most standard semi-batch operations, a constant dosing profile is applied and, hence, the dosing control loop provided by the RC1 evaluation software is sufficient. If a segmented profile is wished, with for each of them a constant rate, then a series of dosing control loop actions can be inserted in the evaluation software program prior to the experiment.

Moreover, with the proposed approach, the temperature reached in case of a cooling failure, $T_g(t)$, can be easily evaluated on-line using Eq. 2.9, p. 16. Based on the constraint of a safety maximum temperature, the optimum feed rate can be defined and adapted, fitting in with the work of Ubrich [127].

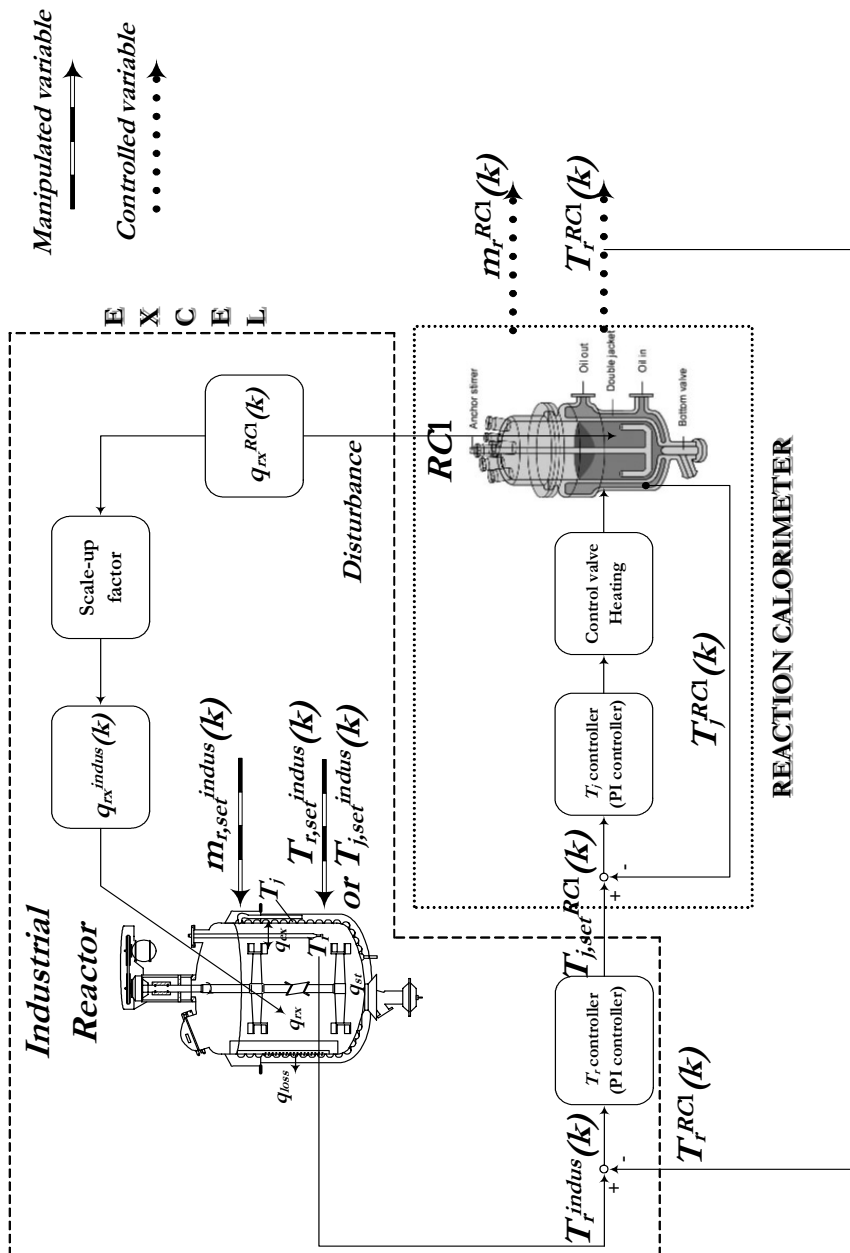


Figure 4.8: Block diagram of the scale-down strategy.

4.6 Conclusions

The new evaluation software developed by Mettler Toledo, WinRC ALR, allows the RC1 and an external data source to communicate, i.e. to send and receive values and to control the RC1 by preset or calculated parameters.

Controlling the jacket temperature of the RC1 rather than the one of the reaction medium allows a faster and more accurate temperature adaptation over time. The proportional and integral parameters of the PI controller can be adapted depending on the temperature ramp that has to be reached or on the heat capacity of the reaction medium.

The invaluable advantage of the scale-down method proposed in § 4.5 is that the kinetics of the reaction are not a prerequisite to predict the thermal behaviour of the process plant, but only the temperature dynamics of the industrial reactor and the instantaneous heat production rate are needed. It is also important to highlight that the modelling of the industrial thermal dynamics needs only to be accomplished once. After that, the temperature course of the reactor during any chemical reaction can be simulated (for more information on the way to characterise the internal heat transfer coefficient h_r of full scale equipment using the RC1, see the «Wilson plot» technique p. 19 & 111).

The dynamics of nine industrial reactors being now characterised and a method to predict their thermal behaviour during a chemical reaction at laboratory scale using the RC1 being elaborated, the next step would be the comparison of laboratory and plant temperature profiles. But before that, the scale-down methodology has to be tested. For this purpose, the power delivered through the calibration probe of the RC1 will be controlled by an external voltage source. This is the topic of the next chapter.

Chapter 5

PUTTING THE SCALE-DOWN STRATEGY INTO PRACTICE

5.1 Introduction

Now that a complete sample of commonly encountered industrial reactors has been characterised and the scale-down methodology has been developed, a logical continuation would be the comparison of temperature evolution between laboratory and plant vessels during chemical reactions. However, in order to test the scale-down procedure proposed in the previous chapter, in particular the two consecutive on-line heat balances, the power provided by the RC1 calibration probe was controlled by an external voltage source. In so doing, the heat release rate provided to the reaction medium is known with great accuracy. If the applied on-line heat balance is correct and in absence of side effects such as mixing energy or local solvent evaporation, the same heat production rate should be found by the on-line heat balance.

It is a crucial point to ensure that the on-line heat balance methodology is correct. Indeed, the temperature of the reaction medium inside the calorimeter is not constant anymore when the scale-down method is applied. Therefore, it is mandatory to test and validate the procedure described in § 4.5 to control that the heat production rate calculated on-line would correspond to that obtained in the full scale reactor. Actually, higher temperatures can generate side reactions and thus lead to a different heat production rate compared with isothermal experiments. Moreover, the reaction enthalpy is temperature-dependent.

The first section of the present chapter explains the way to control the power delivered in the RC1 calibration probe. Then, its application to the scale-down approach will be presented. This will reveal the importance of the reactor dynamics on the temperature evolution. Finally, the hydrolysis of acetic anhydride and a simulation of a polymerisation reaction will be studied as test reactions.

5.2 Calibration probe controlled by an external voltage source

5.2.1 Principle

During normal operating conditions, the RC1 calibration probe is used to calculate the parameter $U \cdot \mathcal{A}$ of the reaction medium at a given temperature. A known and constant power is delivered during a defined time interval (typically 10 min) while the jacket temperature adapts itself in order to maintain isothermal conditions. To calculate $U \cdot \mathcal{A}$, the area under the $(T_r^{RC1} - T_a^{RC1})$ curve in the region of determination is compared with that of the calibration power q_{cal}

$$U \cdot \mathcal{A} = \frac{\int_{t_0}^{t_f} q_{cal} \cdot dt}{\int_{t_0}^{t_f} (T_r - T_a) \cdot dt} \quad (5.1)$$

q_{cal} is normally either 5 W (used with organic solvents or with the 0.8 L SV01 glass reactor) or 25 W. In fact, the RC1 applies a constant voltage of 17 V to the calibration probe, whose resistance varies (57.80 Ω for 5 W and 11.56 Ω for 25 W).

Therefore, by modulating the voltage applied to the probe, it is possible to obtain a varying power over time. In this way, the calibration probe can mimic the thermal effect of a chemical reaction.

5.2.2 Development

In the final version, the power provided by the standard Mettler Toledo 25 W calibration probe (Me-51103807, HC hastelloy) was controlled by an external voltage source composed by an ADLINK[®] cPCI/PCI-6208V 8-Channels 16-Bit Voltage Output Card [132] installed on a Desktop PC (Pentium[®] 4, 2.53 GHz, 512 MB of RAM). Each channel was equipped with a digital to analog converter. The voltage was controlled by a Labview[®] executable [133] (see Fig. 5.1). The card is then connected to an ADLINK[®] DIN-37D termination board [134], which is a universal

screw termination board with a DIN socket. The output voltage is amplified four times by an external voltage source before being transmitted to the calibration probe itself. The executable allows delivering constant, exponential, sinusoidal or polynomial (6th order) powers as a function of time, whereas the probe material allows a maximum power of about 120 W, which is sufficient to simulate most common chemical reactions at this scale.

The development work was jointly executed with Lavanchy [135] in collaboration with electronics technicians at the EPFL.

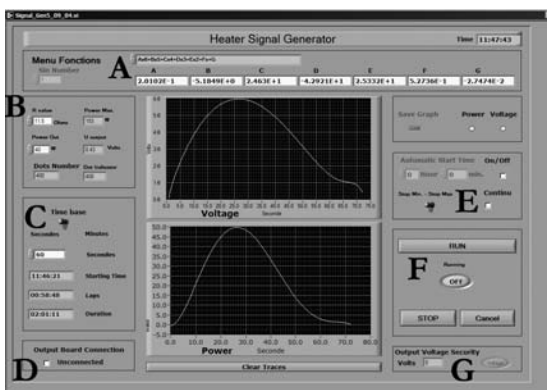


Figure 5.1: Representation of the Labview[®] executable used to control the Mettler Toledo 25 W HC calibration probe, with the voltage signal panel (above) and the corresponding power signal panel (below). A: function selection; B: resistance of the calibration probe (user-defined); C: experiment duration; D: connection to the calibration probe; E: automatic start time; F: run button; G: output voltage security.

In summary, if considering only the thermal aspect, any heat production rate of a chemical reaction can be fitted and reproduced via the calibration probe.

5.2.3 Validation

The controllable calibration probe was validated with experiments within a Dewar[®] reactor whose C_w (in $\text{J}\cdot\text{K}^{-1}$) was determined using a constant power source of 240 W during about 3 min. The Dewar[®], with the inserted Mettler Toledo calibration probe, was filled with water. The Labview[®] executable was then run with a predefined power function and the temperature recorded with a

Pt-100 sensor. Each function of the program has been validated with a least-square fit using the software Madonna[®] [122], the variable parameter being precisely the C_m value of the Dewar[®]. Experiments are validated if the identified value is within 10 % of the mean measurement obtained previously. The somewhat large uncertainty is due to the poor precision of the experiment duration.

5.3 Purely thermal reactions

A hypothetical exothermic reaction was simulated via the calibration probe. Its heat of reaction is approximately 82 kJ and lasts for 1 h. It is simulated using the following 6th order polynomial equation:

$$q_{cal} = 4.412 \cdot 10^{-9} \cdot t^6 - 3.414 \cdot 10^{-6} \cdot t^5 + 4.865 \cdot 10^{-4} \cdot t^4 - 2.543 \cdot 10^{-2} \cdot t^3 + 4.503 \cdot 10^{-1} \cdot t^2 + 2.813 \cdot 10^{-1} \cdot t - 4.396 \cdot 10^{-1} \quad (5.2)$$

with t denoting the time expressed in minutes. Fig. 5.2 shows the corresponding power curve. It corresponds to a reasonable reaction enthalpy at this scale.

This so-called «thermal reaction» was first performed using the classical RC1, filled with water, at two different temperatures in order to find its characteristic parameters (C_p' , UA , q_{loss}) and their thermal dependence. Then, the same signal was delivered by the calibration probe but using the modified RC1 (on-line heat balance) while simulating various industrial reactors.

5.3.1 Classical RC1

1.068 kg of deionised water was introduced in the 2 L glass reactor and heated up to 45 °C. A UA and C_p' determination was performed before the «thermal reaction», then the controllable calibration probe was interlocked under isothermal conditions at 50 °C and another UA and C_p' determination was run after «reaction». As by simulation, the temperature inside reactor R_2 , the slowest one tested in this part, would increase up to about 58 °C if this «thermal reaction» took place in it, the same procedure was carried out at 60 °C in order to take into account the changes of UA , C_p' and q_{loss} with temperature.

The baseline was chosen to be proportional to conversion and the heat balance was calculated by:

$$q_{rx} = q_{ex} + q_{acc} + q_{loss} \quad (5.3)$$

with q_{acc} the accumulation term corresponding to:

$$q_{\text{aux}} = m_r \cdot C_p(T_r) \cdot \frac{dT_r}{dt} \quad (5.4)$$

and q_{ex} , q_{loss} as previously described (see Eqs. 4.6 & 4.8, p. 89).

Fig. 5.2 compares the heat production rates determined at both 50 and 60 °C to that delivered by the probe. It shows that isothermal conditions and great accuracy of temperature measurement permit to reconstruct almost exactly the original signal, the error being less than 1 % (the generally accepted standard deviation being of 5 %). As soon as the probe is interlocked, the classical RC1 detects the heat dissipated. This means that no time delay occurs, no significant heat is accumulated within the probe and no heat loss due to local evaporation takes place. Moreover, with the baseline correction, the heat production rate calculated before and after the «reaction» is precisely zero.

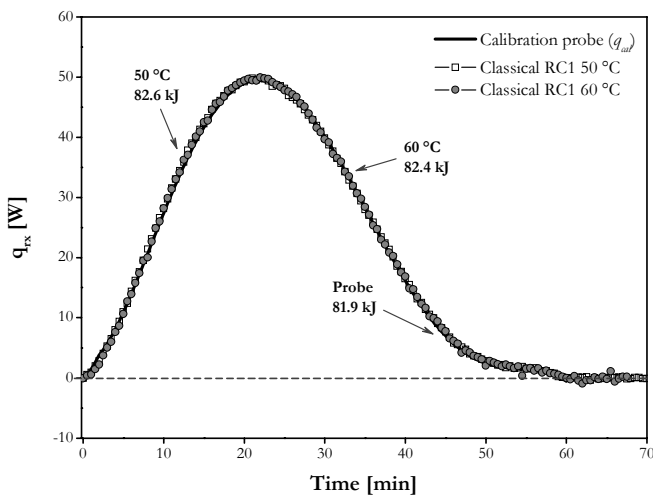


Figure 5.2: Comparison of the controlled power delivered via the calibration probe and the powers of «reaction» determined in the classical RC1 at 50 °C and 60 °C.

Fig. 5.3 shows the corresponding jacket and reaction medium (water) temperatures during this experiment. The fast adaptation of the jacket allows maintaining quasi isothermal conditions, the maximum deviation being of 0.5 °C. In the absence of reaction, the temperature difference between the jacket and reaction medium is obviously more important at 60 °C because the heat losses increase with temperature. It is this type of T_r -dependency that the procedure described in § 4.5, p. 85 has to take into account.

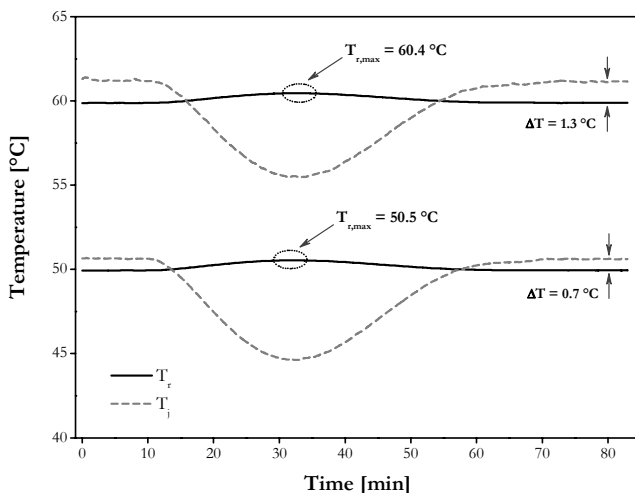


Figure 5.3: Comparison of the reaction medium (solid lines) and jacket (dash lines) temperatures recorded in the classical RC1 during the experiment with the controlled calibration probe.

5.3.2 Modified RC1¹

From the results obtained with the classical RC1, the scale-down method can then be applied. The same amount of water was introduced in the 2 L AP01 reactor and heated up to 50 °C. Once the communication with the external data source (Excel) was established, the same power was delivered by the calibration probe using the Labview[®] executable.

Three different industrial reactors have been simulated:

Table 5.1: Industrial reactors simulated during the experiments with the controlled calibration probe.

Reactor	Nominal volume [L]	Initial mass simulated [kg]	Stirrer speed [rpm]	Setpoint [°C]	Regulation mode
R ₂	49	30	80	50	T_j
R ₄	630	600	50	50	T_r
R ₅	630	600	60	50	T_r

1. Reminder: the term «modified RC1» refers to the RC1 with new WinRC ALR evaluation software combined with the scale-down methodology. The calorimeter *itself* was not modified.

The used conditions correspond each time to an important filling ratio, thus minimising vortex influence on heat transfer area. The main difference, apart from its nominal volume, is that reactor R_2 can work only in T_j -mode (control of solely the jacket temperature). In this case, T_j^{indus} was simulated as constant at 50 °C, whereas for the two other reactors, working in T_r -mode, the *setpoint* was constant at 50 °C, implying a variable T_j setpoint. Before «reaction», both T_r^{indus} and T_j^{indus} were always considered as being stable at 50 °C.

Fig. 5.4 compares the temperature evolutions of the industrial reactors if the same «thermal reaction» as described above, multiplied by the corresponding scale-up factor, took place. Note that these temperatures were recorded in the reaction calorimeter, meaning that if T_r^{RC1} indeed corresponds to that of industrial conditions, T_j^{RC1} is however not the same as T_j^{indus} . It is the RC1 jacket temperature that allows T_r^{RC1} to track T_r^{indus} . This is the reason why T_j^{RC1} *increases* for reactor R_2 but *decreases* for reactor R_4 & R_5 . In comparison, T_j^{indus} decreases down to about 37 °C for R_4 & R_5 . Moreover, T_r^{RC1} corresponds in this case to T_{cf} (see Eq. 2.9, p. 16) since, by definition, there is no accumulation if the probe is switched off when an hypothetical cooling failure occurs.

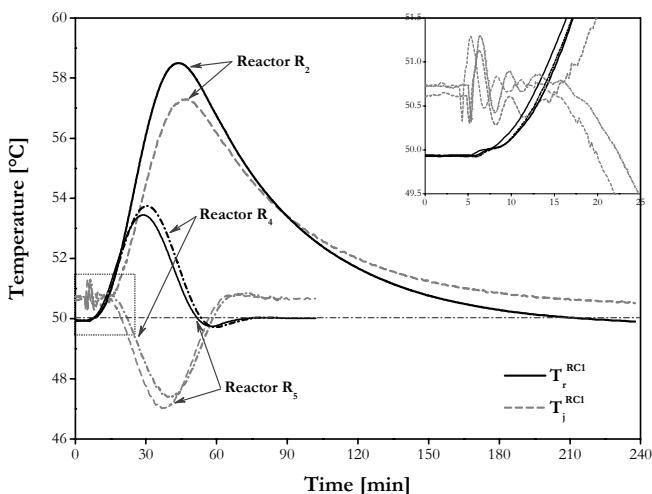


Figure 5.4: Comparison of temperature evolutions between industrial reactors R_2 , R_4 and R_5 obtained in the modified RC1 using the scale-down procedure. AP01 reactor filled with 1.07 kg of deionised water. «Thermal reaction» delivered through the controlled calibration probe.

From the plotted curves, it is obvious that the various dynamics are very different. Although the ratio of heat exchange area to volume of reactor R_2 is the most favourable, it has the slowest dynamics and the poorest temperature control. This difference is explained by the installed heating/cooling system: a thermostat/cryostat with an efficiency corresponding to $\sim 1.5 [^{\circ}\text{C}\cdot\text{min}^{-1}]$ for water (see § 3.4.2, p. 58). Moreover, the fact that only the jacket temperature can be controlled does not contribute to compensate for this problem.

As expected, since the way they are heated up and cooled down and the simulated masses introduced are the same, R_4 & R_5 exhibit comparable behaviours. The slight difference can be explained by the higher heat exchange area (2.5 instead of 2.2 m^2) and, to a lesser extent, by the faster stirrer revolution speed of reactor R_5 . Their behaviour at the beginning of the «reaction» is more or less the same as for reactor R_2 , but as the reaction medium temperature moves away from its setpoint, then the efficiency of their controller becomes evident.

The framed graph in Fig. 5.4, zooming in on the beginning of the experiment, displays oscillations of the jacket temperature that become blurred during the «reaction». The PI parameters applied are therefore relatively aggressive. Nevertheless, they allow a fast adaptation of T_r^{RC1} , the average deviation with the calculated T_r^{indus} being of $0.03 ^{\circ}\text{C}$. Moreover, these oscillations did not have a negative impact on the on-line heat balance. The use of T_a , the corrected jacket temperature (see § 4.5.4, p. 89), can to a large extent overcome this issue.

If it is true that the absolute temperature difference between the three reactors is only about $5 ^{\circ}\text{C}$, when comparing them with the ΔT_{ad} the situation appears more contrasted. A maximum temperature increase of $8.5 ^{\circ}\text{C}$ for reactor R_2 corresponds to 45% of ΔT_{ad} , whereas an increase of $3.4 ^{\circ}\text{C}$ for R_5 corresponds only to 18% , i.e. 2.5 times less. This suggests that the more important ΔT_{ad} the more pronounced the differences between industrial reactors.

As outlined in the introduction, the parameter q_{rx} calculated on-line must correspond to the correct heat production rate within a tolerable standard deviation of 5% . Fig. 5.5 compares two $q_{rx}^{on-line}$ with the power delivered by the calibration probe. In this case, the power exchanged between the jacket and the reaction medium, q_{ex} was calculated by:

$$q_{ex}^{RC1}(\dot{k}) = U \cdot A \cdot (T_r^{RC1}(\dot{k}) - T_j^{RC1}(\dot{k})) \quad (5.5)$$

If the total heat, i.e. the integration of q_{rx} lies in this interval, the signal is shifted by about 1.5 min because the heat capacity of the reactor wall and hence its time constant was not taken into account. Therefore, it became evident that the use of the corrected jacket temperature T_a was necessary, the scale-down method being exclusively based on non-isothermal conditions.

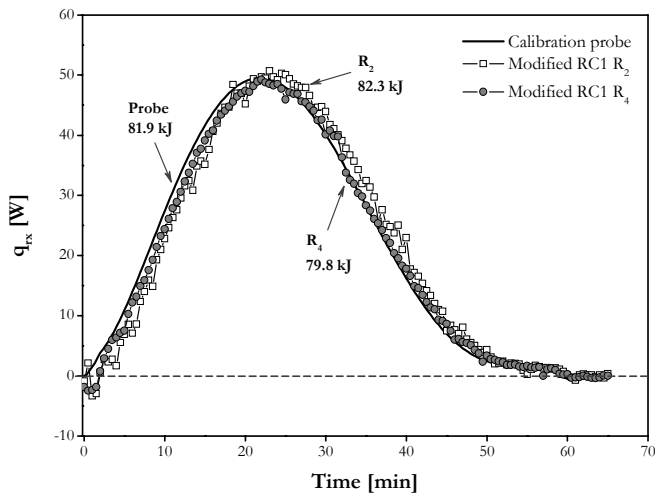


Figure 5.5: Comparison of the controlled power delivered by the calibration probe and the powers of «reaction» determined without T_d -model in the modified RC1 simulating reactors R_2 and R_4 .

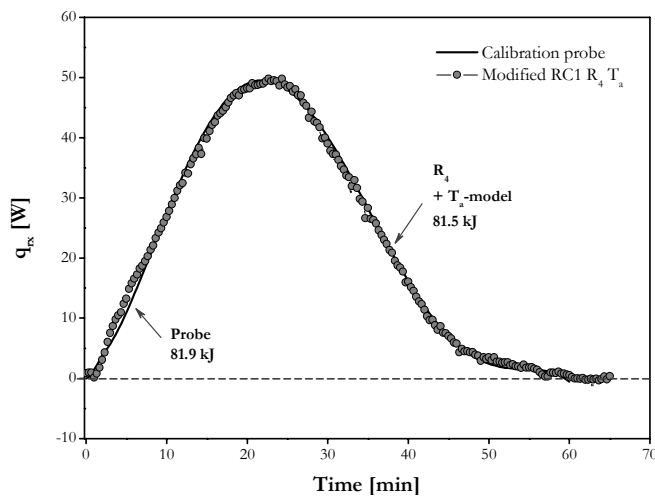


Figure 5.6: Comparison of the controlled power delivered by the calibration probe and the power of «reaction» determined with T_d -model in the modified RC1 simulating reactor R_4 .

When using the T_a -model, not only the integral value, but above all the heat production rate is appreciably more correct. However, compared with isothermal conditions, the signal is more affected by noise, owing to the usual difficulty to obtain reliable calorimetric results in dynamic mode. Note that the situation showed in Fig. 5.6 for reactor R₄ can be generalised to the other ones. These experiments show that the scale-down methodology is correct and robust.

As described in page 80, the reaction medium or jacket setpoint is accessible on-line. If, for safety or quality reasons, the temperature must not exceed 50 °C, the setpoint has to be reduced at the beginning of the experiment. This has been done for reactor R₄. The RC1 was filled with the same amount of deionised water (1.07 kg) and the same power as previously was delivered via the calibration probe. However, as soon as the external data source communication was established, the setpoint of the reaction medium was changed to 45 °C. In the middle of the «reaction», hence after 30 min, it was changed again, this time up to 50 °C. During a second experiment, the setpoint was always set to 45 °C. Fig. 5.7 shows the water and jacket temperatures recorded in the RC1 for these trials. Two combined effects explain the singular shape obtained: that of the setpoint, forcing T_r^{RC1} to decrease at the beginning and that of the «reaction» that rises it again when q_{rx} becomes maximal after 30 min.

Normally, since setpoints and heat production rates are similar, the curves recorded should be perfectly superimposed during the first 30 min. However, a maximum temperature difference of 0.3 °C is observed. Although this corresponds to the intrinsic error of the on-line calculated q_{rx} , the deviation remains in an acceptable domain. However, it should be mentioned that this could become an issue for very exothermic and very temperature sensitive reactions, in which case a greater absolute deviation would occur. But as said previously, an error of 5 % for q_{rx} is generally tolerated when working with bench scale reaction calorimeters.

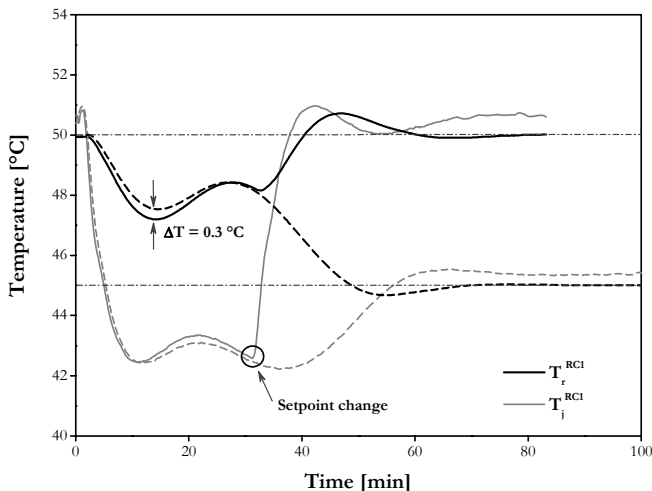


Figure 5.7: Comparison of temperature evolutions obtained in the modified RC1 simulating reactor R_4 . Straight lines: $0 < t < 30$ min: setpoint = 45 °C, $t > 30$ min: setpoint = 50 °C; dash lines: setpoint = 45 °C. AP01 reactor filled with 1.07 kg of deionised water, «thermal reaction» delivered through the controlled calibration probe.

In fact, if q_{rx} is known from previous experiments and assumed to be constant (non temperature dependent), the profiles depicted in Fig. 5.7 could be forecast with the help of the reactor dynamics modelling. After that, the results could be checked with the modified RC1. Changes of heat production rate with temperature due to side reactions would be highlighted. Based on new results, modelling of the reaction path could be improved, and the procedure repeated. At any time, the reaction can be run at plant scale and if small deviations with the laboratory results are observed, the industrial reactor model can also be improved. Therefore, the scale-down methodology proposed here can be a powerful tool for process optimisation, and this at laboratory scale. Moreover, it consists in a cognitive routine, for which each stage provides sufficient information to considerably reduce the time needed to reach a viable process, from both an economic and a safety point of view.

5.4 Hydrolysis of acetic anhydride

5.4.1 Purpose

A test reaction was chosen to control whether the scale-down strategy also works with «usual» chemical reactions (so far, only thermal signals via the calibration probe were used to simulate an exothermic reaction). It is the reaction proposed by the tutorial of the WinRC help files: the hydrolysis of acetic anhydride to form acetic acid, a reaction commonly found in publications dealing with calorimetry.

5.4.2 Experimental conditions

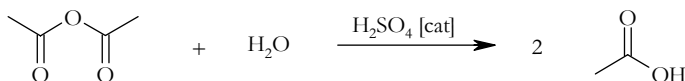


Figure 5.8: Reaction schema of the hydrolysis of acetic anhydride.

The conditions used in the classical RC1 are as follows:

- 650 g of deionised water is added to the inertised 2 L AP01 glass reactor
- 2 g of H_2SO_4 as catalyst is added manually
- 51 g of acetic anhydride is added in 5 min using a ProMinent® pump connected to the RD10 dosing controller
- the temperature of the reaction mass is held constant at 50 °C

With the aim of highlighting the dosing effect, an experiment with 153 g of acetic anhydride added in 10 min (i.e. a dosing profile 1.5 times faster) was also performed. Table 5.2 displays an overview of the experimental conditions. All reactants were used without further treatment.

Table 5.2: General conditions used for the hydrolysis of acetic anhydride.

Property or substance	Type [-]	Mass [g] or speed [rpm]	Temperature [°C]	Dosing time [min]
Water	deionised	650.0	50	batch
H_2SO_4	Fluka 84721	2.0	50	batch
Acetic anhydride	Fluka 45830	51.0/153.0	room	5/10
Stirrer	anchor, glass	100	-	-

Table 5.2: General conditions used for the hydrolysis of acetic anhydride.

Property or substance	Type [-]	Mass [g] or speed [rpm]	Temperature [°C]	Dosing time [min]
Calibration probe	25 W, glass	-	-	-
Inertisation	nitrogen	-	-	-

The same reaction was also performed at 60 °C (for both dosing profiles) and 70 °C (for fast dosing) in order to take $U\mathcal{A}$, Cp_r ' and losses changes with temperature into account.

5.4.3 Classical RC1 results

When using the reaction calorimeter under isothermal conditions, a predefined phase for the $U\mathcal{A}$ and Cp_r ' determination is inserted *before* and *after* reaction. It allows the RC1 to complete the heat balance and to calculate the thermal data of the reaction. The most relevant results for the hydrolysis of acetic anhydride are given in Table 5.3:

Table 5.3: Main results of the hydrolysis of acetic anhydride in the classical RC1.

Temperature [°C]	Dosing [g·min ⁻¹]	Q _{rx} [kJ]	ΔH _{rx} [kJ·mol ⁻¹]	ΔT _{ad} [K]	MTSR [°C]
50	10.2	-27.6	-55.3	10.6	54.5
50	15.3	-84.0	-56.0	32.1	58.3
60	10.2	-30.6	-61.3	11.9	63.6
60	15.3	-83.9	-56.0	32.8	65.2
70	15.3	-82.1	-54.8	31.4	73.1

The determined mean reaction enthalpy corresponds to -56.7 ± 2.6 [kJ·mol⁻¹], a value comparable to that of -56.6 ± 4.0 [kJ·mol⁻¹] at 25 °C found in the literature [136] as well as -56.1 [kJ·mol⁻¹] at 50 °C based on on-line tabulated standard enthalpies of formation and heat capacities [110]. The heat of reaction clearly greater for the experiment at 60 °C is explained by a too aggressive dosing: at each pump stroke, a large amount of acetic anhydride is injected into the reaction medium resulting in a jagged heat production rate. Nevertheless, the reaction enthalpy is situated within the accepted error of 5 %. Moreover, in a general manner, the reaction enthalpy is not affected by a temperature change between 50 and 70 °C. The heat release rates plotted in Fig. 5.9 reveal that the lower the temperature, the greater the accumulation. Apart from this logical effect, more interesting is the fact that a faster dosing does not result in a greater accumulation, on the contrary. The concentration of acetic anhydride being greater in the reaction medium, the reaction kinetic is consequently accelerated, thus reducing the non reacted fraction. Therefore, the maximum temperature of the synthesis reaction (*MTSR*) that could be reached in case of a cooling failure differ only from a few degrees contrary to the adiabatic temperature rise.

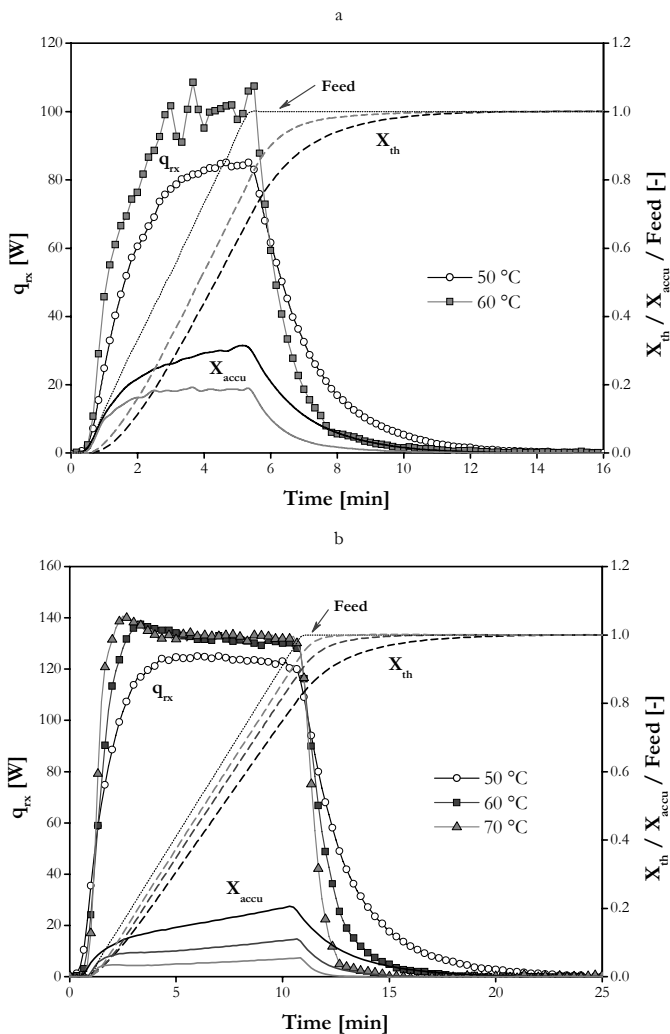


Figure 5.9: Heat production rates (q_{rx}), thermal conversions (X_{th}), thermal accumulations (X_{accu}) and feeds obtained in the classical RC1 for the hydrolysis of acetic anhydride. a: 51 g of acetic anhydride dosed in 5 min; b: 153 g dosed in 10 min.

5.4.4 Modified RC1 results

- Slow dosing profile (51 g of acetic anhydride dosed in 5 min)

The hydrolysis was then repeated using the scale-down procedure, i.e. the reaction calorimeter was forced to follow the investigated dynamic behaviour of the industrial reactor. Three industrial reactors have been simulated (see Table 5.4): the 49 L R_2 (in T_j -mode, with jacket temperature constant at 50 °C), the 630 L R_4 (in T_r -mode, reactor setpoint temperature of 50 °C) and the 25 m³ R_9 (in T_j -mode, with jacket temperature held constant at 50 °C).

Table 5.4: Industrial reactors simulated during the hydrolysis of acetic anhydride.

Reactor	Nominal volume [L]	Initial mass simulated [kg]	Stirrer speed [rpm]	Setpoint [°C]	Regulation mode
R_2	49	30	80	50	T_j
R_4	630	600	50	50	T_r
R_9	25'000	22'000	50	50	T_j

Table 5.5 summaries the results ($T_{r,max}$ is the maximum temperature reached in the RC1 during the reaction). The reaction enthalpies determined on-line are close to that of isothermal experiments, although slightly lower in general.

Table 5.5: Main results of the hydrolysis of acetic anhydride using the scale-down approach.

Simulated reactor	Q_{rx} [kJ]	ΔH_{rx} [kJ·mol ⁻¹]	$T_{r,max}$ [°C]	MTSR [°C]
R_2	-28.4	-57.2	56.5	57.5
R_4	-26.8	-54.0	55.7	57.6
R_9	-26.0	-52.4	57.6	59.5

Using the reaction calorimeter in a classical manner (isothermal conditions) leads to a maximum temperature deviation of about 1.3 °C. Using the scale-down methodology, the behaviour is quite different. Fig. 5.10a shows that industrial reactors working in T_j -mode, with constant jacket temperature, are slower than those working in T_r -mode. The needed time to reach the 50 °C setpoint temperature differs especially. In practice, the jacket setpoint temperature would be adapted as a function of the reaction rate. However, the maximum temperature reached during the reaction as well as the MTSR are not really affected by the choice of the industrial reactor. The main reasons are first that the dosing time (5 min) is by far shorter than the reactors time constants, not leaving enough time for the temperature controller to react until the end of addition, and second that the temperature rise under adiabatic conditions is low ($\Delta T_{ad} = 11$ °C). Note that for simulated reactors R_2 and R_9 , the RC1 jacket temperature needs to heat the reaction medium in order to tracks the temperature modelled in Excel. It proves again that the control of the calorimeter behaviour by the external data source works as intended.

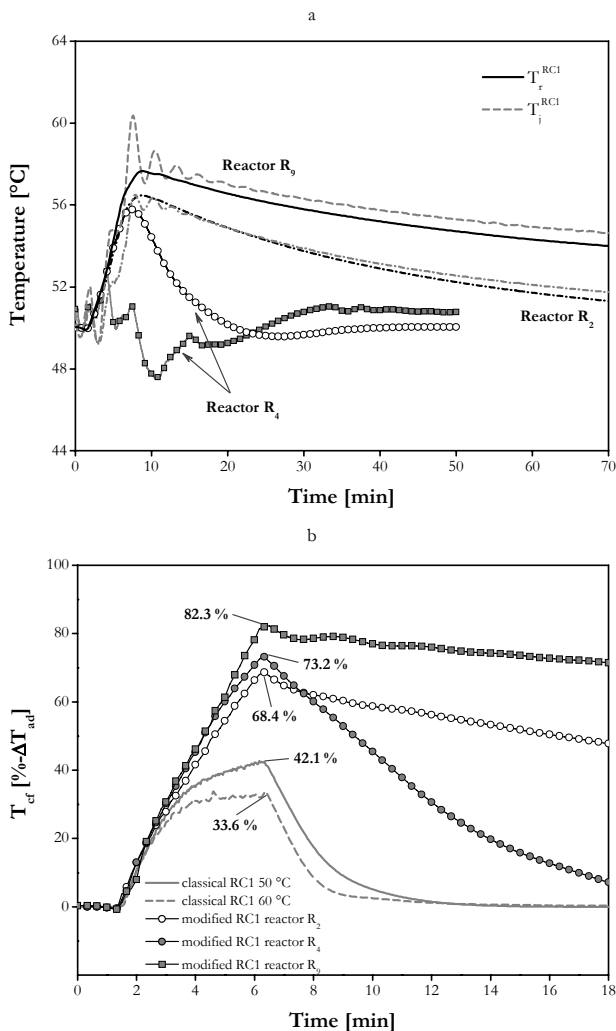


Figure 5.10: Hydrolysis of acetic anhydride (51 g of acetic anhydride dosed in 5 min in 650 g of deionised water). a: comparison of temperature evolutions obtained in the modified RC1 simulating industrial reactors R_2 (49 L) and R_4 (630 L) and R_9 (25 m³); b: comparison of T_{cf} s expressed in percentage of the ΔT_{ad} between the simulated reactors and the isothermal results.

One of the essential applications of the scale-down methodology is to perform a realistic safety analysis of the process, i.e. to predict the temperature course under normal operating conditions and also in case of deviations from these conditions. In this context, the temperature that may be reached in case of a cooling failure (T_{cf}) plays an important role. Fig. 5.10b compares the temperature evolutions in case of a cooling failure between the simulated industrial reactors and the classical RC1 experiments at 50 and 60 °C. T_{cf} is expressed in percentage of the adiabatic temperature rise. It is important to realise that even if thermal accumulations are comparable, $MTSR$ are higher for simulated industrial reactors. The reason is that their *starting* temperatures, when the cooling failure occurs, are higher. This effect is only due to the industrial reactors dynamics and not to the chemical reaction. If, in absolute temperature, $MTSR$ differ by only several degrees, in percentage the variation is much more important. For the biggest simulated reactor, it corresponds to the double of the isothermal experiment (82.3 vs. 42.1 % of ΔT_{ad}). This allows to foresee a totally different deviation, in degrees, in the case of more exothermic reaction and hence of a greater ΔT_{ad} for a same dosing time.

- Wilson plot

So far, the calculation of the inner film coefficient was based solely on the physical and chemical properties of water. Indeed, water represents more than 92 % of the reaction mass. However, for most chemical reactions, either the physical and chemical properties of the reaction medium are unknown, or the medium contains a mixture of diverse solvents, or the reaction mass is heterogeneous. Hence, a more general approach is required. For these cases, the «Wilson plot» method can be used. It allows the determination of the resistance of the inner film inside the reaction calorimeter from calorimetric calibrations at various stirrer speeds in isothermal mode. From the obtained results, reactor specific constants can be derived. Based on these constants, scale-up calculations for reactors of similar geometry and Newtonian fluids can be made (see Eq. 2.15, p. 20, the viscosity ratio at the reactor and wall temperatures being neglected). The determination of the overall heat transfer coefficient U requires the knowledge of the exact heat exchange area, the latter being evaluated visually.

Applying the Wilson method, the most reliable regression results are obtained with calibrations over a wide range of agitator speeds, but attention must be paid to vortex formation at high speeds. Therefore, the filling ratio should be comprised between 70 and 80 % of the total volume, that is, between 1.4 and 1.6 L in the AP01 vessel. At the lower end of the stirring range, the work should not be performed in the transition region between laminar and turbulent flow [61]. Through repeated calibration under the same conditions, the standard deviation of the Wilson plot regression can be reduced.

For this experiment, 1.50 kg of deionised water was introduced in the reaction calorimeter vessel equipped with an anchor stirrer. The UA coefficient was evaluated at 75, 100, 125, 150 and 175 rpm under isothermal conditions at 50 °C. Fig. 5.11 depicts the Wilson regression obtained. The highest deviation arose at maximum agitator speeds since the virtual volume is not exactly defined due to the fluctuating surface and to the fact that the tip of the calibration probe was no more sufficiently immersed in water. This measurement point was therefore not included into the evaluation.

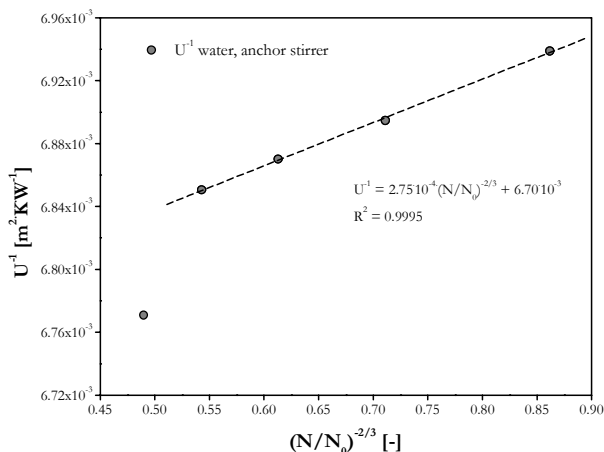


Figure 5.11: Wilson plot: 1.50 kg of deionised water ($T_r = 50^\circ\text{C}$) in 2 L AP01 reactor fitted with an glass anchor stirrer. Arbitrary reference speed N_0 equals to 60 rpm.

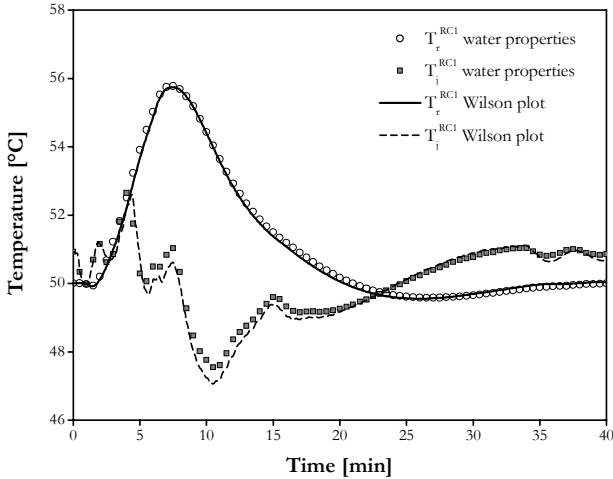


Figure 5.12: Hydrolysis of acetic anhydride: comparison of temperature evolutions within the RC1 between $h_{r,p}$ calculated from the properties of pure water and $h_{r,p}$ determined with the help of the Wilson plot.

Based on the Wilson plot, the internal heat transfer coefficient at plant scale ($h_{r,p}$) in reactor R₄ (nominal volume: 630 L) is equal to about 6'690 [W·m⁻²·K⁻¹] instead of a mean value of 4'340 [W·m⁻²·K⁻¹] calculated from the physical properties of water. In fact, the physical properties of water are such, that the main heat transfer resistance in the RC1 is that of the wall. Consequently, the overall heat transfer coefficient is not significantly affected by the stirrer revolution speed (1.3 % of variation from 75 to 150 rpm).

The hydrolysis of acetic anhydride (51 g of anhydride dosed in 650 g of deionised water in 5 min) was then repeated using the Wilson plot value of the internal heat transfer coefficient of plant equipment, $h_{r,p}$. The recorded temperatures in the RC1 are very similar to previous experiment (see Fig. 5.12), the main heat transfer resistance being also that of the wall for industrial reactor R₄. Note that the heat production rate calculated on-line during this experiment is also comparable. Later on, the estimation of the internal heat transfer resistance at plant scale will always be determined with the help of a Wilson plot.

- Fast dosing profile (153 g of acetic anhydride dosed in 10 min)

As expected, with a faster and larger dosing, the dynamic differences between industrial reactors are more highlighted (see Fig. 5.13).

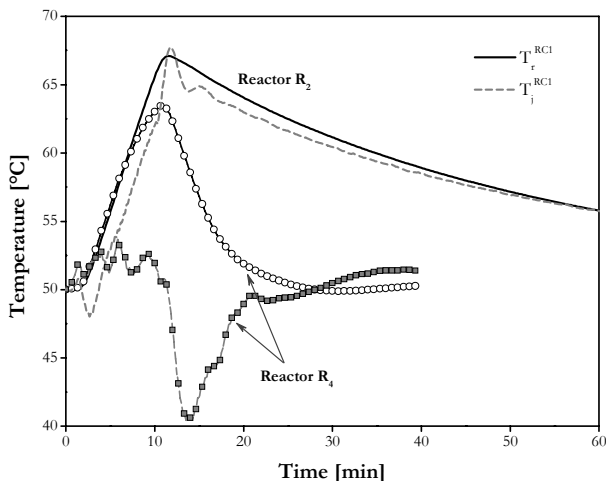


Figure 5.13: Hydrolysis of acetic anhydride (153 g of acetic anhydride dosed in 10 min in 650 g of deionised water): comparison of temperature evolutions obtained in the modified RC1 simulating industrial reactors R_2 (49 L) and R_4 (630 L).

The maximum temperature reached in the smaller reactor would be 67.1 °C, and 63.5 °C in reactor R_4 . In comparison, this difference was only of 0.8 °C during the slower dosing (see Table 5.5).

Note that the simulation conditions of reactors R_2 and R_4 correspond to those given in Table 5.4, except that the initial mass of R_2 was 500 kg instead of 600 kg to avoid overflow.

5.5 Reproduction of a polymerisation reaction

5.5.1 Purpose

In the system studied so far, the variation of the baseline, the overall heat transfer coefficient (U) or the specific heat capacity (Cp_r) during the reaction were limited (about 5 %). The baseline is generally related to two powers: q_{loss} (losses) and q_{st} (stirrer). The losses can have strong changes in non isothermal experiments and/or if the concentration of volatile compound changes during the process. The power that is released by the stirrer can be usually neglected, but it has to be considered if high variations of the apparent viscosity are expected, such as in polymerisation reactions. However, some other non linear changes in the heat transfer coefficient and/or in the

specific heat capacity are not easy to consider. This is why baselines involve very complex effects that are unknown but have to be compensated. For this kind of reaction, a method, called periodical calibration, uses the traditional calibrations during all the experiment to obtain as much values of $U \cdot A$ as possible [137]. In our case, we wanted to test if the solution to evaluate on-line the various parameters (see Fig. 4.7, p. 88) was also valid in more drastic conditions.

Instead of performing a polymerisation, the hydrolysis of acetic anhydride was again used as a test reaction, but this time a thickener was simultaneously dosed with the anhydride to increase the viscosity of the reaction mass. This allows to simulate a reaction of polymerisation with changes of overall heat transfer coefficient during the reaction, but with the advantage of an easy handling. After investigations, it appeared that Xanthan Gum was the appropriate thickener because of its high thickening ability and its cheapness (20 [€·kg⁻¹]).

Xanthan Gum is a polysaccharide produced as a secondary metabolite by a biotechnological fermentation process, based on the culture, in aerobic conditions, of a micro-organism: *Xanthomonas campestris*. Many micro-organisms, bacteria in particular, are capable of metabolising extra-cellular polysaccharides. However, Xanthan is the only bacterial polysaccharide produced industrially on a large scale. It is used in a large number of applications, as a suspending agent, emulsion stabiliser, foam enhancer, or improver of dough volume.

It is an hetero-polysaccharide of high molecular weight. Its main chain is constituted of glucose units (see Fig. 5.14).

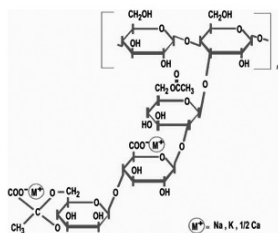


Figure 5.14: Structure of Xanthan Gum repeating unit [138].

Xanthan Gum from Texturant Systems (Degussa) [139] is sold under the brand names Satiaxane™ and Actigum™. For this study, Satiaxane™ CX 90 T (batch n° 20051341) has been used as thickener, because it is not generally affected by changes in pH value and dissolves in most acids or bases. It is an odourless and insipid powder, of white-cream to pale beige colour. The viscosity of a 1 wt-% aqueous solution is between 1'200 to 1'600 cP. The powder was manually dosed during the addition of acetic anhydride. A precise powder measure, with an Archimede's screw, guaranteed the reproducibility of the results.

5.5.2 Experimental conditions

The same conditions as for the hydrolysis of acetic anhydride were used. However, during the dosing of the anhydride, 6.1 g of Satiaxane was simultaneously and added manually. Once again, this reaction was performed twice in the classical RC1 (isothermal conditions), one time at 50 °C and the other time at 60 °C, in order to take the diverse dependencies with temperature into account. Table 5.6 presents an overview of the experimental conditions. All reactants were used without further treatment.

Table 5.6: General conditions used for the hydrolysis of acetic anhydride with Satiaxane™ as thickening agent.

Property or substance	Type [-]	Mass [g] or speed [rpm]	Temperature [°C]	Dosing time [min]
Water	deionised	650.0	50 or 60	batch
H ₂ SO ₄	Fluka 84721	2.0	50 or 60	batch
Acetic anhydride	Fluka 45830	51.0	room	5
Satiaxane	CX 90 T	6.1	room	5
Stirrer	propeller, glass	450	-	-
Calibration probe	5 W, glass	-	-	-
Inertisation	nitrogen	-	-	-

5.5.3 Classical RC1 results

A predefined phase for the U and $C_{p,r}'$ determination was inserted *before* and *after* reaction. The results are given in Table 5.7. They confirm that U drops in a significant manner (about 30 %) thanks to the thickening agent.

Table 5.7: Overall heat transfer coefficients U and specific heat capacity $C_{p,r}'$ determined with the RC1 during the hydrolysis of acetic anhydride, Satiaxane™ used as thickener.

Temperature [°C]	U before rx [W·m ⁻² ·K ⁻¹]	U after rx [W·m ⁻² ·K ⁻¹]	Variation of U [%]	C _{p,r} ' before rx [kJ·kg ⁻¹ ·K ⁻¹]	C _{p,r} ' after rx [kJ·kg ⁻¹ ·K ⁻¹]
50	175.9	120.9	31.3	4.20	5.11
60	182.3	129.6	28.9	4.25	6.42

Note that another UA determination was performed at the end of the experiment and values of about $90 \text{ [W}\cdot\text{m}^{-2}\cdot\text{K}^{-1}]$ were obtained for the overall heat transfer coefficient, thus leading to a final variation of about 50 %. This means that the dissolution of Xanthan Gum is not instantaneous in water and that the mixing time is slower than that of reaction. This effect was also observed visually. It explains the preposterous values of specific heat capacities determined after reaction. In this case, the reaction medium was so viscous and the heat transfer so low that an accurate temperature control was impossible. As water represents more than 90 % of the reaction mass, it has therefore been assumed that Cp_r was solely dependent on temperature and corresponded to that of pure water.

For the integration of the heat generation rate, as the dissolution time of the thickener is different to that of reaction, the baseline was chosen to be proportional to the torque of the stirrer.

Fig. 5.15 shows the heat production rates, thermal conversions and thermal accumulations obtained at 50 and 60 °C. Note that the represented curves of heat production rates were corrected by the baseline to obtain a zero value at the end of the reaction. Raw data generate an offset between the beginning and the end. The results are comparable to those obtained in § 5.4, which means that the addition of Satiaxane™ has not an influence, from the thermal point of view, on the hydrolysis reaction. Once again, the maximum thermal accumulation is greater at 50 °C (29 %) than at 60 °C (15 %), due to a slower reaction rate.

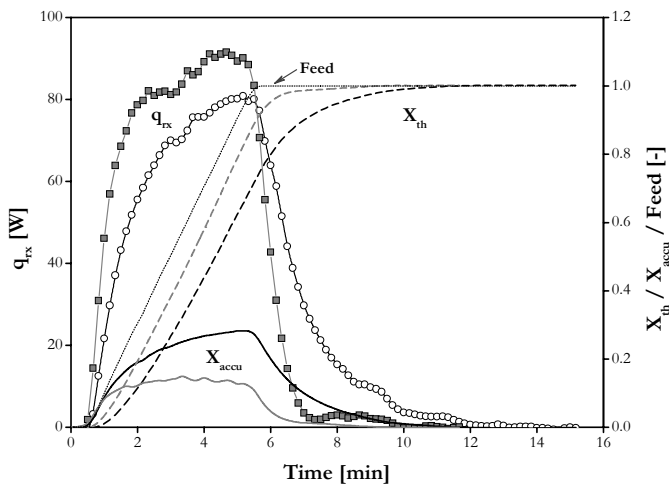


Figure 5.15: Heat production rates (q_{rx}), thermal conversions (X_{th}), thermal accumulations (X_{accu}) and feed obtained in the classical RC1 for the hydrolysis of acetic anhydride with Satiaxane™ used as thickening agent. Black: isothermal conditions at 50 °C; gray: isothermal conditions at 60 °C. Stoichiometry taken into account.

The obtained thermal data are given in Table 5.8. Results at 50 and 60 °C are reproducible.

Table 5.8: Main results of the hydrolysis of acetic anhydride in the classical RC1, Satiaxane™ CX 90 T used as thickening agent.

Temperature [°C]	Q_{rx} [kJ]	ΔH_{rx} [kJ·mol ⁻¹]	ΔT_{ad} [K]	MTSR [°C]
50	-26.9	-53.9	9.9	54.1
60	-27.0	-54.0	9.9	62.7

5.5.4 Modified RC1 results

The same reaction has then been performed in the modified RC1 to simulate the thermal behaviour of industrial reactors R_2 (49 L) and R_4 (630 L), with the same hypothetical conditions as given in Table 5.4. Fig. 5.16 plots the heat production rates (q_{rx}) calculated on-line during the scale-down procedure. It appears that the curves are situated between that at 60 °C (less accumulation, greater heat release rate) and that at 50 °C, and therefore in good agreement with the isothermal experiments. This behaviour is predictable, because the temperature of the reaction medium precisely fluctuates between 50 and 60 °C. The determined reaction enthalpies are also relatively close to the classical RC1 results with -50.6 [kJ·mol⁻¹] for R_2 (6.2 % of deviation) and -54.1 [kJ·mol⁻¹] for R_4 (0.3 % of deviation). However, after about 11 min, the curves are not smooth anymore. The reason for this behaviour is that the viscosity of the reaction medium becomes too important for the temperature to be controlled and, hence, for q_{rx} to be correctly predicted.

This effect is particularly visible on the recorded temperatures (see Fig. 5.17). In both cases, after about 30 min, the reaction medium temperature in the RC1 significantly and spontaneously varies. Because of the increase in viscosity, non homogeneous temperature distribution and, consequently, local aggregates appear. When a warmer zone reaches the tip of the Pt-100 sensor, a hot spot is measured. As a consequence, the jacket temperature tends to rapidly decrease so that T_r does not move away from its setpoint. In summary, the system becomes uncontrollable and the results inconsistent.

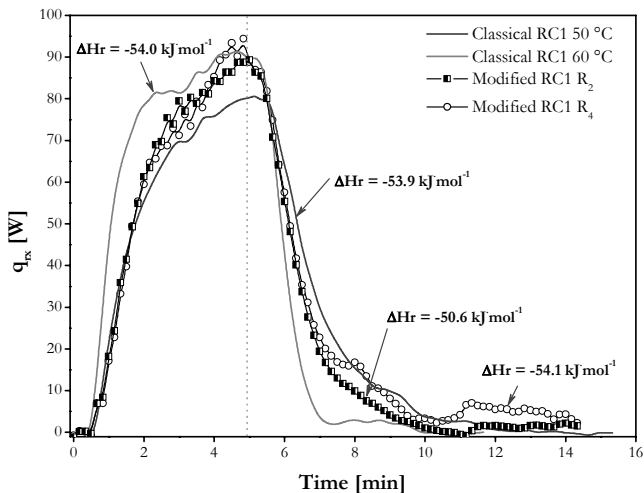


Figure 5.16: Comparison of the heat production rates between classical and modified RC1 for the hydrolysis of acetic anhydride with Satiaxane™ used as thickening agent.

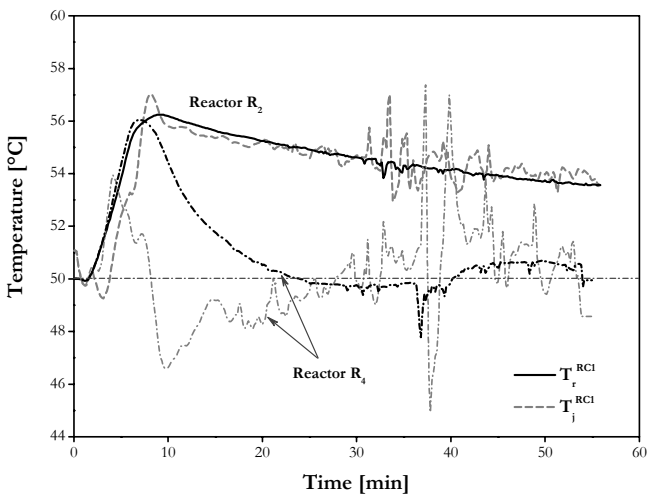


Figure 5.17: Hydrolysis of acetic anhydride with Satiaxane™ used as thickening agent: comparison of temperature evolutions between industrial reactors R_2 and R_4 obtained in the modified RC1 using the scale-down procedure.

5.6 Conclusions

The control of the power delivered by the calibration probe was a very useful tool to prove that the proposed on-line heat balance was accurate. Such a device could have further applications in kinetics analysis as well as in Temperature Oscillation Calorimetry (TOC) [140-143]. As De Luca and Scali [141] state: TOC allows the evaluation of the heat transfer coefficient and the heat capacity, during the course of the reaction, from the elaboration of reactor and jacket temperatures which are forced to oscillate. Such desired oscillations can be produced in two different ways:

- by imposing a sinusoidal variation to the set-point of the reactor temperature obtained by means of an external temperature control system
- by generating a power variation inside the reactor, with different time laws, by means of a thermal resistance, and maintaining the reactor temperature set-point as constant.

The device developed to control the calibration probe could produce the required oscillations. A case of practical relevance is that of batch polymerisation reactors, for which the changes of physical properties from the monomer to polymer are evident, and the possibility of estimating the conversion during the course of reaction is very appealing, because of the difficulties encountered in real-time measurements.

The chosen test reaction, the hydrolysis of acetic anhydride, permitted to reveal the dynamic difference between various industrial reactors. This difference is proportional to the heat production rate of the reaction. Moreover, reaction enthalpies determined on-line are comparable to that of isothermal experiments.

The results of the investigations for reactions accompanied by a strong change in viscosity (as polymerisations), or generally speaking for high viscous reactions, reveal that the on-line calculation of the heat production rate, and, hence, the prediction of the thermal behaviour of industrial reactors, was practicable and correct. Therefore, the developed scale-down approach is not only successful for standard liquid reactions, but also for more «exotic» ones. However, if the system is too viscous (probably from 1'000 cP), then the limitations of the technical capabilities of the RC1 itself make it impossible to study. Nevertheless, it is strongly not advisable that such reactions are conducted in industrial batch reactors, unless their thermal potential is sufficiently low. Otherwise, the use of constant flow stirred tank reactors is mandatory to keep chemical products concentrations at a sufficiently low level. If the temperature has an influence on particle size distribution, like it is generally the case for polymerisations, state observer techniques would be necessary. In summary, if a reaction can be correctly apprehended with the standard reaction calorimeter, then the scale-down approach can be applied.

Chapter 6

COMPARISON OF LABORATORY AND PLANT RESULTS

6.1 Introduction

The fundamental aim of the present work is to forecast the thermal behaviour of full scale equipment during chemical reactions at laboratory scale. A crucial point is to know what precision can be expected from the developed methodology, the difficulties that can be encountered when applying it, and its limitations. This chapter compares the results predicted by the reaction calorimeter RC1 simulating full scale equipment to those indeed recorded in the industrial environment for three different reactions.

The first reaction is a simple semi-batch neutralisation. The second one is a multi-stages reaction with a hydrolysis, a salt formation and finally a bromination. The third one, also a single stage semi-batch reaction, but potentially thermosensitive will allow to highlight, in addition to safety aspects, the effect of the industrial reactor dynamics on the final product quality.

6.2 Neutralisation of KOH by H₂SO₄

6.2.1 Introduction

Potassium hydroxide reacts with sulphuric acid to form dipotassium sulphate and water as shown in Fig. 6.1.



Figure 6.1: Reaction schema of the neutralisation of KOH by H₂SO₄.

This neutralisation reaction was performed by one of the industrial partners in reactors R₃ (nominal volume of 250 L), R₄ (630 L) and R₅ (630 L). A solution of sulphuric acid 50 wt-% was dosed in a 5 wt-% KOH solution previously introduced in the reactor. Thus, the increase of heat transfer area following the dosing was limited. Due to its simplicity, this neutralisation was chosen as the first reaction studied to compare industrial equipment and scale-down approach results. Table 6.1 presents the conditions under which the reaction was performed at plant scale.

Table 6.1: Industrial conditions used during the neutralisation of KOH by H₂SO₄.

Reactor	Initial mass KOH 5 % [kg]	Dosed mass H ₂ SO ₄ 50 % [kg]	Dosing time [min]	Stirrer speed [rpm]	Setpoint [°C]
R ₃	160	15.9	23	300	25
R ₄	400	35.7	19.5	170	25
R ₅	400	35.5	19.5	170	25

Note that the temperature control was always defined in T_r -mode, meaning that the reaction medium temperature was set, whereas that of the jacket resulted from the PID controller installed.

6.2.2 Experimental part

The experimental conditions using the reaction calorimeter RC1 under isothermal conditions are as follows:

- 800 g of a solution KOH 5 wt-% is added to the inertised AP01 reactor (glass, 2 L)
- 71.4 g of a 50 wt-% solution of sulphuric acid is added in 19.5 min using a ProMinent[®] pump connected to the RD10 dosing controller

- the temperature of the reaction mass is held constant at 25 °C
- the inertisation is ensured by a nitrogen flow.

The solution of KOH 5 wt-% was prepared by diluting 46.51 g of pellets of potassium hydroxide 86 wt-% (Fluka, used without further treatment) in 753.49 g of deionised water. 500 g of H_2SO_4 50 wt-% were prepared by adding by portions 260.42 g of sulphuric acid 96 wt-% (Fluka, used without further treatment) in 239.58 g of deionised water.

The experiments using the reaction calorimeter RC1 under isothermal conditions (named «classical RC1» since it is the standard mode of operation) allow to obtain the thermal data of the reaction, with the view to use them to evaluate the on-line heat production rate applying the scale-down methodology. The heat production rate is necessary to forecast, with the help of the calorimeter, the thermal behaviour of plant equipment. It is therefore essential to guarantee that these values are accurate and reliable. As previously said, thanks to the precision of its sensors, its powerful thermostat and its short time constant, the RC1 is generally able to reach a standard deviation lower than 5 % on supplied data. In order to check this, the neutralisation was performed twice at 25 °C. Furthermore, the same reaction was also performed at 30 °C in order to take the $U \cdot A$, $C_{p,r}'$ and heat losses changes with temperature into account.

In the WinRC[®] evaluation software, a predefined phase for the $U \cdot A$ and $C_{p,r}'$ determination was inserted *before* and *after* the reaction of neutralisation. These data are used by the calorimeter for the evaluation of the heat balance.

In order to facilitate the general view, Table 6.2 summarises the experimental conditions:

Table 6.2: General experimental conditions of the neutralisation in the RC1 calorimeter.

Property or substance	Type [-]	Mass [g] or speed [rpm]	Temperature [°C]	Dosing time [min]
KOH 5 wt-%	lab solution	800.0	25 or 30	batch
H_2SO_4 50 wt-%	lab solution	71.4	room	19.5
Stirrer	anchor, glass	100	-	-
Calibration probe	25 W, glass	-	-	-
Inertisation	nitrogen	-	-	-

6.2.3 Classical RC1 results

The obtained thermal characteristics of the neutralisation are given in Table 6.3. Experiments showed that after the pump began the dosing the heat flux increased immediately and reached almost instantaneously a zero value at the end of the dosing (see Fig. 6.3, p. 127). The reaction can therefore be considered as controlled by the dosing and almost no heat accumulation occurs. Despite a rather high reaction enthalpy ($-141 \text{ [kJ}\cdot\text{mol}^{-1}]$), the temperature rise under adiabatic conditions (ΔT_{ad}) remains low due to the important water quantity present in the potassium hydroxide solution. Additionally, results are reproducible, the reaction enthalpy difference being below 3 %. It appears also that this enthalpy does not vary within the temperature interval studied, limited as a matter of fact.

Table 6.3: Main results obtained in the classical RC1 for the neutralisation of KOH by H_2SO_4 .

Temperature [°C]	ΔH_{rx} [kJ·mol ⁻¹]	C_p' [kJ·kg ⁻¹ ·K ⁻¹]	ΔT_{ad} [K]	MTSR [°C]
25	-140.3	3.80	16.9	26.6
25	-143.7	3.81	17.3	26.9
30	-140.5	3.80	16.9	31.0

6.2.4 Modified RC1 results

Based on these results, the Excel sheet containing the complete thermal modelling of the industrial reactor is first of all completed with the necessary data for the scale-down approach, as described in § 4.5.1, p. 85. Obviously, the same initial conditions as those given in Table 6.1 were introduced. Note also that the internal heat transfer resistance of the full scale equipment, $h_{r,p}$, was evaluated with the «Wilson plot» method (see p. 111).

Once the KOH 5 wt-% solution is introduced in the 2 L AP01 glass reactor¹, the temperature is stabilised at that of the simulated industrial reactor. Later on, the communication between the modified RC1 and the external data source (Excel) is established with the help of the Visual Basic window (see Fig. 4.2, p. 80). Once the calorimeter and Excel exchange data (in this case every 10 seconds), the experimental part of the neutralisation is carried on normally with the dosing of sulphuric acid 50 wt-%. While the calorimeter proceeds with the dosing, the scale-down methodology takes place with two on-line heat balances, namely the one over the calorimeter itself to determine q_{rx} and the one over the simulated industrial reactor to forecast, with the help of the thermal dynamics modelling, its hypothetical thermal behaviour. Temperature and, hence, chemical evolutions should therefore mimic the industrial environment.

1. Reminder: to simulate plant reactors, the RC1 has to be «modified», meaning that the EPROM of the calorimeter has to be changed and the new WinRC ALR[®] software run. As regards the apparatus itself, no modification has been done compared with the commercial version. For additional information, see § 4.3, p. 79.

It can be seen, from Fig. 6.2 that with a mean temperature difference lower than $0.5\text{ }^{\circ}\text{C}$ the general trend obtained in the RC1 is very close to that of reactors R_3 , R_4 and R_5 . The predicted temperature evolution is slightly less accurate for reactor R_4 (nominal volume: 630 L). However, the sensibility of the temperature probes themselves, respectively the resolution of the industrial data acquisition system, can be questioned: they react in stages of only $0.5\text{ }^{\circ}\text{C}$. Therefore, the plateau visible in Fig. 6.2b may not exactly correspond to reality. Nevertheless, with a maximum temperature difference of $1.0\text{ }^{\circ}\text{C}$, the precision of the method is satisfactory.

Once again, it is important to realise that if the reaction medium temperatures (T_p) are comparable, the situation is different for that of the jacket (T_j). In fact, the difference between T_j^{indus} and T_j^{RC1} directly reflects their heat transfer capacity. Normally, for exothermic reactions, T_j^{indus} is lower than T_j^{RC1} in order to compensate for the unfavourable heat transfer area to reaction mass ratio (see Table 6.4).

Table 6.4: Comparison of specific heat transfer areas during the neutralisation of KOH by H_2SO_4 .

Reactor	Specific heat transfer area [$\text{m}^2\cdot\text{kg}^{-1}$]
AP01 (2 L)	$4.56\cdot 10^{-2}$
R_3 (250 L)	$9.75\cdot 10^{-3}$
R_4 (630 L)	$6.25\cdot 10^{-3}$
R_5 (630 L)	$6.75\cdot 10^{-3}$

If it is true that this ratio is inversely proportional to the vessel volume, however, the temperature difference is not so contrasted. For the smallest simulated reactor (R_3 , nominal volume 250 L), T_j^{indus} and T_j^{RC1} are very close from each other. First, this means that the jacket dynamics of this plant vessel is comparable to that of the reaction calorimeter, as already outlined in § 3.5.2, p. 64. Second, it also means that the overall heat transfer coefficient U is greater for R_3 than for the RC1. This is explained by its excellent mixing capacity, reducing the inner film coefficient, and above all by its construction material (stainless steel instead of glass).

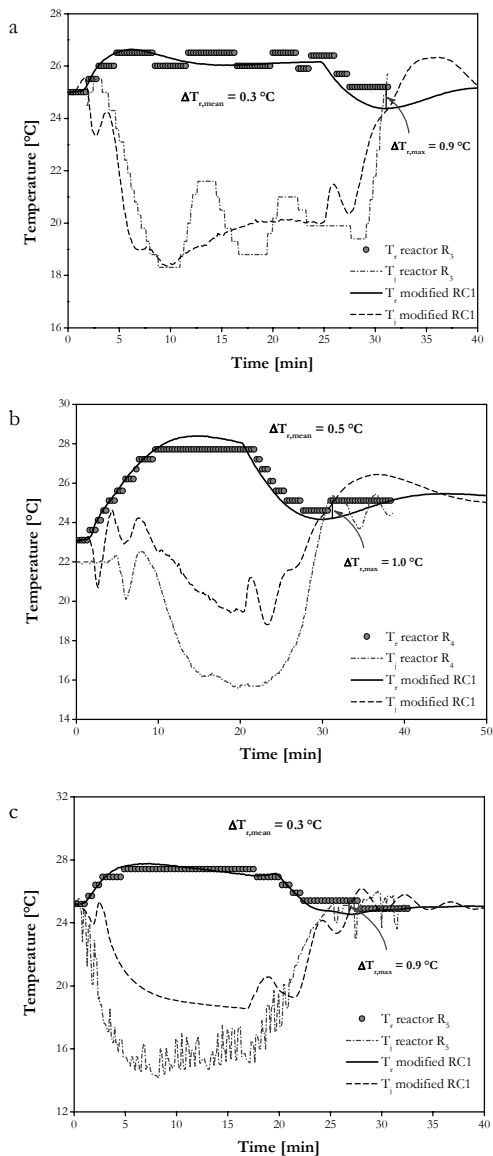


Figure 6.2: Neutralisation of KOH by H₂SO₄: temperatures comparison of modified reaction calorimeter and industrial reactors (a: R₃ (250 L), b: R₄ (630 L), c: R₅ (630 L)).

As regards the reaction itself, the curves of heat production rate depicted in Fig. 6.3 prove that the calculated on-line heat balance over the RC1 is correct, although resulting in slightly lower reaction enthalpies (see Table 6.5). For the simulation of reactor R_4 , the dosing duration was 19.5 min as during isothermal experiments, hence, the curves are superimposed. For reactor R_3 however, the dosing was lengthened to 23.0 min to match the industrial conditions.

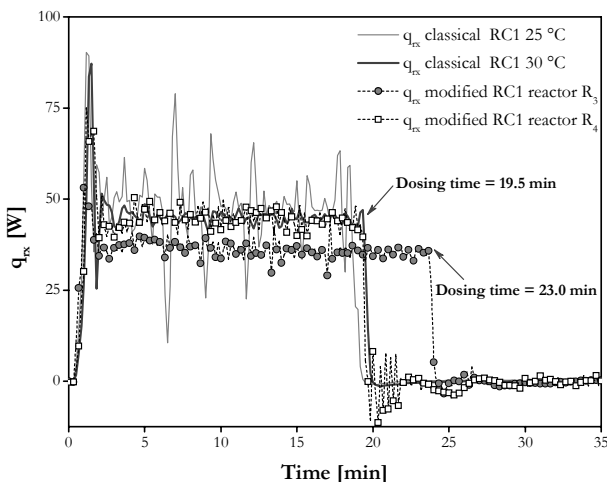


Figure 6.3: Neutralisation of KOH by H_2SO_4 : comparison of heat production rates between classical RC1 results (isothermal conditions) and scale-down procedure simulating industrial reactors R_3 (250 L) and R_4 (630 L).

Table 6.5: Reaction enthalpies determined on-line during the neutralisation of KOH by H_2SO_4 .

Reactor simulated	ΔH_{rx} [kJ·mol ⁻¹]	Error/classical RC1
R_3	-133.0	6.0 %
R_4	-137.5	2.8 %
R_5	-139.0	1.8 %

Note that a peak of heat production rate appears at the beginning of the dosing. It is possible, for some reactions, that the heat flux constantly decreases during the dosing. This is often interpreted as a progressive effect of dilution. In the present case, however, after the first peak the heat flux remains constant until the end of the dosing. Therefore, this peak must rather be interpreted as an artefact not coming from the reaction itself: after the first stroke of the pump, the RD10 dosing

controller requires several seconds to analyse the dosed quantity. Consequently, the dosing is too slow compared to its setpoint. The controller will then tend to compensate this deviation by increasing the dosing rate, an effect directly observable on the heat flux. In fact, this effect was observed in every experiment (see next chapters).

6.3 Three steps reaction

6.3.1 Introduction

This reaction consists first in a semi-batch hydrolysis between acetic anhydride and water contained in the dosed hydrogen bromide 48 wt-%, with glacial acid acetic used as solvent; second of a salt formation, also in semi-batch mode, between hydrogen bromide and compound A; third in a bromination between the salt and dosed bromine (see Fig. 6.4).

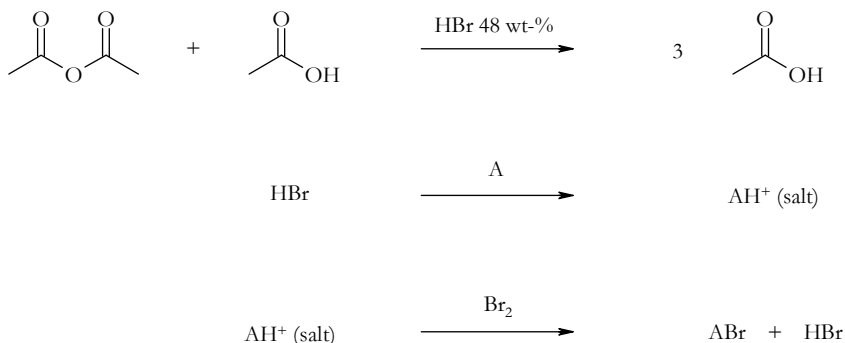


Figure 6.4: Reaction schema of the three steps reaction.

This reaction was industrially performed in reactor R₂ (49 L, T_J -mode).

6.3.2 Experimental part

- First step: hydrolysis

The experimental conditions using the classical RC1 are as follows:

- 441.6 g of acetic anhydride is added to the inertised AP01 reactor
- 264.0 g of glacial acid acetic is added manually

- 267.2 g of hydrogen bromide 48 wt-% is added in 1 h using a ProMinent® pump connected to the RD10 dosing controller
- the temperature of the reaction mass is held constant at 25 °C.

The same reaction was also performed at 30 °C in order to take the various parameters dependencies with temperature into account.

- Second step: salt formation

The experimental conditions using the classical RC1 are as follows:

- the previous reaction mass is heated up to 40 °C
- 160.0 g of compound A is added in 30 min using a ProMinent® pump connected to the RD10 dosing controller
- the temperature of the reaction mass is held constant at 40 °C.

- Third step: bromination

The experimental conditions using the classical RC1 are as follows:

- the previous reaction mass is heated up to 75 °C
- 211.2 g of bromine is added manually in about 1 h with a dosing ampoule
- the temperature of the reaction mass is held constant at 75 °C.

The same reaction was also performed at 85 °C in order to take the various parameters dependencies with temperature into account.

- Cooling

The final reaction mass is finally cooled at room temperature, a process during which a crystallisation phase takes place.

As usual, a predefined phase for the U_A and Cp_r determination was inserted *before* and *after* each reaction step.

6.3.3 Classical RC1 results

The heat production rates and the corresponding thermal conversions and accumulations of the three steps are presented in Fig. 6.5 (a: hydrolysis, b: salt formation and c: bromination). Note that the thermal accumulation is the difference between the feed and the thermal conversion. The stoichiometry has been taken into account in every graph, which means that a final feed value greater than one corresponds to a stoichiometric excess, whereas a final feed value smaller than one corresponds to a stoichiometric default.

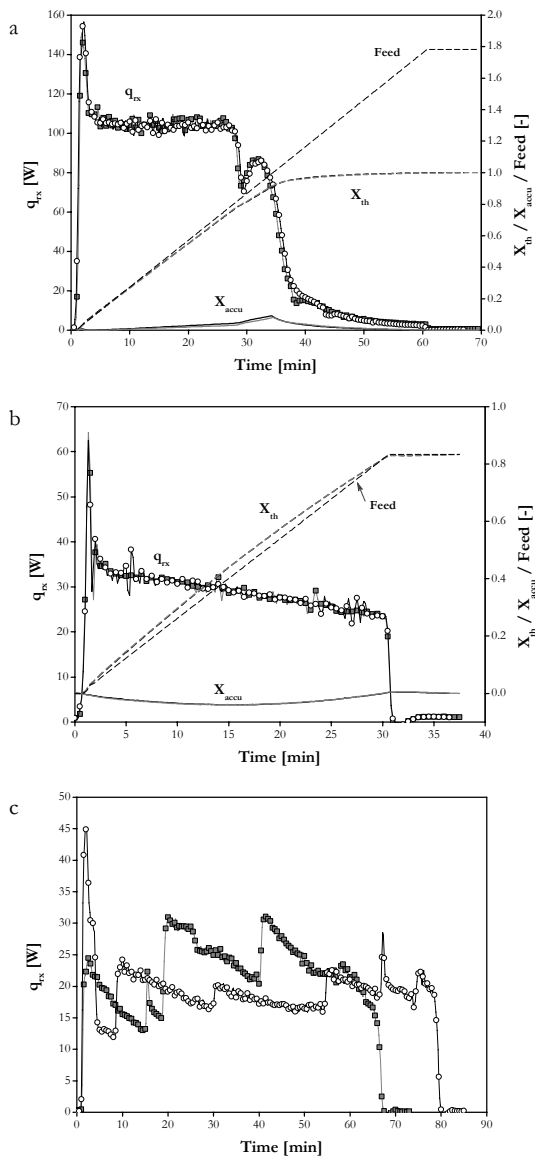


Figure 6.5: Heat production rates (q_{rx}), thermal conversions (X_{th}), thermal accumulations (X_{accu}) and feeds obtained in the classical RC1 for the three steps reaction. Black: isothermal conditions at lower temperatures; gray: isothermal conditions at higher temperatures.

The experimental heat production rates depicted in Fig. 6.5 lead to reaction enthalpies and calorimetric characteristics mentioned in Tables 6.6 to 6.8.

Table 6.6: Main results of the first step (hydrolysis) in the classical RC1.

Temperature [°C]	ΔH_{rx} [kJ·mol ⁻¹]	C_{p_r} [kJ·kg ⁻¹ ·K ⁻¹]	ΔT_{ad} [K]	MTSR [°C]
25	-51.4	1.88	168.5	52.2
30	-50.6	1.86	168.4	50.0

Table 6.7: Main results of the second step (salt formation) in the classical RC1.

Temperature [°C]	ΔH_{rx} [kJ·mol ⁻¹]	C_{p_r} [kJ·kg ⁻¹ ·K ⁻¹]	ΔT_{ad} [K]	MTSR [°C]
40	-38.1	1.96	27.6	40.7
40	-38.1	1.94	27.8	40.8

Table 6.8: Main results of the third step (bromination) in the classical RC1.

Temperature [°C]	ΔH_{rx} [kJ·mol ⁻¹]	C_{p_r} [kJ·kg ⁻¹ ·K ⁻¹]	ΔT_{ad} [K]	MTSR [°C]
75	-69.9	2.01	40.0	75.4
85	-65.9	2.06	37.7	85.4

As regards safety, except for the first step, the thermal potentials are low with adiabatic temperature rises lower than 50 °C. For step 1, the severity is medium with a ΔT_{ad} of about 170 °C. However, the actual value should be lesser because of the large amount of hydrogen bromide dosed and its corresponding specific heat capacity (2.7 [kJ·kg⁻¹·K⁻¹]). Moreover, the maximum achievable temperature due to the synthesis reaction (*MTSR*) is by far lower than the boiling point.

For step 1, the conversion takes place spontaneously during the dosing. After the stoichiometric point, the heat production rate decreases exponentially to the baseline. A modest residual heat is visible leading to a maximal heat accumulation of about 9 % (see Fig. 6.5a).

For step 2, the reaction runs practically dosing controlled and without accumulation. When the dosing is stopped, the heat production rate drops immediately to zero. Astonishingly, the thermal conversion is even higher than the feed (see Fig. 6.5b). It is strongly improbable that this step (salt formation) develops in two stages. Certainly, an additional and likewise spontaneous portion of a mixing heat arises, whose contribution reduces continuously.

For step 3, the main problem is of technical nature: the bromine was dosed with the help of an ampoule. Every peak appearing in the heat production rate (see Fig. 6.5c) corresponds to a manual increase of the flow rate. Therefore, and since bromine was visually instantaneously consumed, the reaction is also dosing controlled with a q_{rx} -profile, in case of a regular dosing, similar to that of step 2. During the crystallisation process, a supplementary heat of -15.8 and -21.0 [kJ·mol⁻¹], for the experiments at 75 and 85 °C respectively, was observed. In all, the reaction enthalpy of the bromination therefore corresponds on average to -86.3 [kJ·mol⁻¹].

6.3.4 Modified RC1 results

The three steps of the reaction were then performed again in the reaction calorimeter mimicking the plant conditions. Fig. 6.6 to 6.8 displays the main results.

- First step (hydrolysis)

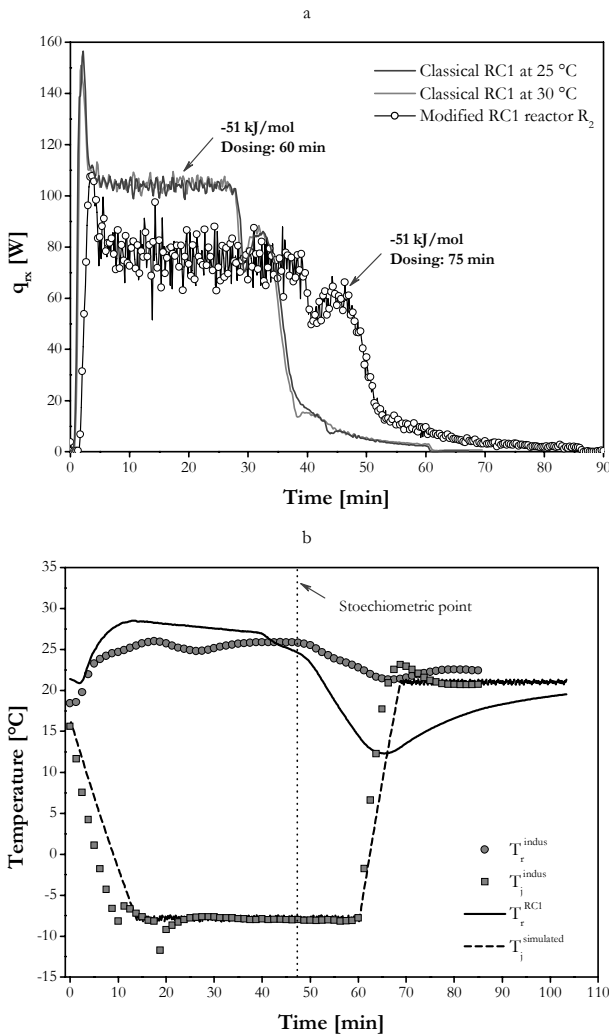


Figure 6.6: First step of the reaction (hydrolysis). a: comparison of heat production rates between classical RC1 (isothermal conditions) and modified calorimeter (scale-down approach); b: comparison of recorded and simulated temperatures between industrial reactor R_2 (49 L) and modified RC1.

- Second step (salt formation)

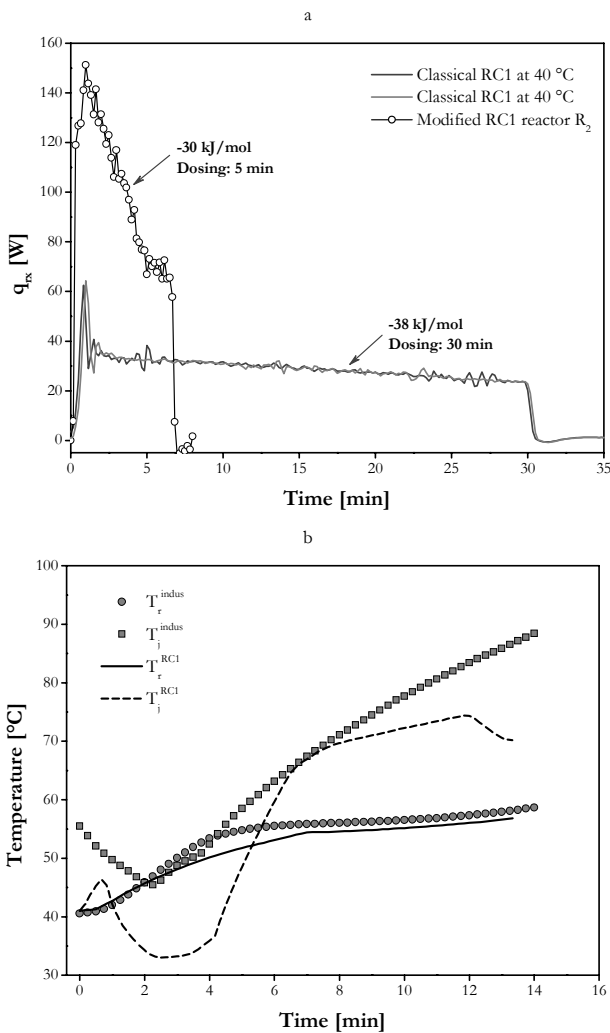


Figure 6.7: Second step of the reaction (salt formation). a: comparison of heat production rates between classical RC1 (isothermal conditions) and modified calorimeter (scale-down approach); b: comparison of recorded temperatures between industrial reactor R_2 (49 L) and modified RC1.

- Third step (bromination)

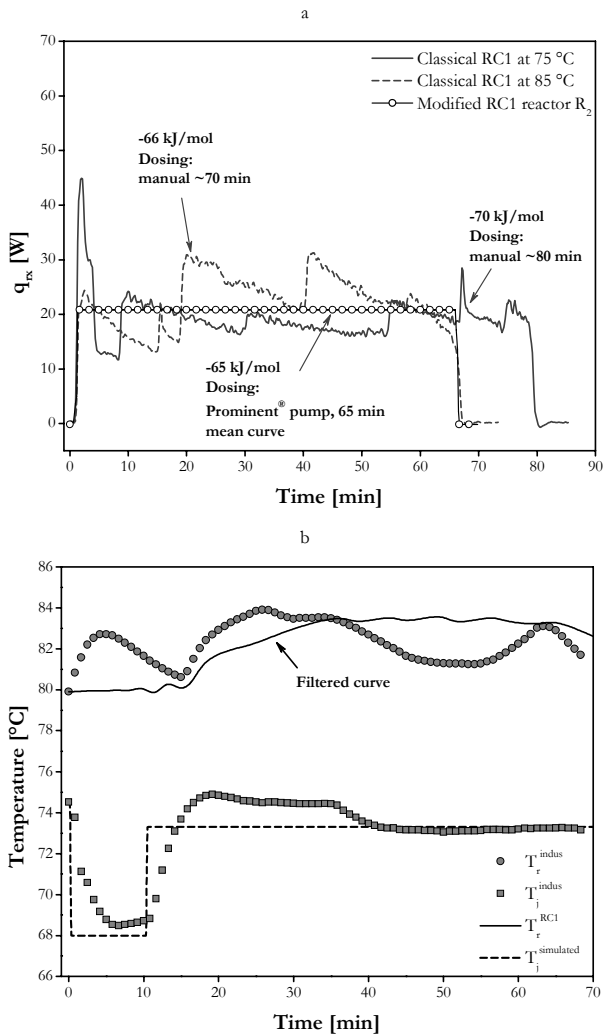


Figure 6.8: Third step reaction (bromination). a: comparison of heat production rates between classical RC1 (isothermal conditions) and modified calorimeter (scale-down approach); b: comparison of recorded and simulated temperatures between industrial reactor R_2 (49 L) and modified RC1.

For the hydrolysis stage, if the reaction enthalpy is indeed correctly determined on-line, the predicted temperature evolution of the reaction medium differs noticeably from that recorded in the industrial reactor. In fact, after investigation, it was established that the hydrogen bromide was dosed manually in portions by the production staff at plant scale. This particularity has been envisaged neither by this thesis author nor by the manager in charge for the project. Therefore, to attempt improving the results, it would have been necessary to adapt the dosing in the calorimeter in consequence. Unfortunately, the industrial dosing profile was not available anymore.

For the salt formation, the results interpretation may be overvalued, since the reaction was performed twice at 40 °C with the classical RC1. The reaction enthalpy determined during the scale-down experiment was lower by 21 % compared to the isothermal conditions. Consequently, the temperature profile differs in several degrees ($\Delta T_{max} = 4$ °C). In this case, it seems that the operational limits of the reaction calorimeter were reached: if the process is very fast (in this case 5 min, with a dT_r/dt of about 3.5 [°C·min⁻¹]) and the temperature variation important, then the accuracy of the on-line heat balance decreases. More precisely, the problem is situated in the reactor time constant. Despite the use of the modified jacket temperature T_a (see p. 89 for information on T_a), this value is no more correct under intense dynamic conditions. A very simple experiment can highlight this phenomenon: suppose, in the absence of any chemical reaction or physical effect, that the jacket temperature of the RC1 is oscillating very rapidly and symmetrically around its setpoint, like a sinusoidal. In this case, the on-line heat balance would calculate a net q_{rx} also oscillating, with of course a zero mean value. This issue is inherent to these extremely fast dynamic situations. Once again, this problem is not due to the developed methodology, but rather to the apparatus itself.

For step 3, it seemed evident that with a manual dosing, no reproducibility could be expected (see Fig. 6.5c, p. 130). Therefore, it was attempted to dose the bromine with a Prominent® pump. However, owing to the very high bromine density, the quantity added at each pump stroke was too high to guarantee a correct profile. Hence, the curves depicted in Fig. 6.8 have been smoothed, but oscillate in reality. As for the first step, it was found that the bromine was also dosed in portions in the industrial reactor, the profile being unknown. Therefore, it is logical that the temperature recorded in the calorimeter differs from that in reactor R₂.

Note that the dashed lines in Fig. 6.6b and 6.8b represent the simulated jacket temperatures of the industrial reactor while applying the scale-down method. They do not represent the jacket temperatures of the reaction calorimeter. This choice of representation was motivated by the fact that if both T_j^{indus} and q_{rx}^{indus} are correctly modelled, then the deviation should only be explained by the dosing profile.

6.4 Alkene oxidation by a peroxycarboxylic acid

6.4.1 Introduction

Alkene compounds are oxidised by peroxycarboxylic acids (also named peracids) to give the corresponding epoxide and, after rearrangement, the ketone (see Fig. 6.9). In this study, the peroxycarboxylic acid was dosed at room temperature in the AP01 reactor containing the alkene and petroleum ether (PE) 100-140 (benzin with boiling point situated between 100 and 140 °C). The final solution was then washed first with deionised water and second with a NaOH 15 wt-% solution. Finally, the ketone was concentrated by distillation.

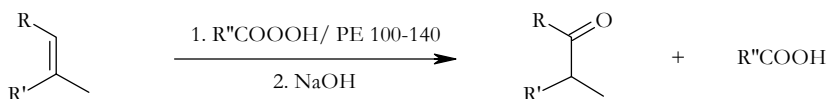


Figure 6.9: Reaction schema of an alkene oxidation by a peroxycarboxylic acid.

This reaction was also performed in the industrial reactor R₄ (nominal volume: 630 L) at a setpoint temperature of 30 °C (*T_r*-mode). The first goal of this chapter is, hence, to carry out at two different temperatures this reaction in the classical RC1 in order to apprehend its thermal characteristics. After that, the temperature evolution of reactor R₄ will be predicted using the proposed scale-down procedure and compared with experimental data. Furthermore, the used peroxycarboxylic acid decomposes itself from 40 °C, meaning that the oxidation is potentially thermosensitive. Therefore, apart from safety aspects, the dynamics of the industrial reactor can play a major role in the *quality* and *selectivity* of the final reaction mixture. The second objective is then to foresee, already at laboratory scale using the modified RC1, the impact of the choice of the industrial reactor on these parameters.

6.4.2 Experimental part

- Reaction

The experimental conditions using the classical RC1 are as follows:

- 230.5 g of the alkene compound is added to the inertised AP01 reactor
- 218.0 g of petroleum ether 100-140 is added manually
- 220.3 g of the peroxycarboxylic acid is added in 3 h using a ProMinent[®] pump connected to the RD10 dosing controller
- the temperature of the reaction mass is held constant at 30 °C.

The same reaction was also performed at 40 °C in order to take the U_A , C_p' and losses changes with temperature into account. Table 6.9 presents an overview of the main experimental conditions.

Table 6.9: General conditions used for the alkene oxidation by a peroxycarboxylic acid.

Property or substance	Type [-]	Mass [g] or speed [rpm]	Temperature [°C]	Dosing time [h]
Alkene	industrial product	230.5	30 or 40	batch
PE 100-140	Fluka 85103	218.0	30 or 40	batch
R ² COOOH	Fluka	220.3	room	3
Stirrer	propeller, glass	450	-	-
Calibration probe	5 W, glass	-	-	-
Inertisation	nitrogen	-	-	-

- Purification

The final reaction mass was then treated with 230.5 g of deionised water, the organic phase washed again first with 115.2 g of deionised water and second with 115.2 g of a NaOH 15 wt-% solution. Finally, the ketone was concentrated during 20 min at 80 °C and about 10 mbar in a vacuum rotavapour.

6.4.3 Classical RC1 results

The main calorimetric characteristics of the oxidation reaction obtained in the classical RC1 are summarised in Table 6.10:

Table 6.10: Main results of the alkene oxidation by a peroxycarboxylic acid in the classical RC1.

Temperature [°C]	ΔH_{rx} [kJ·mol ⁻¹]	C_p' [kJ·kg ⁻¹ ·K ⁻¹]	ΔT_{ad} [K]	MTSR [°C]
30	-330.6	2.04	405.8	68.0
40	-349.8	2.09	419.6	78.1

Fig 6.10 shows the heat production rates, thermal conversions and thermal accumulations obtained at 30 and 40 °C. Note that the baselines were chosen to be «linear from start». This is the reason why q_{rx} is not equal to zero after 4.5 h.

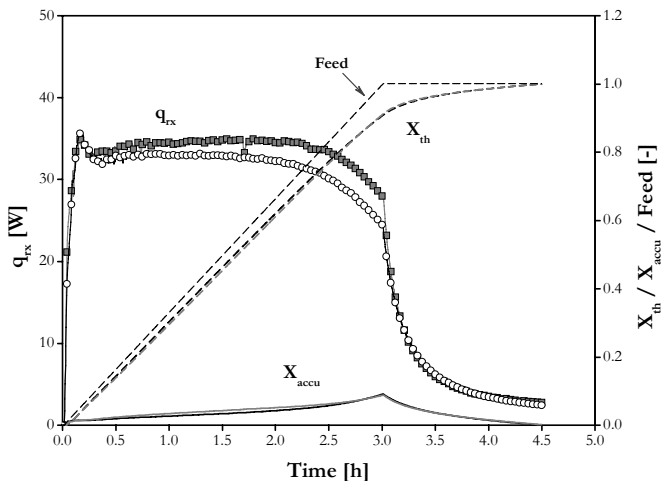


Figure 6.10: Heat production rates (q_{rx}), thermal conversions (X_{th}), thermal accumulations (X_{accu}) and feed obtained in the classical RC1 for the alkene oxidation by a peracid. Black: isothermal conditions at 30 °C; gray: isothermal conditions at 40 °C. Stoichiometry taken into account.

The thermal potential of this reaction is particularly important with adiabatic temperature rises of more than 400 °C. It corresponds to a mean reaction enthalpy of $-340 \text{ [kJ}\cdot\text{mol}^{-1}]$. Therefore, it seems evident that such a reaction can only be performed under semi-batch conditions. Moreover, a cooling capacity of at least $80 \text{ [W}\cdot\text{kg}^{-1}]$ is required for the industrial reactor, otherwise the dosing time has to be lengthened in consequence.

At the end of the dosing, i.e. after 3 h, the curve of heat production rate does not decrease immediately but exponentially reaches zero (see Fig. 6.10). The peroxycarboxylic acid, being immiscible in the organic phase, forms the denser lower phase. The reaction medium is thus biphasic and mass transfer is probably a limiting factor. Note that values given in Table 6.10 correspond to a reaction time of 4.5 h. At laboratory scale, reaction enthalpies of $-410 \text{ [kJ}\cdot\text{mol}^{-1}]$ after complete reaction have been determined by one of the industrial partner. Therefore, the maximal thermal accumulation of 9 % at the end of addition, value rather low, leads to a *MTSR* of 68 and 78 °C, all the same.

The heat production rate is relatively stable until 2 h of addition (about 75 % of the stoichiometric point) and then diminishes slowly. At 40 °C, q_{rx} is slightly higher due perhaps to slow decomposition of the peracid.

6.4.4 Modified RC1 results

From the results obtained in the classical RC1, the scale-down method was then applied to two different industrial reactors (see Table 6.11). R_4 was chosen with the intention to compare predicted temperature evolution with experimental data, whereas R_9 (the largest reactor characterised) should reveal, due to its slower dynamics, a completely different temperature evolution and, hence, final product quality. Note that a jacket temperature of 5 °C for R_9 corresponds to the lowest possible temperature of the indirect cooling system (water). Therefore, the 25 m³ reactor was simulated with its maximal cooling capacity.

Table 6.11: Industrial reactors simulated in the modified RC1 for the alkene oxidation.

Reactor	Nominal volume [L]	Initial mass simulated [kg]	Stirrer speed [rpm]	Setpoint [°C]	Regulation mode
R_4	630	179.4 ^a	150	30	T_r
R_9	25'000	11'000	50	5	T_j

a. This amount corresponds to that actually introduced in the 630 L during the industrial process.

The same experimental conditions as described in § 6.4.2 were used. After the reaction mass was stabilised at 30 °C, the dosing and the external data source communication were conjointly launched. As by simulation the temperature of the reaction mass would reach about 120 °C in reactor R_9 (q_{rx} (766 kW) being on average 3 times greater than q_{ex} (237 kW)), the dosing time of the peroxycarboxylic acid was doubled (6 h). In this case, the temperature should reach 75 °C assuming a same heat production rate profile, an acceptable value from the safety point of view, since the calorimeter is well inertised and no excess of acid is dosed.

- Comparison of industrial reactors dynamics

Fig. 6.11 compares the heat production rates between the classical and modified RC1 experiments. As regards q_{rx} , the simulation of industrial reactor R_4 does not match the isothermal experiments but results in a lower power from 2.5 h. For a same reaction time, the difference in reaction enthalpies corresponds to 7 %. It can also be seen that the reaction power drops abruptly at the end of dosing for reactor R_9 . Assuming same final conversion, the reaction enthalpy calculated differs from 8 % (-314 vs. -340 [kJ·mol⁻¹]). For such a long reaction, small deviations of $U \cdot A$, Cp_r or q_{loss} calculated on-line can lead to significant errors at the end.

The R_9 dynamics being slower and its cooling capacity lesser, the temperature of the reaction medium continually increases (see Fig. 6.12, p. 142) and so for the reaction kinetic. Moreover, the higher the temperature, the faster the peracid decomposition. Therefore, a maximal thermal accumulation of only 2 % was observed during the simulation of the 25 m³.

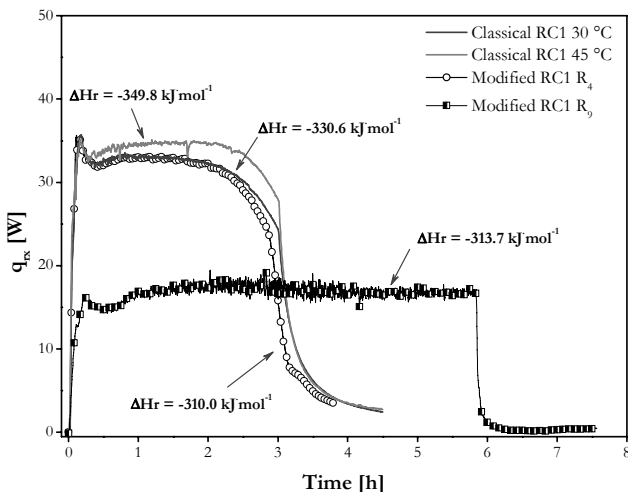


Figure 6.11: Comparison of the heat production rates between classical and modified RC1 for the alkene oxidation by a peroxydicarboxylic acid. Classical RC1 and simulation of reactor R_4 ; dosing time (t_{dos}) = 3 h; simulation of reactor R_9 ; t_{dos} = 6 h.

The main calorimetric data obtained with the modified RC1 are listed in Table 6.12. *MTSR* values of these two reactors differ only in 17 °C, first because the thermal accumulation is four times more important in the 630 L and second because the dosing time was doubled for the 25 m³.

Table 6.12: Main results of the alkene oxidation by a peroxydicarboxylic acid in the modified RC1.

Reactor [-]	ΔH_{rx} [kJ·mol ⁻¹]	ΔT_{ad} [K]	<i>MTSR</i> [°C]
R_4	-310.0	368.6	60.4
R_9	-313.7	380.8	77.4

The difference between the two industrial reactors dynamics is illustrated in Fig. 6.12. If *MTSR* are comparable, the temperature profiles exhibit very contrasting behaviours. Despite a slower dosing, the heat production rate would not be totally evacuated by the cooling system of the 25 m³ reactor. As heat accumulates, the temperature progressively increases. Consequently, the power exchanged with the utility fluid also increases, until equilibrium at about 70 °C. Note that the $U \cdot A$, C_p , and q_{loss} parameters, although being not evaluated at 70 °C, have been extrapolated to this temperature from

the two isothermal experiments at 30 and 40 °C. The fast response of the 630 L reactor to a setpoint overshoot and its excellent heat transfer characteristics allow to maintain a quasi constant temperature of 35 °C during the entire course of the reaction. At the end of the dosing, the setpoint (30 °C) is reached in less than 15 min.

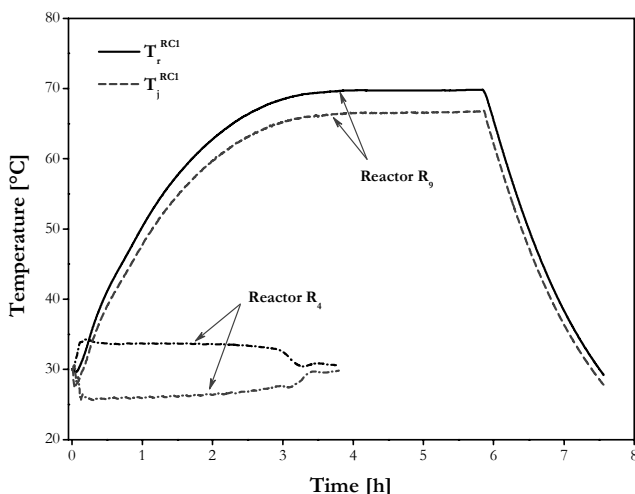


Figure 6.12: Alkene oxidation by a peracid: comparison of reaction medium (T_r) and jacket (T_j) temperatures recorded in the modified RC1. Simulation of industrial reactors R₄ (630 L, $T_{r\text{-mode}}$, $T_{set} = 30^\circ\text{C}$) and R₉ (25 m³, $T_{j\text{-mode}}$, $T_j = 5^\circ\text{C}$). Dosing time: R₄: 3 h, R₉: 6 h.

As previously said, this oxidation reaction has been conducted in the reactor R₄ by one of the industrial partners with the same experimental conditions presented in Table 6.11. The generated temperature evolution was followed by Pt-100 probes and recorded as function of time. If we compare the temperature of the reaction medium with that obtained in the calorimeter simulating this industrial reactor, we can conclude that the general trend is respected with a mean absolute difference of 0.5 °C (see Fig. 6.13). And this, despite the poor temperature precision of $\pm 0.5^\circ\text{C}$ for the plant reactor. The maximum difference of 1.8 °C at the beginning of the reaction probably results from a slight different flow rate of acid. However, in general, the level of confidence in the scale-down method can be qualified of high and allows, in a great extend, to reduce the unpleasant surprises that could arise during the process transfer from laboratory to plant scale.

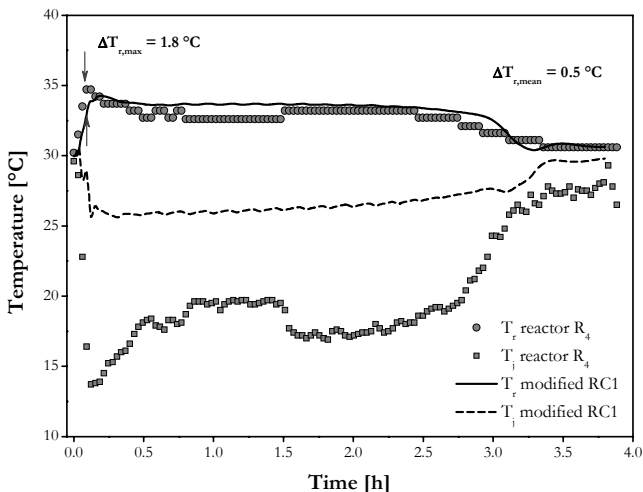


Figure 6.13: Alkene oxidation by a peroxycarboxylic acid: comparison of plant and modified RC1 reaction medium (T_r) and jacket utility fluid (T_j) temperatures.

It is clear that if T_r are comparable, T_j are quite different. Their divergence directly reflects the difference of heat transfer with scale. With a smaller volume to surface ratio, the industrial reactor needs a lower jacket temperature to get a same T_r .

- Effect of reactor dynamics on reaction selectivity

Finally, one of the goals of the developed method is also to predict the final quality and selectivity of any chemical reaction taking place in any industrial vessel that has been previously modelled. In this intention, the concentrated ketones (see p. 138) were analysed by gas chromatography (GC) by one of the industrial partner. The three experiments performed in the classical RC1 lead to a mean ketone selectivity of $79.0 \pm 0.7 \%$ (Fig. 6.14). In the first experience, the used stirrer was a glass anchor. This engendered a dead zone under the agitator shaft and the position of the stirrer had to be modified (see also Fig. 7.2, p. 150). However, the final concentrations were similar to those with a propeller stirrer despite a slightly poorer alkene conversion.

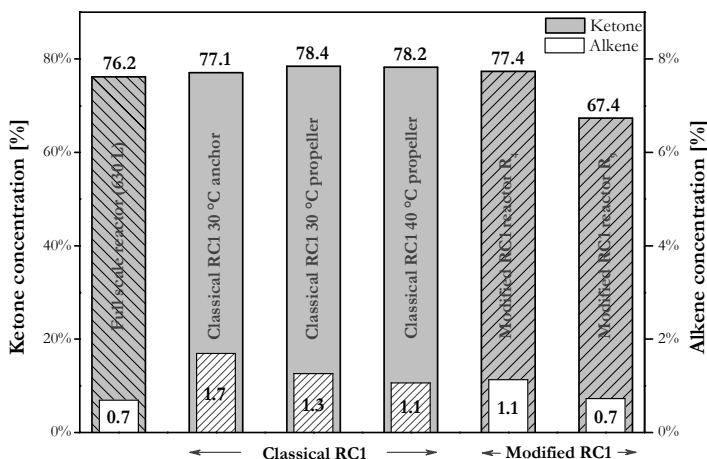


Figure 6.14: Alkene oxidation by a peroxycarboxylic acid: comparison of alkene and ketone final concentrations (GC analysis) between industrial reactor R₄, classical and modified RC1.

GC results reveal that the alkene conversions of the modified RC1 experiments are similar to isothermal experiments with a mean value of 99.1 %. The sample analysis of the simulated 630 L (78.3 % of selectivity) is in good accordance with the temperature profile situated between 30 and 40 °C. Moreover, it well tallies with GC analysis of the full scale experiment (76.7 % of selectivity). However, for the simulated 25 m³, the selectivity decreases by 14.1 % (compared with isothermal experiments) to 67.9 %. Furthermore, the reaction is more «dirty» with the apparition of supplementary peaks on GC results. Therefore, it seems that higher temperatures can disturb the reaction path by degradation of the peracid.

6.5 Conclusions

In this chapter, the comparisons of thermal dynamics between the modified reaction calorimeter RC1 and various industrial reactors were presented. The heat production rates determined on-line lead to values situated in the tolerable error of 5 %. The scale-down approach meets well with plant reality. The few observed differences rather result from technical issues or process deviations than from the proposed method. Moreover, it has been demonstrated that the industrial reactor dynamics can lead to quality divergences in case of thermosensitive reactions. With the present work, they can be highlighted and apprehended already in the 2 L reaction calorimeter RC1.

The results obtained for the three steps reaction are, for technical and inherent reasons, less satisfactory. However, the positive point is that it is the laboratory results that revealed the dosing anomaly at full scale equipment. This suggests once again that the developed method is accurate and robust.

Chapter 7

CONCLUSIONS

7.1 Summary of the main results

In this work, a methodology for driving process profitability and safety has been developed. Combining calorimetric measurements and heat transfer modelling, it allows to manage and optimise plant performances at laboratory scale from the productivity, selectivity and safety point of view and, thus, to reduce the development time, i.e. time-to-market.

First, the heat transfer dynamics of nine industrial reactors have been modelled. These reactors differ in sizes (ranging from 40 L to 25 m³), construction material and temperature control system. The use of standard heat balance equations and parameters identification was sufficient to correctly describe both reaction medium and jacket temperatures evolutions during heating/cooling experiments. The mean absolute temperature difference was typically in the order of one degree. Moreover, it has been shown that for specific stirrers configurations a visual evaluation of the vortex formation was inevitable. Once the complete dynamic model is identified, the thermal behaviour of the industrial reactors can be numerically simulated. The model can handle jacket and reaction medium setpoint changes, variation of stirrer revolution speed as well as semi-batch operations.

Second, a methodology operating at laboratory scale using the reaction calorimeter RC1 and predicting the thermal behaviour of full scale equipment during a chemical process has been developed. It is based on two on-line heat balances, one over the reaction calorimeter to determine q_{rx}^{RC1} and the other over the industrial reactors dynamics to compute T_r^{indus} . These two heat

balances are calculated in an Excel sheet. A Visual Basic window allows to establish the connection between the reaction calorimeter and the Excel sheet. Moreover, this window gives an user on-line access to some basic functions, mainly the temperature control mode of the industrial reactor (either T_r -mode or T_j -mode) and the temperature setpoint of the reactor. The reaction calorimeter is then forced to track the calculated T_r^{indus} , the latter being the setpoint of the RC1. According to the present work, controlling the jacket temperature of the RC1 instead of that of the reaction medium allows a faster and more robust temperature dynamic adjustment. The great advantage of the proposed methodology is that the modelling of the reaction kinetics is *not* necessary.

The precision of the on-line heat balance over the RC1 was tested by simulating the heat release rate of a reaction through the control of the power delivered by the calibration probe with an external voltage source. In this way, the heat provided to the reaction medium was known with great accuracy. With the help of the T_a -model, the error on q_{rx} lies in the acceptable 5 % range for bench scale calorimeters, especially for non isothermal conditions. The chosen test reaction, the hydrolysis of acetic anhydride, has highlighted that the thermal dynamics of industrial reactors can influence the reaction medium temperature evolution and hence the global safety. The simulation of a polymerisation reaction with the help of a thickener permitted to conclude that the proposed method was also applicable to reactions accompanied with large variations of the reaction medium viscosity.

Finally, comparison of reaction medium temperature evolutions predicted within the 2 L reaction calorimeter RC1 with that actually recorded at plant scale were presented, first for a neutralisation, second for a three steps reaction and third for an alkene oxidation. For the neutralisation of KOH by H_2SO_4 , the results precisely tallied with mean temperature differences less than 0.5 °C. Due to technical difficulties, the three steps reaction did not give very satisfactory results. Extreme dynamic conditions with temperature ramps of almost 4 [°C min⁻¹] have reduced the accuracy of the on-line heat balance. However, the laboratory experiments revealed that the dosing rate was not constant during the plant process, an unexpected characteristic beforehand. For the alkene oxidation by a peroxycarboxylic acid, the temperature evolution obtained in the RC1 tangibly agreed with the 630 L reactor, in which the reaction was also performed. The mean ΔT_r was of 0.5 °C. Moreover, the effect of the reactor thermal dynamics on the final reaction selectivity was clearly observable on the gas chromatography analyses. Because of its slower dynamics, smaller cooling capacity and more unfavourable heat transfer area to volume ratio, the simulated 25 m³ reactor generated a final selectivity about 13 % lesser than the simulated 630 L.

7.2 Outlooks

7.2.1 *Mixing effects*

As outlined in the introduction, a successful process development, and more precisely a correct scale-up, has to take three main time constants into account:

- *reaction* time constant
- full scale equipment *dynamics* time constant
- *mixing* time constant.

As this thesis only dealt with the first two items, its logical continuation would be the scale-down of mixing effects, or «mix-down». The methodology developed here with the combination of reaction calorimetry and full scale heat transfer dynamics modelling could be extended to mixing issues occurring during large scale-up. It would lead to a complete tool, allowing process engineers to rapidly identify the key parameters involved during the phase linking a new process concept with its commercial exploitation. The purpose of this conclusion is not to solve mixing problems, but rather first to illustrate with simple examples what we consider as mixing issues, and second to give some of the aspects we think are relevant in the mixing field.

7.2.2 *Mixing issues*

Mixing effects can be highlighted with a very simple experiment. Filling up the reaction calorimeter RC1 with various amounts of any liquid and performing for each of them an UA evaluation leads to the situation depicted in Fig. 7.1 (example given for deionised water). The more the mass of liquid introduced, the smaller the overall heat transfer coefficient U . This suggests that the flow field generated by the downward propeller is less dense with larger amount of liquid, a situation on the whole intuitive. Moreover, vortex formation and vortex depth are dependent on stirrer revolution speed [119, 120, 144]. In the case of a semi-batch reaction, with large quantity of reactant dosed, not only the heat transfer area will vary (this evolution being easily calculable) but also the overall heat transfer area. The evolution of U with the amount of reaction mass is probably not easy to estimate. It depends on geometrical characteristics (reactor and stirrer diameters, number of agitator stages, presence or not of baffles), stirrer revolution speed and physical characteristics of the reaction medium. Moreover, this dependency can also evolve during the course of the reaction. It may be the case when a dosed substance has different physical properties than the reaction mass or when the reaction implies a large variation of the physical characteristics, like for polymerisation reaction with high apparent viscosity changes.

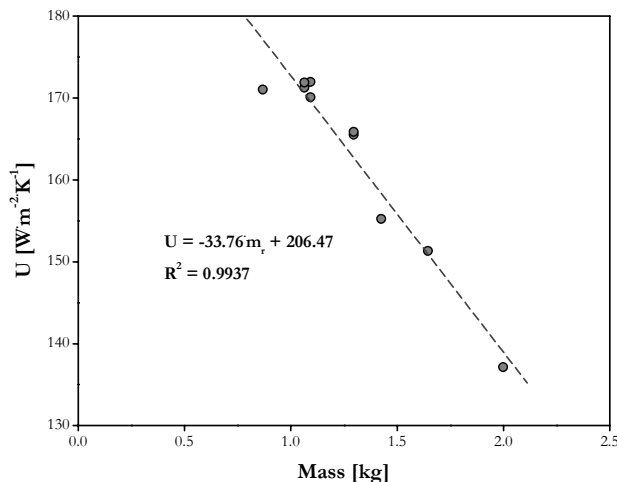


Figure 7.1: Overall heat transfer coefficient U vs. mass of liquid. Results obtained in the RC1 with the following experimental conditions: 2 L AP01 glass reactor filled with deionised water, constant temperature at 50 °C, downward propeller with constant revolution speed of 400 rpm.

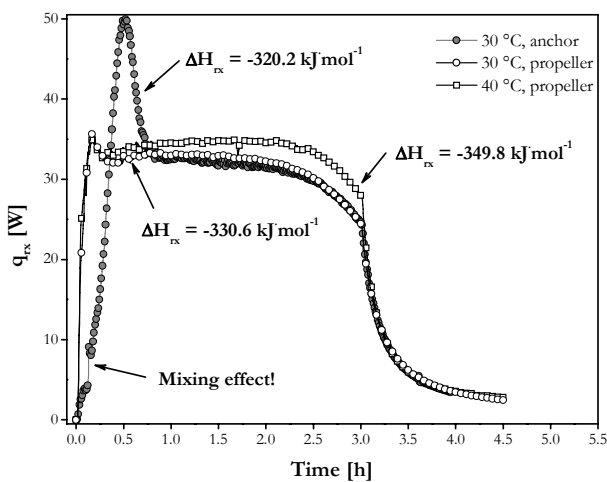


Figure 7.2: Alkene oxidation by a peracid: comparison of heat production rates obtained in the classical RC1 between anchor (100 rpm) and downward propeller (450 rpm) stirrers.

Another edifying example is illustrated in Fig. 7.2. It represents the heat production rates obtained in the classical RC1 for the alkene oxidation by a peroxycarboxylic acid (see § 6.4, p. 137). The first experiment was performed using an anchor stirrer and the corresponding q_{rx} is given by the ●-curve, the two other experiments were performed with a downward propeller stirrer.

With the anchor stirrer (100 rpm), a dead zone under the agitator shaft was observable during the dosing of peracid. This resulted in a lower heat release rate since still acid only very slowly reacts. After around 7 min of reaction, the anchor was manually more deeply immersed into the reaction mass. Consequently, the dead zone was stirred, an effect directly visible by the peak of heat production rate on Fig. 7.2. Thanks to its axial-flow characteristics (see Table 3.1, p. 47), the whole reaction medium was well mixed when using the downward propeller (400 rpm).

The above example clearly illustrates that q_{rx} may be strongly dependent on the stirrer configuration and hence on the mixing field. Therefore, the heat flux calculated on-line during the RC1 experiment may not correspond to that of full scale equipment because of different mixing characteristics. However, the 630 L industrial reactor having a very efficient mixing device installed, as it is also the case in the RC1 with the downward propeller, the temperature profiles are comparable (see Fig. 6.13, p. 143).

7.2.3 Continuation of the project - a few general guidelines

Normally, laboratory scale experiments can be carried out easily and the effects of tank geometry and process parameters could be studied at low cost. However, the scale-up of stirred tanks from laboratory scale to pilot and full-scale plant is not straightforward, in the same way for the scale-down. Depending on the physical process limiting the performance of the mixing vessel, it is commonly suggested that at least one of the mixing characteristics such as the power input per unit volume, impeller discharge flow, impeller tip speed, Re number, should be maintained constant. The most significant problem in scale-up occurs when different physical processes become limiting at different scales. Industrial scale reactors must perform several functions simultaneously (dispersion, reaction, and heat transfer) which do not scale-up in the same manner. Thus, the direct scale-up of mixing tanks from laboratory to industrial scale is not always successful [145].

Nowadays, computers offer unprecedented computational power to address complex chemical process operational and design issues. Moreover, numerical simulation techniques provide a great flexibility concerning the geometrical parameter variations. To employ such techniques for optimisation purposes, an integrated approach combining geometry variation, flow simulation and mathematical optimisation is desirable [146]. Numerical techniques, when dealing with mixing issues, often use dimensional analysis. Its advantage lies in the scale-invariance of the dimensionless frame, thus enabling the only reliable scale-up [147]. It may be therefore advisable to establish a complete list of the relevant parameters that describe the process.

The last two decades have seen the more widespread use of Computational Fluid Dynamics (CFD). CFD is the use of computers to analyse problems in fluid dynamics. The most fundamental consideration in CFD is how one treats a continuous fluid in a discretised fashion on a computer. One method is to discretise the spatial domain into small cells to form a volume mesh or grid, and then to apply a suitable algorithm to solve the equations of motion (Navier-Stokes equations for viscid, and Euler equations for inviscid flow). The general methodology is the following [148]:

- The geometry (physical bounds) of the problem is defined.
- The volume occupied by the fluid is divided into discrete cells (the mesh).
- The physical modelling is defined - for example, the equations of motions, enthalpy and species conservation.
- The boundary conditions are defined. This involves specifying the fluid behaviour and properties at the boundaries of the problem. For transient problems, the initial conditions are also defined.
- The equations are solved iteratively as a steady-state or transient.
- The resulting solution is analysed and visualised.

Three further recent publications can be cited: the one of Brucato et al. [149], where macro-mixing models were found to be sufficient in characterising process selectivity for a classical test set of fast reactions, the one of Farmer et al. [150] that outlines the numerical models available for analysing CFD of complex processes and complicated geometries and finally the one of Kumaresan & Joshi [151] that undertakes a systematic investigation of the effect of axial flow impeller designs on the flow pattern and mixing time.

Another approach is the use of stochastic models. As aforementioned, the increase of reactor volume is traduced in practice by an increase of the hydrodynamic characteristic time constants (e.g., mixing and circulation times). However, when scaling-up a reactor, the spatial dimension is also involved. This becomes problematic when dealing with circulation problem for which the spatial dimensions are very important because it affects the shape of the circulation times distribution. In their work, Delvigne et al. [152] propose a simple procedure to translate the hydrodynamic characteristics of a big scale bioreactor at the level of a scale-down reactor comprising a perfectly mixed part and a plug-flow part. This procedure involves two steps:

- the first one leading to the determination of a concentration field at a given inhomogeneity degree
- the second one involving the use of structured parameters coming from stochastic simulation.

From our point of view, it seems also essential to determine which mixing process is limiting. Generally three mixing length and time scales are used to describe the scale-up and scale-down of single phase stirred reactor processes in turbulent flow:

- micro-mixing: at the scale of turbulence; function of viscosity, density and power/volume
- meso-mixing: at the scale of the feed tube and impeller; function of feed tube location, feed rate, power/volume, impeller pumping rate
- macro-mixing: at the scale of the reactor; function of feed rate, impeller pumping rate.

Finally, some practical mixing guidelines in laboratory systems can be listed according to Machado [153]:

- Run at agitation rates to maintain turbulent flow, $Re > 2000$.
- Use standard reactor set-up.
- Use baffles or off-centre mixing to generate complete circulation patterns with top-to-bottom mixing.
- Confirm mixing uniformity visually and take digital pictures for the record.
- For multiphase processes:
Measure time for phases to separate: short times (seconds) suggest difficult mixing problem and need for shear and high power to volume ratio; long times (minutes) suggest circulation is more critical than shear and scale-up is more straightforward.
Estimate mixing gas liquid mass transfer rates using gas induction impeller.

REFERENCES

1. www.seeburger.com/fileadmin/COM/pdf/SEEBURGER_Chemical_engl.pdf.
2. CEFIC, *Summary of Business Impact Assessments of New Chemicals Policy*. Consultation Document concerning Registration, Evaluation, Authorisation and Restrictions of Chemicals (REACH), 2003.
3. Martin, V., *The Implementation of Known Technologies in Process Development: A Philosophy*. RXE User Forum Europe, Flims, 2005.
4. Mitchell, M., *Space Exploration at CRD La Jolla*. RXE User Forum Europe, Flims, 2005.
5. Tirronen, E. and Salmi, T., *Process development in the fine chemical industry*. Chemical Engineering Journal, 2003. **91**(2-3): p. 103-114.
6. Bonvin, D., *Optimal operation of batch reactors--a personal view*. Journal of Process Control, 1998. **8**(5-6): p. 355-368.
7. Stoessel, F., *Safety issues in scale-up of chemical processes*. Curr Opin Drug Discov Devel, 2001. **4**(6): p. 834-9.
8. Sie, S.T. and Krishna, R., *Process development and scale up .1. Process development strategy and methodology*. Reviews in Chemical Engineering, 1998. **14**(1): p. 47-88.
9. Bollyn, M., Van den Bergh, A., and Wright, A., *Fast scale-up combination of reaction calorimetry and reactor simulation*. Chemie-Anlagen + Verfahren, 1996. **29**(4): p. 95-6, 98, 100.
10. Grewer, T., Frurip, D.J., and Keith Harrison, B., *Prediction of thermal hazards of chemical reactions*. Journal of Loss Prevention in the Process Industries, 1999. **12**(5): p. 391-398.
11. Stoessel, F., *What Is Your Thermal Risk*. Chemical Engineering Progress, 1993. **89**(10): p. 68-75.
12. Gygax, R., *Chemical reaction engineering for safety*. Chemical Engineering Science, 1988. **43**(8): p. 1759-1771.
13. Toulouse, C., Cezerac, J., Cabassud, M., Le Lann, M.V., and Casamatta, G., *Optimisation and scale-up of batch chemical reactors: impact of safety constraints*. Chemical Engineering Science, 1996. **51**(10): p. 2243-2252.
14. Hemminger, W. and Höhne, G., *Calorimetry*. 1984: Verlag Chemie.
15. Landau, R.N., *Expanding the role of reaction calorimetry*. Thermochimica Acta, 1996. **289**(2): p. 101-126.
16. Regenass, W., *The development of heat flow calorimetry as a tool for process optimization and process safety*. Journal

- of Thermal Analysis, 1997. **49**(3): p. 1661-1675.
17. Stoessel, F., *La sécurité des procédés chimiques*. 2004: Ecole Polytechnique Fédérale de Lausanne.
 18. Hansen, L.D. and Hart, R.M., *The art of calorimetry*. Thermochimica Acta, 2004. **417**(2): p. 257-273.
 19. www.calorimeters.net/downloads/arc.pdf.
 20. www.systag.ch/e530isc5.htm.
 21. [www.rcforum.com/www_MT_com/wr_LA_RC1\(cal\)Products/rc1e_midtemp.htm](http://www.rcforum.com/www_MT_com/wr_LA_RC1(cal)Products/rc1e_midtemp.htm).
 22. www.belgroup.co.uk/home/reactor-systems/process-scale-up/similar-en.html.
 23. www.systag.ch/e310inrc.htm.
 24. www.chemisens.com/system/systemframe.htm.
 25. Boersma, S.L., *A Theory of Differential Thermal Analysis and New Methods of Measurement and Interpretation*. Journal of the American Ceramic Society, 1955. **38**(8): p. 281-284.
 26. Tian, M., *Utilisation de la Méthode Calorimétrique en Dynamique Chimique: Emploi d'un Micro-Calorimètre à Compensation*. Bulletin de la société chimique de France, 1923. **33**: p. 427-428.
 27. Calvet, E., *A new compensated differential microcalorimeter*. Compt. rend., 1948. **226**: p. 1702-1704.
 28. Andersen, H.M., *Isothermal kinetic calorimeter applied to emulsion polymerization*. Journal of Polymer Science, Polymer Chemistry Edition, 1966. **4**(4): p. 783-791.
 29. Koehler, W., Riedel, O., and Scherer, H., *Isothermal calorimeter controlled by beating pulses. I*. Chemie Ingenieur Technik, 1972. **44**(21): p. 1216-1218.
 30. Regenass, W., *Thermoanalytische methoden in der chemischen verfahrensentwicklung*. Thermochimica Acta, 1977. **20**(1): p. 65-79.
 31. Giger, G., Aichert, A., and Regenass, W., *A heat flux calorimeter for data-oriented process development*. Swiss Chem, 1982. **4**(3a): p. 33-36.
 32. Hub, L. and Kupr, T., *Calorimeter*, (Sandoz-Patent-G.m.b.H., Fed. Rep. Ger.), 1979. Patent n° DE2840595
 33. Schildknecht, J., *Reaction calorimeter for applications in chemical process industries: Performance and calibration*. Thermochimica Acta, 1981. **49**(1): p. 87-100.
 34. Litz, W., *The thermokinetic reactor (TKR) and its possible applications in chemical research and engineering*. Journal of Thermal Analysis, 1983. **27**(1): p. 215-228.
 35. Regenass, W., *Simulation as Aid in Development of Chemical Processes*. Chimia, 1971. **25**(5): p. 154-&.
 36. Regenass, W., *Calorimetric monitoring of industrial chemical processes*. Thermochimica Acta, 1985. **95**(2): p. 351-368.
 37. Karlsen, L.G. and Villadsen, J., *Isothermal reaction calorimeters—I. A literature review*. Chemical Engineering Science, 1987. **42**(5): p. 1153-1164.
 38. Stoessel, F., *Design Thermally Safe Semibatch Reactors*. Chemical Engineering Progress, 1995. **91**(9): p. 46-53.
 39. Landau, R.N. and Blackmond, D.G., *Scale-up Heat-Transfer Based on Reaction Calorimetry*. Chemical Engineering Progress, 1994. **90**(11): p. 43-48.
 40. Regenass, W., *Thermal Methods for the Determination of Overall Reaction-Rates*. Chimia, 1983. **37**(11): p. 430-437.

41. Snee, T.J., Bassani, C., and Lighthart, J.A.M., *Determination of the Thermokinetic Parameters of an Exothermic Reaction Using Isothermal, Adiabatic and Temperature-Programmed Calorimetry in Conjunction with Spectrophotometry*. Journal of Loss Prevention in the Process Industries, 1993. **6**(2): p. 87-94.
42. Stoessel, F. and Ubrich, O., *Safety assessment and optimization of semi-batch reactions by calorimetry*. Journal of Thermal Analysis and Calorimetry, 2001. **64**(1): p. 61-74.
43. Kletz, T.A., *Inherently safer plants*. Plant/Operations Progress, 1985. **4**(3): p. 164-167.
44. Kletz, T.A., *Inherently safer design: the growth of an idea*. Process Safety Progress, 1996. **15**(1): p. 5-8.
45. Gygax, R., *Thermal process safety*. Expert Commission for Safety in the Swiss Chemical Industry ed. Vol. 8. 1991.
46. Hugo, P., Steinbach, J., and Stoessel, F., *Calculation of the maximum temperature in stirred tank reactors in case of a breakdown of cooling*. Chemical Engineering Science, 1988. **43**(8): p. 2147-2152.
47. Abel, O., Helbig, A., Marquardt, W., Zwick, H., and Daszkowski, T., *Productivity optimization of an industrial semi-batch polymerization reactor under safety constraints*. Journal of Process Control, 2000. **10**(4): p. 351-362.
48. Erwin, S., Schulz, K., Moritz, H.-U., Schwede, C., and Kerber, H., *Increased reactor performance versus reactor safety aspects in acrylate copolymerization*. Chemical Engineering & Technology, 2001. **24**(3): p. 305-311.
49. Lerena, P., Wehner, W., Weber, H., and Stoessel, F., *Assessment of hazards linked to accumulation in semi-batch reactors*. Thermochimica Acta, 1996. **289**(2): p. 127-142.
50. Ubrich, O., Srinivasan, B., Lerena, P., Bonvin, D., and Stoessel, F., *Optimal feed profile for a second order reaction in a semi-batch reactor under safety constraints; Experimental study*. Journal of Loss Prevention in the Process Industries, 1999. **12**(6): p. 485-493.
51. Semenov, N., *Theories of combustion processes*. Zeitschrift für Physik, 1928. **48**: p. 571-582.
52. Townsend, D.I. and Tou, J.C., *Thermal hazard evaluation by an accelerating rate calorimeter*. Thermochimica Acta, 1980. **37**(1): p. 1-30.
53. Fierz, H., Finck, P., Giger, G., and Gygax, R., *Thermally stable operating conditions of chemical processes*. Institution of Chemical Engineers Symposium Series, 1983. **82**(Loss Prev. Saf. Promot. Process Ind., Vol. 3): p. A12-A21.
54. Alos, M.A., Zaldivar, J.M., Strozzi, F., Nomen, R., and Sempere, J., *Application of parametric sensitivity to batch process safety: Theoretical and experimental studies*. Chemical Engineering & Technology, 1996. **19**(3): p. 222-232.
55. Alos, M.A., Nomen, R., Sempere, J.M., Strozzi, F., and Zaldivar, J.M., *Generalized criteria for boundary safe conditions in semi-batch processes: simulated analysis and experimental results*. Chemical Engineering and Processing, 1998. **37**(5): p. 405-421.
56. Nomen, R., Sempere, J., Serra, E., and Barrera, A., *A Comparison of Calorimetric Measurements from Different Devices*. RC User Forum Europe, Interlaken, 1995.
57. Leggett, D.J., *Safe process development from reaction hazards testing*. Thermochimica Acta, 2001. **367-368**: p. 351-365.
58. Regenass, W., *Achieving safe processes for chemical production*. Swiss Chem, 1983. **5**(9a): p. 37-41.
59. Stoessel, F., Fierz, H., Lerena, P., and Kille, G., *Recent developments in the assessment of thermal risks of*

- chemical processes*. Organic Process Research & Development, 1997. **1**(6): p. 428-434.
60. Grob, B. and Riesen, R., *Reaction calorimetry for the development of chemical reactions*. Thermochemica Acta, 1987. **114**(1): p. 83-90.
 61. Choudhury, S., Utiger, L., and Riesen, R., *Heat transport in agitated vessels: scale-up methods*. Mettler-Toledo publication, (00724218).
 62. Bürl, M., *Ueberprüfung einer neuen Methode zur voraussage des Waermeneberganges in Ruebrkesseln*. Diss ETHZ, 1979. **6479**.
 63. Wilson, E.E., *A basis for rational design of heat transfer apparatus*. Trans. Am. Soc. Mech. Engrs, 1915. **37**: p. 47-82.
 64. Chilton, T.H., Drew, T.B., and Jebens, R.H., *Heat Transfer Coefficients in Agitated Vessels*. Industrial & Engineering Chemistry, 1944. **36**(6): p. 510-516.
 65. Uhl, V.W. and Gray, J.B., *Mixing, Theory and Practice*. Vol. 1, Chapter 3.5. 1966: Academic Press.
 66. Lake, R.J., *Practical Simulation and Scale-up Methods for Assessing Cooling of Exothermic Batch Reactions*. Chemistry & Industry, 1977(7): p. 250-255.
 67. Kumpinsky, E., *Experimental Determination of Overall Heat-Transfer Coefficient in Jacketed Vessels*. Chemical Engineering Communications, 1992. **115**: p. 13-23.
 68. Landau, R.N., Blackmond, D.G., and Tung, H.H., *Calorimetric Investigation of an Exothermic Reaction - Kinetic and Heat-Flow Modeling*. Industrial & Engineering Chemistry Research, 1994. **33**(4): p. 814-820.
 69. Bollyn, M., van den Bergh, A., and Wright, A., *Accelerated scale-up*. Mettler-Toledo publication, (51724866).
 70. de Buruaga, I.S., Echevarria, A., Armitage, P.D., delaCal, J.C., Leiza, J.R., and Asua, J.M., *On-line control of a semibatch emulsion polymerization reactor based on calorimetry*. Aiche Journal, 1997. **43**(4): p. 1069-1081.
 71. De Valliere, P., *State and parameter estimation in batch reactors for the purpose of inferring on-line the rate of heat production*, ed. D. ETH. Vol. 8847. 1989, Zürich. 196 p.
 72. Wilson, D.I., Agarwal, M., and Rippin, D.W.T., *Experiences implementing the extended Kalman filter on an industrial batch reactor*. Computers & Chemical Engineering, 1998. **22**(11): p. 1653-1672.
 73. Krämer, S. and Gesthuisen, R., *Simultaneous estimation of the heat of reaction and the heat transfer coefficient by calorimetry: estimation problems due to model simplification and high jacket flow rates--theoretical development*. Chemical Engineering Science, 2005. **60**(15): p. 4233-4248.
 74. Ubrich, O., Srinivasan, B., Lerena, P., Bonvin, D., and Stoessel, F., *The use of calorimetry for on-line optimisation of isothermal semi-batch reactors*. Chemical Engineering Science, 2001. **56**(17): p. 5147-5156.
 75. Hergeth, W.-D., Jaeckle, C., and Krell, M., *Industrial Process Monitoring of Polymerization and Spray Drying Processes*, in *Polymer Reaction Engineering*. 2003. p. 663-714.
 76. Zogg, A., Fischer, U., and Hungerbühler, K., *Identification of kinetic and thermodynamic reaction parameters from online calorimetric and IR-ATR data using a new combined evaluation algorithm*. Chemical Engineering Science, 2004. **59**(24): p. 5795-5806.
 77. Kupr, T. and Hub, L., *Industrial reaction calorimeter*. Experientia, Supplementum, 1979. **37**(Angew. Chem. Thermodyn. Thermoanal.): p. 334-342.
 78. Schneider, M.A., Maeder, T., Ryser, P., and Stoessel, F., *A microreactor-based system for the study of fast exothermic reactions in liquid phase: characterization of the system*. Chemical Engineering Journal (Amsterdam,

- Netherlands), 2004. **101**(1-3): p. 241-250.
79. Luyben, W.L., *Process Modeling, Simulation, and Control for Chemical Engineers*. 1973: McGraw-Hill. 558 p.
 80. www.answers.com/topic/feedback-1?method=6.
 81. www.answers.com/feedforward.
 82. Bilous, O. and Amundson, N.R., *Chemical Reactor Stability and Sensitivity*. 2. *Effect of Parameters on Sensitivity of Empty Tubular Reactors*. *Aiche Journal*, 1956. **2**(1): p. 117-126.
 83. Barkelew, C.H., *Chemical Engineering Progress Symposium Series*, 1959. **55**: p. 37-47.
 84. Barkelew, C.H., *Stability of adiabatic reactors*. *ACS Symposium Series*, 1984. **237**: p. 337-359.
 85. Morbidelli, M. and Varma, A., *Parametric Sensitivity and Runaway in Tubular Reactors*. *Aiche Journal*, 1982. **28**(5): p. 705-713.
 86. Morbidelli, M. and Varma, A., *Parametric sensitivity and runaway in fixed-bed catalytic reactors*. *Chemical Engineering Science*, 1986. **41**(4): p. 1063-1071.
 87. Morbidelli, M. and Varma, A., *A Generalized Criterion for Parametric Sensitivity - Application to Thermal-Explosion Theory*. *Chemical Engineering Science*, 1988. **43**(1): p. 91-102.
 88. Haldar, R. and Rao, D.P., *Experimental Studies on Parametric Sensitivity of a Batch Reactor*. *Chemical Engineering and Technology*, 1992. **15**: p. 34-38.
 89. Haldar, R. and Rao, D.P., *Experimental Studies on Semibatch Reactor Parametric Sensitivity*. *Chemical Engineering and Technology*, 1992. **15**: p. 39-43.
 90. Wang, Q.-G., *Structure and synthesis of PID controllers*. *Automatica*, 2003. **39**(4): p. 758-759.
 91. Miklovicova, E., Latifi, M.A., Msaad, M., and Hejda, I., *PID adaptive control of the temperature in batch and semi-batch chemical reactors*. *Chemical Engineering Science*, 1996. **51**(11): p. 3139-3144.
 92. Ziegler, J.G., *Optimum settings for automatic controllers*. *Transactions of the American Society of Mechanical Engineers*, 1942. **64**: p. 759-768.
 93. Voda, A.A. and Landau, I.D., *A Method for the Auto-calibration of PID Controllers*. *Automatica*, 1995. **31**(1): p. 41-53.
 94. Ubrich, O., *Choosing the correct temperature control parameters with RC1*. Mettler-Toledo publication.
 95. Seborg, D.E., Edgar, T.F., and Mellichamp, D.A., *Process dynamics and control*. 1989: John Wiley & Sons. 717 p.
 96. Wolf, A., Swift, J.B., Swinney, H.L., and Vastano, J.A., *Determining Lyapunov Exponents from a Time-Series*. *Physica D*, 1985. **16**(3): p. 285-317.
 97. Strozzi, F. and Zaldivar, J.M., *A General-Method for Assessing the Thermal-Stability of Batch Chemical Reactors by Sensitivity Calculation Based on Lyapunov Exponents*. *Chemical Engineering Science*, 1994. **49**(16): p. 2681-2688.
 98. Alos, M.A., Strozzi, F., and Zaldivar, J.M., *A new method for assessing the thermal stability of semibatch processes based on lyapunov exponents*. *Chemical Engineering Science*, 1996. **51**(11): p. 3089-3094.
 99. Bhat, N. and McAvoy, T.J., *Use of neural nets for dynamic modeling and control of chemical process systems*. *Computers & Chemical Engineering*, 1990. **14**(4-5): p. 573-582.
 100. www.mathworks.com/access/helpdesk/help/toolbox/nnet/nnet.shtml.
 101. Zaldivar, J.M., Hernandez, H., and Panetsos, F., *Control of Batch Reactors Using Neural Networks*.

- Chemical Engineering and Processing, 1992. **31**(3): p. 173-180.
102. Galvan, I.M., Zaldivar, J.M., Hernandez, H., and Molga, E., *The use of neural networks for fitting complex kinetic data*. Computers & Chemical Engineering, 1996. **20**(12): p. 1451-1465.
 103. Galvan, I.M. and Zaldivar, J.M., *Application of recurrent neural networks in batch reactors; Part I. NARMA modelling of the dynamic behaviour of the heat transfer fluid temperature*. Chemical Engineering and Processing, 1997. **36**(6): p. 505-518.
 104. Galvan, I.M. and Zaldivar, J.M., *Application of recurrent neural networks in batch reactors - Part II: Nonlinear inverse and predictive control of the heat transfer fluid temperature*. Chemical Engineering and Processing, 1998. **37**(2): p. 149-161.
 105. Dirion, J.L., Cabassud, M., Lelann, M.V., and Casamatta, G., *Design of a Neural Controller by Inverse Modeling*. Computers & Chemical Engineering, 1995. **19**: p. S797-S802.
 106. Cabassud, M., Dirion, J.-L., Etteguie, B., Le Lann, M.V., and Casamatta, G., *Elaboration of a neural network system for semi-batch reactor temperature control: An experimental study*. Chemical Engineering and Processing, 1996. **35**(3): p. 225-234.
 107. Dirion, J.-L., Cabassud, M., Le Lann, M.V., and Casamatta, G., *Development of adaptive neural networks for flexible control of batch processes*. The Chemical Engineering Journal and the Biochemical Engineering Journal, 1996. **63**(2): p. 65-77.
 108. Verein Deutscher Ingenieure-Wärmeatlas. 2002, Berlin: Springer.
 109. Yaws, C.L., McGraw-Hill Chemical Properties Handbook *Physical, Thermodynamics, Environmental Transport, Safety & Health Related Properties for Organic & Inorganic Chemical*. 1998: McGraw-Hill Professional Publishing.
 110. webbook.nist.gov/chemistry.
 111. www.aspentech.com/includes/product.cfm?IndustryID=0&ProductID=77.
 112. www.prosim.net/english.html.
 113. Fletcher, P., *Heat-Transfer Coefficients for Stirred Batch Reactor Design*. Chemical Engineer-London, 1987(435): p. 33-37.
 114. Bondy, F. and Lippa, S., *Heat-Transfer in Agitated Vessels*. Chemical Engineering, 1983. **90**(7): p. 62-71.
 115. Ekato, *Handbook of Mixing Technology*. 1991.
 116. Ekato, *Recherche et Développement dans la technologie de l'agitation*. 1981, Versailles: Ekato.
 117. Clark, M.W. and Vermeulen, T., *Incipient Vortex Formation in Baffled Agitated Vessels*. Aiche Journal, 1964. **10**(3): p. 420-422.
 118. www.on-line.vismix.com.
 119. Markopoulos, J. and Kontogeorgaki, E., *Vortex Depth in Unbaffled Single and Multiple Impeller Agitated Vessels*. Chemical Engineering & Technology, 1995. **18**(1): p. 68-74.
 120. Zlokarnik, M., *Stirring Theory and Practice*. 2001: Wiley-vch.
 121. Zaldivar, J.M., Hernandez, H., and Barcons, C., *Development of a mathematical model and a simulator for the analysis and optimisation of batch reactors: Experimental model characterisation using a reaction calorimeter*. Thermochimica Acta, 1996. **289**(2): p. 267-302.
 122. www.berkeleymadonna.com.

123. Felder, R.M. and Rousseau, R.W., *Elementary Principles of Chemical Processes*. 2nd ed. 1986: Wiley Series.
124. Regenass, W., *Calorimetry for Process Optimization and Process Safety Scope*. RC User Forum USA, Hilton Head, 1996.
125. www.mathworks.com.
126. Mettler-Toledo, *RC1 Instruction Notes*. 2004.
127. Ubrich, O., *Improving Safety and Productivity of Isothermal Semi-Batch Reactors by Modulating the Feed Rate*. Vol. Thèse N° 2245. 2000, Lausanne: Ecole Polytechnique Fédérale.
128. D'Angelo, F.A., Brunet, L., Cognet, P., and Cabassud, M., *Modelling and constraint optimisation of an aromatic nitration in liquid-liquid medium*. Chemical Engineering Journal, 2003. **91**(1): p. 75-84.
129. Wang, S. and Hofmann, H., *Strategies and methods for the investigation of chemical reaction kinetics*. Chemical Engineering Science, 1999. **54**(11): p. 1639-1647.
130. Duh, Y.S., Hsu, C.C., Kao, C.S., and Yu, S.W., *Applications of reaction calorimetry in reaction kinetics and thermal hazard evaluation*. Thermochimica Acta, 1996. **285**(1): p. 67-79.
131. Nomen, R., Sempere, J., and Lerena, P., *Heat flow reaction calorimetry under reflux conditions*. Thermochimica Acta, 1993. **225**(2): p. 263-276.
132. www.adlinktech.com/PD/web/PD_detail.php?cKind=FN&pid=16&seq=&id=&sid=.
133. www.ni.com/labview/.
134. www.adlinktech.com/PD/web/PD_detail.php?cKind=FN&pid=98&seq=&id=&sid=.
135. Lavanchy, F., *Development of reaction calorimetry applied to supercritical CO2 and methanol-CO2 critical mixture: - heat transfer, heat flow, and hydrodynamics -*. Ecole Polytechnique Fédérale. 2005, Lausanne. 255 p.
136. Becker, F. and Maelicke, A., *Thermokinetic measurements based on heat flow calorimetry*. Zeitschrift fuer Physikalische Chemie (Muenchen, Germany), 1967. **55**(516): p. 280-295.
137. Nomen, R., Sempere, J., Bueno, A., and Lopes da Cunha, R., *Approach to the Baselines Problem in RC1 Operations*. RC User Forum Europe, Zermatt, 1993.
138. www.texturant-systems.com/texturant/html/e/products/xanthan/mole.htm.
139. www.texturant-systems.com/texturant/html/e/products/xant.htm.
140. Freire, F.B. and Giudici, R., *Temperature oscillation calorimetry by means of a Kalman-like observer: The joint estimation of Q_r and UA in a stirred tank polymerization reactor*. Macromolecular Symposia, 2004. **206**(Polymer Reaction Engineering V): p. 15-28.
141. De Luca, P.G. and Scali, C., *Temperature oscillation calorimetry: Robustness analysis of different algorithms for the evaluation of the heat transfer coefficient*. Chemical Engineering Science, 2002. **57**(11): p. 2077-2087.
142. Maschio, G., Ferrara, I., and Lister, D.G., *Determination of the heat transfer coefficient in polymerization reactors by temperature oscillation calorimetry*. DECHEMA Monographien, 2001. **137**(7th International Workshop on Polymer Reaction Engineering, 2001): p. 543-550.
143. Tietze, A., Pross, A., and Reicher, K.H., *Temperature-oscillation calorimetry in stirred tank reactors*. Chemie Ingenieur Technik, 1996. **68**(1-2): p. 97-100.
144. Rieger, F., Dittl, P., and Novak, V., *Vortex Depth in Mixed Unbaffled Vessels*. Chemical Engineering Science, 1979. **34**(3): p. 397-403.
145. Li, M., White, G., Wilkinson, D., and Roberts, K.J., *Scale up study of retreat curve impeller stirred tanks using*

- LDA measurements and CFD simulation*. Chemical Engineering Journal, 2005. **108**(1-2): p. 81-90.
146. Schafer, M., Karasozen, B., Uludag, Y., Yapici, K., and Ugur, O., *Numerical method for optimizing stirrer configurations*. Computers & Chemical Engineering, 2005. **30**(2): p. 183-190.
 147. Zlokarnik, M., *Problems in the application of dimensional analysis and scale-up of mixing operations*. Chemical Engineering Science, 1998. **53**(17): p. 3023-3030.
 148. en.wikipedia.org/wiki/Computational_fluid_dynamics.
 149. Brucato, A., Ciofalo, M., Grisafi, F., and Tocco, R., *On the simulation of stirred tank reactors via computational fluid dynamics*. Chemical Engineering Science, 2000. **55**(2): p. 291-302.
 150. Farmer, R., Pike, R., and Cheng, G., *CFD analyses of complex flows*. Computers & Chemical Engineering, 2005. **29**(11-12): p. 2386-2403.
 151. Kumaresan, T. and Joshi, J.B., *Effect of impeller design on the flow pattern and mixing in stirred tanks*. Chemical Engineering Journal, 2006. **115**(3): p. 173-193.
 152. Delvigne, F., Destain, J., and Thonart, P., *A methodology for the design of scale-down bioreactors by the use of mixing and circulation stochastic models*. Biochemical Engineering Journal, 2006. **In Press, Corrected Proof**.
 153. Machado, R., *Practice and science of mixing in the scale-up of RCI reactors*. RXE User Forum Europe, Flims, 2005.

APPENDIX

A.1 Identification program

Typical Berkeley Madonna program for the identification of the outside heat transfer coefficient h_j (example presented: reactor R₂ filled with 27 kg of toluene, 80 rpm, «stair-shape» experiment). Note that the model parameters were evaluated using the complete set of heating/cooling experiments.

```
{PRODUCTION: VESSEL TJ_MODE}
```

```
METHOD stiff
```

```
STARTTIME = 0
```

```
STOPTIME=28795
```

```
DT = 0.1
```

```
DTMAX = 10
```

```
TOLERANCE = 0.01
```

```
{PARAMETERS FOR IDENTIFICATION}
```

```
a = 0
```

```
{regression parameter, W/(m2*K2)}
```

```
b = 401.7
```

```
{regression parameter, W/(m2*K)}
```

```
{Data}
```

```
Alat = 0.258
```

```
{heat transfer area between water and reactor wall, m2}
```

```
Alatg = 0.082
```

```
{heat transfer area between water and air, m2}
```

```
mCpw = 31683
```

```
{mass times Cp of reactor wall, stirrer and temperature probe, J/K}
```

```
dr = 0.40
```

```
{reactor diameter, m}
```

```
rr = dr/2
```

```
{reactor radius, m}
```

$n = 80/60$	{agitator speed, s-1}
$da = 0.25$	{agitator diameter, m}
$g = 9.81$	{gravitational constant, m/s ² }
$dsteel = 0.012$	{reactor stainless steel wall thickness, m}
$lambdasteel = 52$	{reactor stainless steel wall thermal conductivity, W/(m*K)}
$denamel = 0.0012$	{reactor enamelled wall thickness, m}
$lambdaenamel = 1.2$	{reactor enamelled wall thermal conductivity, W/(m*K)}
$C = 0.33$	{agitator constant, W/(m ² *K)}
$Ne = 0.20$	{Power number}
$Tro = 244.62$	{initial reactor temperature, °K}
$mr = 30$	{mass of water introduced, kg}

{Physical properties of toluene}

$\rho = -1.0800E-06*Tr^3 + 3.8809E-04*Tr^2 - 8.6396E-01*Tr + 1.1161E+03$	
{toluene density, kg/m ³ }	
$\lambda = 1.1852E-07*Tr^2 - 3.3591E-04*Tr + 2.1885E-01$	
{toluene thermal conductivity, W/(m*K)}	
$Cpr = (1.7472E-10*Tr^4 - 2.2475E-07*Tr^3 + 1.1059E-04*Tr^2 - 2.1360E-02*Tr + 2.8335E+00)*1000$	
{toluene specific heat capacity, J/(kg*K)}	
$\mu = \exp(6.2156E+07*(1/Tr)^3 - 5.6957E+05*(1/Tr)^2 + 2.7782E+03*(1/Tr) - 1.2760E+01)$	
{toluene viscosity, Pa}	

{ENERGY BALANCE}

{Exchange with jacket}

$z = C*(n^{2/3}*da^{4/3})/(dr*g^{1/3})$	
$\gamma = (\rho^{2*\lambda^2*Cpr*g/\mu})^{1/3}$	
$hr = z*\gamma$	{film heat transfer due to water, W/(m ² *K)}
$hw = 1/(dsteel/\lambda dsteel + denamel/\lambda daenamel)$	{film heat transfer due to reactor wall, W/(m ² *K)}
$hj = a*Tjtol + b$	{film heat transfer due to the utility fluid, W/(m ² *K)}
$U = 1/(1/hj + 1/hw + 1/hr)$	{overall heat transfer coefficient, W/(m ² *K)}
$qex = U*Alat*(Tr - Tjtol)$	{rate of heat exchange, W}

{Pagit}

$P = Ne*\rho*n^3*da^5$	{power supplied by agitator}
------------------------	------------------------------

{Qloss}

$dg = 0.007$	{glass wall thickness, m}
$\lambda dag = 1.25$	{glass wall thermal conductivity, W/(m*K)}

Tambient = 295.15 {ambient temperature, °K}
hig = 8.1 {film heat transfer coefficient due to air, W/(m^2*K)}
hwg = lambdag/dg {film heat transfer due to glass, W/(m^2*K)}
Ug = 1/(1/hig+1/hwg+1/hr) {overall heat transfer coefficient for losses, W/(m^2*K)}
qloss = Ug*Alatg*(Tr-Tambient) {losses through glass wall, W}

{Tr}

init Tr=Tro {initial reactor temperature, °K}
d/dt (Tr)=(P-qex-qloss)/(mr*Cpr+mCpw) {reactor temp. time dependence, °K/s}
LIMIT Tr <= 473.15

{Tj}

Tjmax=437.637
Tjmin=174.467
tauc=3178.22
taur=3801.48

init Tjtol = 226 {initial mean jacket temperature, °K}
Tjsettol = if TIME <= 2579 then 263.15 else if TIME <= 5504 then 283.15 else if TIME <= 7869 then 303.15 else if TIME <= 11199 then 323.15 else if TIME <= 13584 then 343.15 else if TIME <= 15989 then 363.15 else if TIME <= 18529 then 333.15 else if TIME <= 20899 then 313.15 else if TIME <= 23699 then 293.15 else if TIME <= 26104 then 273.15 else 253.15

d/dt (Tjtol) = if TIME <= 15989 then if Tjtol<Tjsettol then (Tjmax-Tjtol)/tauc else 0 else if Tjtol>Tjsettol then (Tjmin-Tjtol)/taur else 0 {jacket temp. time dependence, °K/s}

A.2 Experiments performed in industrial reactors

A.2.1 First set of reactors

Table A.1: Summary of experiments conducted within the 40 L industrial reactor R_I.

Experiments	Solvent	Mass [kg]	Stirrer [rpm]	Setpoint high [°C]	Setpoint low [°C]
1-3	water	10	80/120/160	150	-10
4-6	water	20	40/80/100	150	-10
7-9	water	35	80/120/160	150	-10
10	water	35	80	30/50/70/90	60/40/20

Table A.1: Summary of experiments conducted within the 40 L industrial reactor R₁.

Experiments	Solvent	Mass [kg]	Stirrer [rpm]	Setpoint high [°C]	Setpoint low [°C]
11-13	toluene	9	80/120/160	150	-50
14-16	toluene	18	80/120/160	150	-50
17-19	toluene	30	80/120/160	150	-50
20	toluene	30	80	-10/10/30/50/70	60/40/20/0/-20

Table A.2: Summary of experiments conducted within the 49 L industrial reactor R₂.

Experiments	Solvent	Mass [kg]	Stirrer [rpm]	Setpoint high [°C]	Setpoint low [°C]
1-3	water	5	80/120/160	150	-10
4-6	water	15	80/160/240	150	-10
7-9	water	30	80/160/240	150	-10
10	water	30	80	30/50/70/90	60/40/20
11-12	toluene	4	120/160	150	-50
13-15	toluene	12	80/160/240	150	-50
16-18	toluene	27	80/160/240	150	-50
19	toluene	27	80	-10/10/30/50/70/90	60/40/20/0/-20

A.2.2 Second set of reactors

Table A.3: Summary of experiments conducted within the 250 L industrial reactor R₃.

Experiments	Solvent	Mass [kg]	Stirrer [rpm]	Setpoint high [°C]	Setpoint low [°C]
1-3	water	80	100/200/300	130	-22
4-6	water	160	100/200/300	130	-22
7-9	water	240	100/200/300	130	-22
10-12	toluene	70	100/200/300	130	-22
13-15	toluene	140	100/200/300	130	-22
16-18	toluene	210	100/200/300	130	-22

Table A.4: Summary of experiments conducted within the 630 L industrial reactor R₄.

Experiments	Solvent	Mass [kg]	Stirrer [rpm]	Setpoint high [°C]	Setpoint low [°C]
1-3	water	200	50/110/170	130	-22
4-6	water	400	50/110/170	130	-22
7-9	water	600	50/110/170	130	-22
10	water	600	50	20/50/70/90/110	90/70/50/20/0
11-13	toluene	174	50/110/170	130	-22
14-16	toluene	348	50/110/170	130	-22
17-19	toluene	522	50/110/170	130	-22

Table A.5: Summary of experiments conducted within the 630 L industrial reactor R₅.

Experiments	Solvent	Mass [kg]	Stirrer [rpm]	Setpoint high [°C]	Setpoint low [°C]
1-3	water	200	60/110/170	130	-22
4-6	water	400	60/110/170	130	-22
7-9	water	600	60/110/170	130	-22
10-12	toluene	174	60/110/170	130	-22
13-15	toluene	348	60/110/170	130	-22
16-18	toluene	522	60/110/170	130	-22

A.2.3 Third set of reactors

Table A.6: Summary of experiments conducted within the 4 m³ industrial reactor R₆.

Experiments	Solvent	Mass [kg]	Stirrer [rpm]	Setpoint high [°C]	Setpoint low [°C]
1-2	water	1'600	25/33	20	80
3-4	water	2'750	25/33	20	80
5-6	water	3'900	25/33	20	80
7	water	3'900	33	20/40/60/80	60/40/20

A.2.4 Fourth set of reactors

Table A.7: Summary of experiments conducted within the 6.3 m³ industrial reactor R₇.

Experiments	Solvent	Mass [kg]	Stirrer [rpm]	Setpoint high [°C]	Setpoint low [°C]
1	water	2'000	65	80 (T_F -mode)	30 (T_F -mode)
2	water	4'000	65	80 (T_F -mode)	30 (T_F -mode)
3-5	water	6'300	20/65/115	80 (T_F -mode)	30 (T_F -mode)
6	water	6'300	65	80 (T_J -mode)	30 (T_J -mode)

Table A.8: Summary of experiments conducted within the 16 m³ industrial reactor R₈.

Experiments	Solvent	Mass [kg]	Stirrer [rpm]	Setpoint high [°C]	Setpoint low [°C]
1-2	alcohol	2'997	23/55	80	20
3-4	alcohol	7'004	23/55	80	20
5-6	alcohol	10'515	23/55	80	20

Table A.9: Summary of experiments conducted within the 25 m³ industrial reactor R₉.

Experiments	Solvent	Mass [kg]	Stirrer [rpm]	Setpoint high [°C]	Setpoint low [°C]
1-2	water	7'019	23/50	80	20
3-4	water	13'686	23/50	80	20
5-6	water	21'689	23/50	80	20
7-8	methanol	5'004	23/50	50	15
9-10	methanol	11'008	23/50	50	15
11-12	methanol	17'011	23/50	50	15

Note that for reactors R₈ & R₉ masses correspond to that of the electronic balance, but are for sure not exact to the nearest kilo.

A.3 Identified modelling parameters

Table A.10: Identified parameters of the heat balance model.

Reactor	P1 [W m ⁻² K ⁻²]	P2 [W m ⁻² K ⁻¹]	P3 [-] ^[°C for R5]	T _{j,max} [K]	T _{j,min} [K]	τ _b [s]	τ _c [s]
R ₁	3.7	-727.7	-	390.1	163.2	2244.9	3223.1
R ₂	0	401.7	-	437.6	174.5	2736.8	3493.2
R ₃	14.9	-3024.4	0.02	451.8	-	308.4	149.3
R ₄	11.4	-2202.6	0.38	412.4	64.5	332.1	332.1
R ₅	11.0	-1981.1	68.01	392.9	0.5	329.6	329.6
R ₆	6.2	-757.3	-	-	-	-	-
R ₇	1.9	274.8	-	-	-	-	-
R ₈	4.9	773.4	-	-	-	-	-
R ₉	24.8	-1367.3	-	-	-	-	-

Note that for reactors R₄ and R₅, τ_b = τ_c (model modification) and that for R₅, $p_3(T_{j,set} - T_{j,0})$ (see Eqs. 3.22 & 3.23, p. 55) was replaced by p_3 .

INDEX

A

Accumulation 6, 10, 16, 21, 98, 141
Activation energy 17, 24
Adiabatic
 control 39
 definition 10
 temperature rise 16, 111, 124, 131, 139

B

Baseline 89, 99, 114, 132
 choice of 98, 117, 138
 effects 115
Batch 3, 16, 41, 67
Block diagram 91–93
Brine 24, 26, 59, 66

C

Calibration probe 88, 112
 external voltage source 96–98, 148
 temperature oscillations 120
 thermal reactions 98
 types 78
Calorimetry 21, 149
 current trend 23
 modes of operation 10
 reaction 5, 9–24
 temperature oscillation 120
Cognitive routine 105
Controller

 cascade 32
 definition 29
 I 32
 P,I,D 30
 PI 32, 82–84
 proportional band 31, 55
 saturation 32
Conversion 16, 20, 39, 120, 143
 in scale-down approach 87–88
Cooling failure 5, 16, 101, 111
CPA 202 12

D

DSC 11

E

Enthalpy 7, 107, 124, 132, 139, 152
Excel 80, 124, 148
 communication 80–84
External data source 79–81, 104, 124

F

Feedback control 20, 29, 30, 32, 54
Feedforward control 29
Froude number 47, 51

G

Gain 31

H

Heat
 losses 53, 61, 85, 123
 resistance 18, 60, 68, 90, 111, 113, 124
 transfer 9, 11, 19, 53, 59, 85, 125
Heat balance 5
 equations 43, 44, 85
 industrial reactor 90
 jacket temperature 53–54
 on-line 20, 95, 136
 RC1 89
 reaction calorimetry 10–12
Heat flow 10, 11, 49, 71, 89
 calorimetry 12
 kinetics 14–15, 20
Heating/cooling
 capacity 18, 22, 38
 curves 57
 experiments 56
 reactor designs 24–28
 system 102

I

Isoperibolic
 control 38
 definition 10
 instruments 10

J

Jacket 18, 24, 29, 44, 53, 83, 125

mass flow rate 61

K

Kalman filter 21, 43

L

Lyapunov exponents 33–34

M

Madonna 57, 98, 163

Matlab 80

Mixing 3, 6, 117

- designs 47
- effects 20, 149
- enthalpy 23
- issues 149–151
- nozzle 26
- power of 45

Modelling 59, 64, 69

- dynamics 105, 124
- general equations 44–55
- kinetics 4, 148
- parameters 169

N

Neural networks 34–35

Nusselt

- constant 47
- correlation 49

O

On-line 79, 115

- monitoring of chemical reactions 20–21
- scale-down methodology 85–89

P

Parametric sensitivity 17, 29–30, 33

Peltier elements 11

Polymerisation 20

- reproduction of 114–119

Power

- equation 46
- number 47
- of reaction 89

Process development 3, 18, 149

Pump 78, 107, 124, 136, 153

Q

Quality 1, 4, 28, 67, 90, 104, 137, 140, 143

R

RC1

- apparatus 78–79
- characteristics 6
- classical 82, 85, 98, 106, 107, 116, 123, 124, 129, 138
- external data source 79–81
- history 13
- modified 82, 98, 100, 109, 118, 124, 132, 140, 144
- picture 12
- scale-down methodology 85–93
- temperature control strategy 81–84

RD10 78, 127

Reaction

- hydrolysis 106–114
- neutralisation 122–128
- oxidation 137–144
- three steps 128–136

Reactor

- dynamics 6, 96, 140, 143
- material 45, 125
- size 6, 18, 53, 77
- wall 46, 50, 64, 89

Return on investment 2

Reynolds number 47, 49

S

Safety 6, 14–18, 27, 39, 92, 104, 147

- analysis 111
- aspects 4
- choice of reactor 137
- inherent design 15

margins 90

- reaction calorimetry 14

Scale-down

- history 22
- methodology 6, 77–78, 85–91
- mixing effects 149, 152

Scale-up

- factor 90
- principle 3, 18
- time constants 149

Sedex 11

Segment time 81

Semi-batch 3, 16, 20, 89, 149

Sensitivity 88

Sikarex 11

Simular 12

Steam 24, 54, 70

Stirrer

- dead zone 151
- effect of 151
- heat capacity of inserts 46
- heating/cooling experiments 56
- in Wilson plots 18, 111
- power due to 46
- types 47
- Visimix 52
- with scale-down approach 85

Syscalo 12

T

Temperature

- control 81, 102, 117, 147
- dependence 18, 85, 95
- difference 11, 52, 53, 59, 84, 125, 147
- jacket corrected 89
- Pt-100 46, 78, 118

Thickener 115, 117, 148

Time constant 6, 38, 102, 123, 136

Time to maximum rate 16

Timer event 80–81, 87

Tj-mode 41, 54, 55, 56, 58, 80, 82, 83, 84, 101, 109, 128

Tr-mode 41, 54, 56, 80, 82, 101, 109, 122, 137

U

Utility fluid 24, 46, 49, 54

V

Variable

controlled 91

manipulated 91

Viscosity 20, 48, 49, 60, 115, 148

Visimix 50, 52, 64

Visual Basic 80, 148

Vortex 51, 59, 64, 101, 111, 147,
149

W

Water

cold 54, 66

deionised 81, 98, 106, 112, 123,
137, 138, 149

factory 24, 25

superheated 24, 26

Wilson plot

concept 19

example 111–113

WinRC 78, 79, 80, 83, 123

Benoît ZUFFEREY

Swiss
benoit.zufferey@a3.epfl.ch

Born - 10/22/1977
Single

KEY SKILLS

Analytical – Proactive – Open-minded – Results-oriented

EDUCATION

- 2002 - 2005: **PhD** at the Swiss Federal Institute of Technology Lausanne (EPFL) under the supervision of Prof. **Francis Stoessel** in the Group of Chemical Process Safety and in partnership with **Ciba SC, Firmenich, Mettler-Toledo, Roche**, the **Swiss Institute for the Promotion of Safety & Security** and **Syngenta**
- 1997 - 2002: Master in **Chemical Engineering** at the EPFL

PROFESSIONAL EXPERIENCE

2002 - 2005:	PhD	EPFL (24 months) - BASEL (15 months)
---------------------	------------	---

- **Thesis** entitled: “Scale-down Approach: Chemical Process Optimisation using Reaction Calorimetry for the Experimental Simulation of Industrial Reactors Dynamics”
- Development of a methodology for driving **process profitability and safety**
Combining calorimetric measurements and modelling, allows to manage and optimise plant performance at laboratory scale and to reduce time-to-market.
- Computer’s **modelling** of industrial reactors heat transfer dynamics
- **Award** for the best contribution at the RXE Forum organised by Mettler-Toledo
Democratically elected by the 150 participants, the price consisted in CHF 1000.- and a free trip to the next RXE Forum in the US to hold the award-winning lecture.
- First inventor of a **Patent** deposited by Mettler-Toledo at the European Patent Office

2004 - 2005:	Assistant	EPFL
---------------------	------------------	-------------

- 8th semester lecture: **Chemical Process Safety**
- 8th semester lecture: **Process Development**
Supervisor of the Aspen Plus software’s training lecture for minimising energy costs, improving yields and throughput, and increasing operating profitability and return on capital employed.

2001 - 2002:	3 months traineeship and diploma work	LONZA AG, Visp
---------------------	--	-----------------------

- Development and characterisation of structured catalysts
- Kinetic modelling and computer’s optimisation of a direct esterification

1998 - 2000:	7 weeks practical training	ORGAMOL SA, Evionnaz
---------------------	-----------------------------------	-----------------------------

- Laboratory and production assistant

LANGUAGES

French: Mother tongue
English: Fluent, spoken and written
German: Fluent, spoken and written

COMPUTER KNOWLEDGE

Scientific software: **Aspen**, Madonna, **Matlab**, **Visual Basic**, **Labview**, BatchReactor, **VisiMix**
Office software: MS Office 2003, **FrameMaker**, EndNote, Origin, ISIS Draw, **Photoshop CS**

EXTRA CURRICULAR ACTIVITIES

Table tennis:

- Top-level (2nd league)

Piano:

- Since 1982
- Member of a trio, regular concerts

Politics:

- Political secretary since November 2003 (700 members)
- Responsible for the recruitment of new members
- Co-maker of the party's youth movement
- Coordinator of a group reacting towards the current political scene